Expedition 347 summary[1]

T. Andrén, B.B. Jørgensen, C. Cotterill, S. Green, E. Andrén, J. Ash, T. Bauersachs, B. Cragg, A.-S. Fanget, A. Fehr, W. Granoszewski, J. Groeneveld, D. Hardisty, E. Herrero-Bervera, O. Hyttinen, J.B. Jensen, S. Johnson, M. Kenzler, A. Kotilainen, U. Kotthoff, I.P.G. Marshall, E. Martin, S. Obrochta, S. Passchier, N. Quintana Krupinski, N. Riedinger, C. Slomp, I. Snowball, A. Stepanova, S. Strano, A. Torti, J. Warnock, N. Xiao, and R. Zhang[2]

Chapter contents

[1] Andrén, T., Jørgensen, B.B., Cotterill, C., Green, S., Andrén, E., Ash, J., Bauersachs, T., Cragg, B., Fanget, A.-S., Fehr, A., Granoszewski, W., Groeneveld, J., Hardisty, D., Herrero-Bervera, E., Hyttinen, O., Jensen, J.B., Johnson, S., Kenzler, M., Kotilainen, A., Kotthoff, U., Marshall, I.P.G., Martin, E., Obrochta, S., Passchier, S., Quintana Krupinski, N., Riedinger, N., Slomp, C., Snowball, I., Stepanova, A., Strano, S., Torti, A., Warnock, J., Xiao, N., and Zhang, R., 2015. Expedition 347 summary. *In* Andrén, T., Jørgensen, B.B., Cotterill, C., Green, S., and the Expedition 347 Scientists, *Proc. IODP,* 347: College Station, TX (Integrated Ocean Drilling Program). doi:10.2204/iodp.proc.347.101.2015

[2] **Expedition 347 Scientists' addresses.**

Abstract

Integrated Ocean Drilling Program Expedition 347 aimed to retrieve sediments from different settings of the Baltic Sea, encompassing the last interglacial–glacial cycle to address scientific questions along four main research themes:

1. Climate and sea level dynamics of marine isotope Stage (MIS) 5, including onsets and terminations;
2. Complexities of the latest glacial, MIS 4–MIS 2;
3. Glacial and Holocene (MIS 2–MIS 1) climate forcing; and
4. Deep biosphere in Baltic Sea Basin (BSB) sediments.

These objectives were accomplished by drilling in six subbasins: (1) the gateway of the BSB (Anholt), where we focused on sediments from MIS 6–5 and MIS 2–1; (2) a subbasin in the southwestern BSB (Little Belt) that possibly holds a unique MIS 5 record; (3, 4) two subbasins in the south (Bornholm Basin and Hanö Bay) that may hold long complete records from MIS 4–2; (5) a 450 m deep subbasin in the central Baltic (Landsort Deep) that promises to contain a thick and continuous record of the last ~14,000 y; and (6) a subbasin in the very north (Ångermanälven River estuary) that contains a uniquely varved (annually deposited) sediment record of the last 10,000 y.

These six areas were expected to contain sediment sequences representative of the last ~140,000 y, with paleoenvironmental information relevant on a semicontinental scale because the Baltic Sea drains an area four times as large as the basin itself.

The location of the BSB in the heartland of a recurrently waning and waxing ice sheet, the Scandinavian Ice Sheet, has resulted in a complex development: repeated glaciations of different magnitudes, sensitive responses to sea level and gateway threshold changes, large shifts in sedimentation patterns, and high sedimentation rates. Its position also makes it a unique link between Eurasian and northwest European terrestrial records. Therefore, the sediments of this largest European intracontinental basin form a rare archive of climate evolution over the latest glacial cycle. High sedimentation rates provide an excellent opportunity to reconstruct climatic variability of global importance at a unique resolution from a marine-brackish setting. Comparable sequences cannot be retrieved anywhere in the surrounding onshore regions. Furthermore, and crucially, the large variability (salinity, climate, sedimentation, and oxygenation) that the BSB has under-

doi:10.2204/iodp.proc.347.101.2015

gone during the latest glacial cycle makes it optimal for new research on the deep biosphere and its evolution and biogeochemical processes in a changing environment. The BSB also provides a model for how postglacial diffusive penetration of seawater ions has altered the chemical environment and microbial physiology in the subseafloor biosphere.

It is envisaged that the transect of drilled sites, from west to east and from south to north, in this repeatedly glaciated and environmentally very dynamic region will add totally new scientific insights into a variety of research fields. These involve, for example, regional and global issues on the timing and forcing of rapid climate and sea level changes, on mechanisms behind hypoxia-driven processes in intracontinental sea basins, and on the glacial history of the SIS and its interaction with the climate system. The drilled sites will also give new insight into the controlling mechanisms for prokaryotic communities and underlying biogeochemical processes in the seabed. New data will show how the highly variable environment has affected the phylogenetic diversity of the microbial communities and which biogeochemical processes predominate today in the deep glacial and interglacial deposits. An extraordinary large set of biological, physical (including a variety of dating and paleomagnetic methods), chemical, and biogeochemical methods, as well as a set of novel approaches, have been applied to the drilled sediments.

Introduction

The Baltic Sea Basin (BSB) is one of the world's largest intracontinental basins, occupying 373,000 km^2 with a drainage area four times this size. Its mean depth is 54 m, although a few relatively deep basins exist (e.g., the Eastern Gotland Basin [248 m] and the Landsort Deep [459 m]) (Fig. **F1**). The BSB has served as a depositional sink throughout the last several hundred thousand years, and the sediments comprise a unique high-resolution archive of the paleoenvironmental history of the large drainage area, the basin itself, and the neighboring sea areas. The location of the BSB in the heartland of a recurrently waning and waxing ice sheet, the Scandinavian Ice Sheet (SIS), has resulted in complex development characteristic of many glaciated regions of the Northern Hemisphere. Repeated glaciations of different magnitudes, sensitive responses to sea level and gateway threshold changes, large shifts in sedimentation patterns, and high sedimentation rates have shaped its development. The geographical location of the BSB also makes it a unique link between the Eurasian and the northwestern European terrestrial records and, as such, also serves as a link to North Atlantic marine records and Greenland ice cores. Analyses of terrestrial, marine, and ice archives combined with numerical modeling (e.g., Levine and Bigg, 2008) have shown that North Atlantic Ocean circulation plays an important role in the global climate system, affecting North America and Europe in particular but also closely linked to, for example, the Asian monsoon system (Wang et al., 2001). The position of the BSB roughly halfway between North Atlantic-Greenland and Asia represents a link that preserves the continental response to oceanic forcing. However, long high-resolution marine records showing continental response to this oceanic forcing are scarce.

Therefore, the sediments of this largest European intracontinental basin form a unique archive of climate evolution over the latest glacial cycle. The high sedimentation rates (100–500 cm/1000 y) of the BSB provide an excellent opportunity to reconstruct climatic variability of global importance at unique resolution from a marine-brackish setting. Some of the sedimentary record can be resolved on interannual timescales—for example, those controlled by changes in Meridional Overturning Circulation (MOC), the North Atlantic Oscillation (NAO), and the Arctic Oscillation (AO). This makes the BSB unique for sampling sediments from the latest glacial cycle. Comparable sequences cannot be retrieved anywhere in the surrounding onshore regions. The extreme climatic changes have also had a profound effect on the biota, both in the BSB and in the surrounding terrestrial ecosystems. Shifts between marine, brackish, and freshwater have been accompanied by changes in temperature, oxygen, nutrients, and biological productivity. These large-scale variations in the environment of the BSB have controlled the composition of biotic communities in the past and may be reflected in the buried deposits where the extant deep biosphere controls sediment geochemistry and nutrient cycling.

Background

Regional background

The location of the BSB at a glaciation-sensitive high northern latitude has resulted in highly dynamic development during its recent geological history. Areas of the BSB have been repeatedly covered by recurring Quaternary glaciations over northern Europe, with subsequent deglaciations resulting in largely differential uplift across the region of the BSB and its drainage area. The latest interglacial–glacial cycle is an excellent analog of the various processes that the basin has been exposed to during previous glacial cycles, with geological deposits in the Baltic Basin and

the surrounding region acting as archives of its history.

The Eemian interglacial (~130–115 k.y. before present [BP]) is partly documented in the North Greenland Ice Core Project (NGRIP) ice core (North Greenland Ice Core Project Members, 2004) and in low-resolution deep-sea records (land-sea correlation, Sánshez-Goñi et al., 1999). However, detailed Eemian marine shelf records from northern Europe are very scarce and generally contain only fragmented paleoenvironmental information. The same is true of the early Weichselian interstadials (marine isotope Stage [MIS] 5c and MIS 5a).

The buildup to the Last Glacial Maximum (LGM), MIS 3 (~60 to 25 k.y. BP), is characterized by many rapid switches between short cold and longer warm periods. The latter are known as Dansgaard-Oeschger (D/O) events, which are evident in both the Greenland ice cores and deep-sea records. The D/O events are part of the "Bond cycles," each one ending with a Heinrich event disrupting North Atlantic thermohaline circulation and causing cooling in the Northern Hemisphere (e.g., Dickson et al., 2008; Grimm et al., 2006; Bond et al., 2001). The complexity of these cycles is intricate: although warming can destabilize ice sheets and produce surges and icebergs, a cooler climate increases sea ice cover and consequently increases Earth's albedo and promotes further ice sheet growth. However, the feedback from increased sea ice cover in the North Atlantic on the SIS, and hence the climatic effects on northwestern Europe, is presently poorly understood.

The long-term paleoenvironmental development since the LGM at ~20 k.y. BP (MIS 2) is fairly well understood, and the drastic climatic shifts during the Last Termination as recorded in the Greenland oxygen isotopic record are mirrored in the Baltic varved glacial clay record (Andrén et al., 1999, 2002).

The Late Pleistocene and Holocene climatic history of Central and Northern Europe is closely connected to the large-scale meteorological processes of the wider North Atlantic region, which also controlled the climate development of the North American continent. Different terminologies are used for the glacial history of Europe and North America. Table T1 provides a correlation of terminologies used for the two regions and the approximate ages and marine isotope stages.

Geological history of the Baltic Sea Basin during the latest glacial cycle

The BSB has undergone many glaciations during the Quaternary. During the last interglacial (the Eemian), the BSB was a larger and more saline sea than the present Baltic Sea (Funder et al., 2002). A thin and incomplete marine Eemian sediment sequence has been found as a thrusted sequence in a coastal cliff in the western Baltic (e.g., Kristensen and Knudsen, 2006; Gibbard and Glaister, 2006), but no complete sequence of sediments deposited during the Eemian has been recovered in situ from any part of the Baltic Sea. Consequently, we have incomplete knowledge about the BSB during the Eemian interglacial. Two subsequent early Weichselian glacial advances (MIS 5d and MIS 5b) may have only reached as far south as ~60.5°N, leaving the central and southern BSB free of ice. Glacial events during MIS 4 were recorded in sediments from (north)western Finland at ~64°N (Salonen et al., 2007), and the first Baltic ice lobe advance into Denmark is dated to 50–55 k.y. BP (Houmark-Nielsen, 2007; Larsen et al., 2009). Based on these records, an isolated lake probably covered large parts of the BSB until at least 60 k.y. BP. This portion of the BSB acted as a depocenter between 55 and 60 k.y. BP, and accumulated sediments most likely hold a high-resolution record of climate-related changes across the large catchment area of the BSB.

The complex Danish glacial stratigraphy and several ^{14}C dates (26–35 ^{14}C k.y. BP; Andrén and Björck, unpubl. data) of peat and lake (35 and 65 m below present sea level, respectively) sediments covered and underlain by till and clays in the southern BSB indicate a highly oscillating ice margin. These data show that the southern BSB was partly free of ice on several occasions during MIS 3 prior to the LGM at ~22 k.y. BP when the Weichselian ice sheet covered the entire BSB (Houmark-Nielsen and Kjær, 2003; Larsen et al., 2009). It also implies that the central parts of the Hanö and Bornholm Basins were lacustrine systems during ice-free conditions and that glacial erosion, at least locally, was insignificant, leaving much of the MIS 3 and older archives intact. Furthermore, glacial erosion must have been minimal in the deepest basins during these inferred surge-like events. This part of the BSB may therefore hold a record of Heinrich and D/O events and answer questions about what if any role the SIS played in these enigmatic oscillations.

Deglaciation and early postglacial stages

The deglaciation of the southern BSB between 22 and 16 k.y. BP was highly complex, with major deglacial phases interrupted by intriguing stillstands and re-advances (Houmark-Nielsen and Kjær, 2003; Larsen et al., 2009) (Table T2). The Baltic Ice Lake (BIL), dammed in front of the retreating ice front (Fig. F2), released large amounts of freshwater into the North Atlantic during the early stage of the de-

glaciation between ~16 and 11.7 k.y. BP. This occurred both through Øresund and south central Sweden (Gyldenholm et al., 1993; Björck, 1995; Majoran and Nordberg, 1997; Jiang et al., 1998). During the final drainage of the BIL at ~11.7 k.y. BP, almost 8000 km^3 of freshwater was released rapidly into the North Atlantic (Jakobsson et al., 2007), but the effects on North Atlantic thermohaline circulation may have been only minor (Andrén et al., 2002) (Fig. F3). However, it has also been suggested that this sudden freshwater discharge may have triggered the cold Preboreal oscillation (Björck et al., 1996) and ice advances in northern Norway (Hald and Hagen, 1998).

The next Baltic Sea stage, the Yoldia Sea (YS) stage, coincides with the onset of the Holocene epoch (Walker et al., 2009) and the associated rapid warming. In fact, the thicknesses of glacial varves in the northwestern Baltic proper and $\delta^{18}O$ values in the Greenland Ice Core Project (GRIP) ice core display a noticeably similar pattern over a 150 y Younger Dryas to the Preboreal transition period (Andrén et al., 1999, 2002). These records show a distinct increase in sedimentation rate as the ice sheet began to melt and rapidly retreat (Fig. F3). The following few hundred years were characterized by rapid deglaciation of the SIS. Relative sea level changes of the YS stage of the Baltic Sea history played an important role and were the result of a combination of rapid regression in the recently deglaciated regions and normal regression rates in southern Sweden (1.5–2 m/100 y).

Despite the fact that the passage westward to the North Sea was open and the YS was at the same topographic level as the North Sea, it took ~300 y before saline water could enter through the fairly narrow straits of the south-central Swedish lowland (Fig. F4). This brackish phase has been documented by varve lithology, geochemistry, and marine/brackish fossils, such as *Portlandia* (*Yoldia*) *arctica*. Occasionally, this phase is represented by sulfide banding, implying a halocline. The maximum duration of this brackish phase has been estimated to 350 y (Andrén et al., 2007), although some records indicate that it only lasted 70–120 y (Andrén and Sohlenius, 1995; Wastegård et al., 1995). Because of the high isostatic rebound rate in south-central Sweden, the strait rapidly shallowed, which, together with the large outflow of meltwater from the retreating ice sheet, prevented further inflow of saline water to the Baltic Sea (Fig. F4). This turned the YS into a freshwater basin again, although there was still an open connection to the North Sea in the west. At the end of the YS stage, the ice sheet had receded to the north and most of today's BSB was deglaciated, with the exception of the Bothnian Bay.

As the outlets west of Lake Vänern became shallower, subsequent damming forced the water level inside the Baltic Basin to rise, and the next stage, the Ancylus Lake (AL) stage, began. The sediments of this large freshwater lake generally contain little organic material, which may be explained partly as a result of the meltwater inflow to the Baltic from the final deglaciation of the SIS and is also due to the young soils of the recently deglaciated drainage area. Together, this created an aquatic environment with low nutrient input and hence low productivity. This environment did not promote the formation of a halocline but led to a well-mixed oxygenated water body. The relatively common sulfide-banded sediment of this stage can probably be explained by H_2S diffusion from younger organic-rich sediments (Sohlenius et al., 2001).

Areas south of Stockholm–Helsinki that experienced shoreline regression since the deglaciation now entered a transgressive phase, marking the onset of the AL stage of the Baltic Sea history. This stage is documented by several shore displacement curves from this area but also by simultaneous flooding of pine forests growing along the coasts of the southern Baltic Basin. In the southernmost Baltic, a transgression is recorded by submerged pine trees and peat deposits dated between 11.0 and 10.5 k.y. BP (Andrén et al., 2007).

Whereas areas to the north experienced a slow regression, the extent of the transgression in the south varied depending on whether areas were isostatically rising or submerging (Fig. F5). A large number of ^{14}C dates from peat as well as tree remains (mainly pine) from the beaches suggest the time span of this so-called Ancylus transgression can be estimated to ~500 y. The isobases over southern Sweden show that the water level of the Baltic was higher than the sea in the west, indicating that the AL was dammed. The total impact of this damming is estimated to have raised the Baltic ~10 m above the level of the North Sea (Björck et al., 2008), meaning that the isostatically submerging areas in the southernmost Baltic experienced a transgression larger than that.

The transgression and flooding in the south, as a result of the differences in isostatic rebound between the northern and southern Baltic Basin, would have resulted in a new outlet in the south. Because the outlet through Øresund had been uplifted more than other possible outlets farther south, it is likely that the new outlet was located somewhere in these southern areas (Fig. F1). Available data indicate that the Darss sill area, between Darss and Møn, was inundated by the AL. The idea of a sudden and large drainage of the AL through the so-called Dana River flowing through Mecklenburg Bay and Fehmarn

Belt, along the east side of Langeland and out through the Great Belt to Kattegat as proposed by von Post (1929) was proven impossible by Lemke et al. (2001). However, initial erosion of soft Quaternary deposits from the riverbed might have opened a connection and caused an initial lowering of the AL by ~5 m, followed by a period of rising sea level. It has been proposed that this resulted in a complex river system through Denmark comprising river channels and lakes (Bennike et al., 2004) with a steadily lower fall-gradient as sea level rose. As the sea level in Kattegat had reached the level of the AL inside the Baltic Basin, it was possible for saltwater to penetrate all the way through the long river system into the Baltic. The first weak inflows of saline water are recorded simultaneously in the Bornholm Basin (Andrén et al., 2000b) and the Blekinge archipelago (Berglund et al., 2005) at ~9.8 k.y. BP. It is therefore possible to define the end of the AL stage as being concurrent with the time at which the AL level was at the same approximate level as the North Sea and the first signs of any marine influence since the YS stage are recorded. This period of low and fluctuating saline influence lasted longer than a millennium and has been named the initial Littorina Sea stage (Andrén et al., 2000b).

Littorina Sea stage

The onset of the next stage of Baltic Sea history, the Littorina Sea (LS) stage, can often be recognized as a marked lithologic change in Baltic Sea cores. The onset may be represented by a distinct increase in organic carbon content and an increasing abundance of brackish-marine diatoms (e.g., Sohlenius et al., 2001). Whether this sudden increase in organic carbon content is exclusively coupled to changes in primary production or if it is partly due to a better preservation of organic carbon during anoxic conditions has been a matter of discussion (Sohlenius et al., 1996). Flocculation of clay particles and subsequent rapid sedimentation resulting in an increase in the Secchi depth has also been proposed as contributing to an increase in primary production (Winterhalter, 1992). The distribution of trace elements in sediments, especially the enrichment of barium and vanadium, which is linked to cycling of organic carbon, implies that increased productivity in the basin is a plausible cause of the rise in organic carbon content (Sternbeck et al., 2000).

The global melting of the large ice sheets over a couple of millennia caused a 30 m rise in absolute sea level (Lambeck and Chappell, 2001). A consequence of this is the flooding of the Øresund, believed to be the main mechanism behind the onset of the LS stage. The outlets/inlets at Øresund and Great Belt widened and became deeper, resulting in greater flow of increasingly saline water (Fig. F6). Maximum postglacial salinity was reached at ~6 k.y. BP (e.g., Westman and Sohlenius, 1999). Gustafsson and Westman (2002) proposed, based on model calculations, that the salinity variations during the last ~8 k.y. BP are only partly explained by changes in the morphology and depths of the sills in the inlet area. They suggest that a major cause of the salinity changes may have been variation in the freshwater input to the basin. It was demonstrated that the freshwater supply to the basin may have been 15%–60% lower than at present during the phase of maximum salinity around 6 k.y. BP. Climate-driven long-term freshwater discharge variability may also have been an important factor controlling salinity and stratification, hence the distribution of hypoxia in the Baltic Sea during the last ~8 k.y. (Zillén et al., 2008). Periods of deepwater hypoxia in the open Baltic Basin are evident in the sediment record as extended sections of laminated sediment (Sohlenius and Westman, 1998; Zillén et al., 2008). These are considered a direct result of this salinity stratification together with increased primary production. Increased upward transport of nutrients from the anoxic bottom water has been suggested as an explanation for the enhanced primary productivity at the Ancylus–Littorina stage transition (Sohlenius et al., 1996). The LS experienced a sustained period of hypoxia between 8 and 4 k.y. BP (Zillén et al., 2008). The inflowing marine water in the Baltic Sea probably caused the release of phosphorus from the sediments, thereby enhancing the growth of nitrogen-fixing cyanobacteria (Bianchi et al., 2000; Borgendahl and Westman, 2007; Kunzendorf et al., 2001).

Because of dating uncertainties of reworked "old" carbon in the sediment, it has not been possible to absolutely date the transition from fresh to brackish water. In general, ^{14}C dates between 8.5 and 8 k.y. BP are very common for the onset of this shift in salinity and sedimentary regime (Sohlenius et al., 1996; Sohlenius and Westman, 1998; Andrén et al., 2000a). However, an optically stimulated luminescence (OSL)-based age-depth model presented by Kortekas et al. (2007) suggests an age of 6.5 k.y. BP for the same shift in the Arkona Basin. ^{14}C ages of both bulk sediment and bivalves from the same core give ages older than the OSL ages yet younger than the expected ^{14}C age of 8.5–8 k.y. BP. As diatom analyses were not carried out by Kortekas et al. (2007), it may be that the shift dated was not the same as that determined in the other studies.

A climatic event at 8.2 k.y. BP has been recognized in both marine and terrestrial records from northern

Europe (e.g., Alley et al., 1997; Klitgaard-Kristensen et al., 1998; Tinner and Lotter, 2001; Snowball et al., 2002). A drift gyttja layer dated to 8.2–8.1 k.y. BP from coastal sites in the Blekinge area in the southern BSB has been interpreted as representative of a regional catastrophic event, possibly the result of disturbance in the climate regime in the North Atlantic region (Berglund et al., 2005). In the central Bornholm Basin, a similar stratigraphic unit is recorded and dated to ~8.0 k.y. BP. As it is associated with a hiatus, the dating is uncertain (Andrén et al., 2000b; Andrén and Andrén, 2001), but it may be related to the drift gyttja layer in the Blekinge area and the associated catastrophic event. The full consequence of the short climatic cooling during the 8.2–8.1 k.y. BP event in the BSB is presently not well understood.

The present Baltic Sea

Around 6–5 k.y. BP, the eustatic sea level rise gradually ceased and the remaining slow rebound resulted in shallowing of the Øresund and Great Belt Strait and decreased salinities in the BSB. There have been several attempts to estimate the paleosalinity of the Baltic Basin, for example that of Gustafsson and Westman (2002). They use the presence or absence of mollusks and a silicoflagellate species to infer different salinity intervals of the last 8 k.y. Using stable carbon isotopes, Emeis et al. (2003) reconstruct Baltic salinity fluctuations throughout the Holocene. However, a comparison of these two salinity reconstructions (Zillén et al., 2008) shows large discrepancies. The reconstruction by Gustafsson and Westman (2002) shows decreasing salinity following a maximum value between 5 and 6 k.y. BP, whereas the study by Emeis et al. (2003) suggests increasing salinity during the last 2 k.y. Using the strontium isotopic ratio in carbonate mollusk shells, Widerlund and Andersson (2006) infer paleosalinity and quantified salinity with a precision greater than ±5%. A drawback with the method, however, is that it can only be used when carbonate shells are preserved in the sediments. Donner et al. (1999) suggest salinity ~4 higher than present in the coastal areas of the Gulf of Finland and the Gulf of Bothnia between ~7.5 and 4.5 k.y. BP based on the $^{18}O/^{16}O$ ratio in mollusk shells.

After ~4 k.y. BP, salinity decreased and oxygen conditions improved considerably in the bottom waters (Gustafsson and Westman, 2002). This coincided with the onset of the neoglaciation in northern Europe with a more humid and cold climate (Snowball et al., 2004). Such a decrease in salinity may be the result of a shift to colder and wetter conditions, which probably increased the net precipitation in the watershed, leading to increased freshwater supplies to the basin (Gustafsson and Westman, 2002). This scenario, in combination with increased wind stress over the Baltic Sea, would lead to more efficient exchange of oxygen across the halocline because of a weakened halocline and enhanced vertical mixing (Conley et al., 2002). This scenario would also explain the reduction of the hypoxic zone around 4 k.y. BP as a result of more oxic bottom water conditions (Zillén et al., 2008).

The causes for widespread hypoxia during the middle–late Littorina Sea stage of Baltic Sea history are not fully understood, but the fact that it occurred simultaneously with the growing population around the Baltic Basin may indicate forcing via eutrophication as a result of increased anthropogenic influence. Population growth and large-scale changes in land use that occurred in the Baltic Sea watershed during the Medieval Period between AD 750 and 1300 has been suggested as a triggering mechanism behind the expansion of hypoxia at that time (Zillén et al., 2008; Zillén and Conley, 2010). Alternative hypotheses suggest that the development of hypoxia in the open Baltic Sea over the past 1000 y is mainly driven by the climate system (e.g., Kabel et al., 2012). It is therefore likely that the late record of hypoxia in the Baltic Sea may be a result of multiple stressors, the interaction of climatic and anthropogenic influences.

Around the turn of the last century, hypoxia again appeared in the Baltic Sea recorded as laminated sediments deeper than 150 meters below seafloor (mbsf) in the Eastern Gotland Basin (Hille et al., 2006). This period corresponds to the onset of the Industrial Revolution when the European population size increased rapidly (about six-fold since AD 1800) and great technological advances took place in agriculture and forestry (Zillén and Conley, 2010). It also correlates with climate warming that has lasted most of the twentieth century. The present-day eutrophication (e.g., Elmgren, 2001) may be partly explained by the ongoing climate warming (Andrén et al., 2000a; Leipe et al., 2008). Superimposed on this climate warming are the effects of increased nutrient discharge related to a growing population and the intensive use of synthetic fertilizers on arable land after World War II (Elmgren, 1989). It is a major scientific challenge for the future to understand and predict the interactions between climate and anthropogenic forcing on the Baltic Sea ecosystem.

Microbial life in the Baltic seabed

The Baltic seabed holds a record of past biota of plants and animals that lived in the BSB ecosystem or in the surrounding catchment area. The fossil re-

mains are evidence of strong changes in the living communities that resulted from shifts in climate and environment during the glacial–interglacial history. The seabed also harbors extant communities of living microorganisms that thrive on fossil organic matter that is now buried deeply beneath the seafloor.

Such microorganisms have been found abundantly tens to hundreds of meters deep in the sediments of the worlds' oceans, with total numbers that equal those of all microorganisms in the water column (Kallmeyer et al., 2012) (Fig. F7). These microorganisms play a key role in the slow degradation of organic matter and remineralization of nutrients. With increasing depth and age of the deposits, the remaining organic matter becomes increasingly recalcitrant and the availability of nutrients and energy for the microorganisms becomes very low. The combination of large microbial communities and very low carbon flux means that the individual cells gain little energy and therefore have correspondingly slow growth and long generation times of hundreds to thousands of years (D'Hondt et al., 2004; Parkes et al., 2005; Biddle et al., 2006; Hoehler and Jørgensen, 2013).

Many fundamental questions remain before we understand the life of these microorganisms in the deep subseafloor biosphere. It is not understood whether the deep biosphere is inhabited by a unique community of organisms that are specifically adapted to this mode of life under apparent long-term starvation. It is also not understood whether the diversity of microorganisms from past sediment surfaces still dominates the microbial biome after they have been buried for thousands of years, thus remaining as a "paleome" from former times (Inagaki et al., 2005).

The BSB provides unique possibilities to address these and many other questions. In contrast to most other sediments cored during IODP, the surface environment of the BSB has changed dramatically over its glacial–interglacial history so that the abundance and diversity of the buried microbial communities can now be related to both the present and the past environment.

Scientific objectives

The scientific objectives of Expedition 347, Baltic Sea Paleoenvironment, can be summarized with four overarching themes.

Theme 1: climate and sea level dynamics of MIS 5

Deposits from the last interglacial (Eemian, MIS 5e; ~130–115 k.y. BP) have been described from a number of marine and terrestrial sites, but the interglacial is only partly documented in the NGRIP ice core (North Greenland Ice Core Project Members, 2004). A land-sea correlation of European pollen zones and marine isotope stages was presented for the first time by Sánchez Goñi et al. (1999), who demonstrate a delay between the beginning of MIS 5e and the European terrestrial Eemian (discussed by Kukla et al., 2002). High-resolution Eemian marine shelf records (here correlated with MIS 5e) from northern Europe are, however, very scarce and usually contain only fragmented paleoenvironmental information. The same is valid for the early Weichselian stadials and interstadials (MIS 5d–MIS 5a) that were captured in the NGRIP ice core.

Data from marine sediments in the Nordic Seas show three substantial sea-surface temperature fluctuations during MIS 5e (Fronval and Jansen, 1996). The study implies that the last interglacial at high northern latitudes was characterized by rapid changes in Polar Front movement, ocean circulation, and oceanic heat fluxes. This may have resulted in appreciable temperature changes in neighboring land areas, which differs from Holocene climate development, with only minor fluctuations on a general cooling trend.

From onshore Eemian (MIS 5e) records, we know that the BSB Eemian began with a lacustrine phase covering ~300 y before marine conditions were established (Kristensen and Knudsen, 2006). Higher mean sea-surface and sea bottom temperatures (~6°C) and salinities (~15) than today characterized the first ~4 k.y. of the Eemian Baltic Sea (Kristensen and Knudsen, 2006; Funder et al., 2002). During the first 2–2.5 k.y., a pathway existed between the Baltic Basin and the Barents Sea through Karelia, but the degree to which this was important for the general ocean circulation and the climate of northern Europe is debatable (Funder et al., 2002). The circulation pattern and high salinities may have created strong salinity stratification and the development of a permanent halocline, resulting in hypoxic bottom conditions during a large part of the Eemian. This hypoxia would simulate conditions similar to those developed in the Baltic Sea during the last 8000 y. Also, the difference between the warm and well-ventilated southwestern Eemian BSB and the cold, stagnant conditions of its easternmost parts implies that the ocean–continental climate gradient from west to east in northern Europe was steeper than during the Holocene (Funder et al., 2002). After ~6 k.y. of the interglacial, the Eemian Baltic Sea was characterized by a falling sea level and decreased salinity, as observed in diatom and foraminifer records (Eiríksson et al., 2006; Kristensen and Knudsen, 2006), but its

further development during the subsequent MIS 5 stadials and interstadials is largely unknown.

Theme-specific scientific objectives

Scientific objectives specific to this theme are as follows:

- To increase our understanding of the climate system and the sea level dynamics of the last interglacial, including the climatic oscillations at the transition between MIS 6 and MIS 5e and during the initial, climatically oscillating part of the latest glacial (MIS 5d–MIS 5a).
- To better understand the links between oceanic and terrestrial climate systems, including ocean circulation patterns, during the highly variable MIS 5.
- To analyze environmental conditions during the warmest interval of MIS 5e to elucidate a possible future scenario with respect to a warmer climate and higher sea level.
- To understand how the anthropogenically unaffected Eemian (MIS 5e) Baltic Sea ecosystem responded to different environmental forcing factors to distinguish anthropogenic factors from natural driving mechanisms behind presently threatened semienclosed basin environments and ecosystems.

Theme 2: complexities of the latest glacial, MIS 4–MIS 2

Since the confirmation of high climate variability during the latest glacial in the MIS 4–MIS 2 interval from the GRIP and Greenland Ice Sheet Project 2 ice core records (Johnsen et al., 1992; Grootes et al., 1993), paleoclimatologists have been presented with several corresponding records, both from the marine and terrestrial North Atlantic margins (Rasmussen et al., 1997; Dickson et al., 2008; Grimm et al., 2006; Wohlfarth et al., 2008). The huge ice sheets in Eurasia—of which the SIS was the largest—and North America played major roles in this high degree of climatic variability. The impact of sea ice and icebergs (e.g., Dokken et al., 2003), as well as glacial advances and retreats, upon the North Atlantic marine system because of their interaction with MOC suggests they were key influences on the variable climate pattern of the latest glacial. The direct effects of this variability were best registered in areas proximal to the ice sheets. It is therefore essential to gather modern and detailed stratigraphic information from the "sediment trap areas" of these two main glaciated regions, of which the Baltic Basin is the main one for the SIS, to decipher, date, and analyze the recurrent stages of ice-covered and ice-free conditions.

Only fragments of the Baltic glacial history are known. However, we do know that a Baltic glacial event occurred during MIS 4 as recorded in sediments from northwestern Finland at ~64°N (Salonen et al., 2007), whereas the first Baltic ice lobe advance into Denmark is dated to ~55–50 k.y. BP (MIS 3) (Houmark-Nielsen, 2007). It is likely that freshwater lakes covered the deeper subbasins of the central and southern BSB until at least 60 k.y. BP, when the sea level was >50 m lower than today (Lambeck and Chappell, 2001; Siddall et al., 2003). The Hanö Bay, the Bornholm Basin, and the Landsort Deep acted as depocenters for several tens of millennia (~40–60 ka) through the first half of the latest glacial. The BSB also experienced a dynamic and variable glacial–interstadial development during the remaining parts of the glacial.

We have several indications that the southern Baltic may contain relatively complete stratigraphies of MIS 3. From detailed correlations and dating of southwestern Baltic glacial stratigraphies (Houmark-Nielsen and Kjær, 2003; Houmark-Nielsen, 2007, 2008), it is concluded that the southwestern Baltic experienced two major ice advances during MIS 3, at ~50 and 30 k.y. BP. However, the latter is highly debated (Kjellström et al., 2010), as well as the general asynchroneity of MIS 3 ice advances at the western margin of the SIS (Mangerud, 2004) compared to the ice margins in the south (Houmark-Nielsen et al., 2005). This enigmatic period between ~50 and 25 k.y. BP, with its partly incompatible records, is followed by complex glaciation in the southern BSB (Houmark-Nielsen and Kjær, 2003) leading up to the LGM. Furthermore, previous offshore studies in the southern Baltic have documented the presence of marine-brackish sediments, dated to MIS 3 or older, that were overridden by a glacier (Klingberg, 1998) at Kriegers Flak (Fig. **F1**) and two varved clay sequences—the upper one dating from the last deglaciation—separated by an organic-rich layer dated to >35 k.y. ^{14}C BP (bulk date) in Hanö Bay (Björck et al., 1990). Also, and maybe even more significant, an ongoing study of the shallow Kriegers Flak area shows a surprisingly complex stratigraphy with a variety of lithologic units, including gravel-sand-silt, clays of glaciolacustrine and brackish origin, interstadial lacustrine gyttja (lake mud), and peat with ages of 39 and 41 k.y. BP sandwiched between several glacial diamicts (Anjar et al., 2010).

A complicating and key factor for BSB history is the geographic location and altitude (in relation to sea level) of the critical threshold or "gateway" between

the open ocean and the BSB, which determines whether and how much oceanic water can enter the BSB. Today, the two main thresholds are the Øresund (–7 m) and the Great Belt (approximately –20 m). However, the bedrock threshold of the BSB is today situated 60 m below sea level and is located in the buried Alnarp-Esrum bedrock valley, which runs through southwestern Skåne in Sweden and northernmost Själland in Denmark, 120 km long and 6 km wide (Fig. F1). From deep cores taken in the 1970s from this main aquifer, fluvial and lacustrine sediment units were ^{14}C dated. The ages summarized by Anjar et al. (2010) imply that the valley was sediment filled during the later part of MIS 3. The valley thus served as an outlet river for the complete BSB until it was filled up by sediments. Clearly, the age of this last infilling is crucial for the younger sedimentary history of the basin, including the relationship between sea level and the BSB during MIS 3. Analysis of 128 cores acquired for planning of the Kriegers Flak windmill park indicates that complex stratigraphies occur in this shallow part of the BSB, but the records remain incomplete (Anjar et al., 2010). These results imply that the nearby deep basins of Bornholm Basin and Hanö Bay may hold more complete stratigraphies. The >35 k.y. ^{14}C BP organic mud between two units of undisturbed varved clay in Hanö Bay shows that this basin contains long records of sedimentation history, which is also supported by seismic data. These subbasins are controlled by bedrock topography and may potentially contain better preserved pre-LGM sediment records in comparison with other deep subbasins carved out by the youngest glacial ice streams. In these cases, older sediments have been stripped off and redeposited as arcuate end moraines along the Baltic coasts.

Theme-specific scientific objectives

We hypothesize that deeper bedrock-controlled basins in the southern BSB were left largely untouched by the erosive powers of surging glaciers, a hypothesis supported by the Kriegers Flak and Hanö Bay records. By combining shallow offshore drilling and land-based stratigraphy around the southern Baltic with more complete sedimentary archives in the two deep basins of the southern BSB, we will be able to address the following crucial scientific objectives:

- To understand the SIS response, in time and space, to North Atlantic climate forcing during the latest glacial event and to what extent SIS dynamics had an impact on the North Atlantic climate system.
- To determine the feedbacks between the water body of the BSB, the SIS, and the North Atlantic circulation.
- To decipher to what degree the glacial oscillations of the SIS margin were synchronous on both sides of the main ice divide, centered along the Scandinavian Mountain Chain, and whether the advances into the southern BSB can be recognized as large-scale surges.
- To investigate whether the substantial ice advances into the southernmost BSB occurred because they were triggered by rapid North Atlantic warming periods that paved the way for Heinrich events or whether large parts of the BSB were ice free during most of MIS 3.
- To understand more comprehensively how well the highly oscillating climate pattern of MIS 3 at the northeast margin of the North Atlantic was recorded as long and continuous buried sediment sequences in the BSB and to enhance our knowledge on how this huge drainage area reacts to these large-scale circulation changes. The southern BSB may hold unique archives of this time period, as many large rivers drain into the basin, therefore making these archives relevant on a semicontinental basis.
- To better constrain the model of the SIS with its global and regional isostatic and eustatic impacts. This requires better knowledge of glaciation chronology and dynamics and of the BSB threshold history; long archives of this development are believed to exist at some of the proposed drill sites.

Theme 3: deglacial and Holocene (MIS 2–MIS 1) climate forcing

Deglaciation of the southern BSB between 22 and 16 k.y. BP was complex, with major deglacial phases interrupted by some intriguing stillstands and re-advances (Houmark-Nielsen and Kjær, 2003), possibly as surges. Near-complete varved sedimentary records of this dynamic period may be found in the basin of Hanö Bay and Bornholm Basin. Low-lying areas were dammed in front of the retreating ice margin, forming the BIL, and huge amounts of freshwater were released into the North Atlantic during this dynamic phase of the deglaciation between ~16 and 11.7 k.y. BP (Gyldenholm et al., 1993; Björck, 1995; Majoran and Nordberg, 1997; Jiang et al., 1998). During the final drainage of the BIL at ~11.7 k.y. BP, almost 8000 km^3 of freshwater was released rapidly into the North Atlantic (Jakobsson et al., 2007). However, the effects on North Atlantic thermohaline circulation may only have been minor (Andrén et al., 2002). It has also been suggested that this freshwater release may have triggered the Preboreal oscillation (Björck et al., 1996), as well as ice advances in northern Nor-

way (Hald and Hagen, 1998). Earlier studies have suggested that the Younger Dryas cold period was caused by freshwater runoff from the Laurentide (American) ice sheet (Marshall and Clark, 1999), but the influence of the Baltic region has not been studied in detail. The oceanographic effects of the drainage should be detectable in varved sediments at the Anholt Loch site.

At ~10 k.y. BP, the complete BSB was deglaciated. During the course of deglaciation, varved glacial clay was deposited in front of the retreating ice sheet. This record has been used to date the ice recession and postglacial events; varves are still being deposited in the Ångermanälven River estuary, providing a link to present time (Cato, 1985). Although we know that this long varve series should contain at least 10,000 varve years in the estuary, it has not been possible to explore the potential of this record. We know that correlation exists between maximum daily discharge and mean varve thickness during the last 2000 y in the Ångermanälven River (Sander et al., 2002).

Because of the region's geographic location, it is possible to use these unique laminated sediment archives to reconstruct atmospheric (e.g., shifts in NAO and AO variability) and oceanic (e.g., effects of changes in the strength of MOC) circulation patterns during the Holocene. These patterns might also reflect changes in Equator-to-pole teleconnections (e.g., in El Niño Southern Oscillation) related variability. In addition, the site reflects the precipitation records over a wide area and helps to integrate the abundant lake record data available.

Laminated sediments are used as a proxy for hypoxic bottom water conditions and are formed during periods with strong permanent salinity stratification, probably as a result of increased evaporation/decreased precipitation and possibly also by enhanced primary productivity. Laminated sediments in the deep basins of the Baltic Sea (e.g., Andrén et al., 2000b; Zillén et al., 2008) indicate that the open Baltic Sea ecosystem has experienced several regime shifts during its environmental history. These high-resolution sediment records provide an excellent archive to study long-term patterns such as atmospheric circulation (similar to the variability of the NAO, its trend and strength) during the Holocene.

Precipitation and evaporation are critical parameters for understanding the function of the ecosystems of the Baltic Sea, as they affect salinity through dilution, vertical mixing, and river inflow. These parameters are closely related to changes in atmospheric circulation, which modify the inflow of saline waters. Salinity (together with temperature) determines stratification and thus controls the extent of hypoxia and the "health" of the ecosystem in this enclosed sea.

The sensitivity of the BSB system to changes in sea level/salinity, productivity, hydrology/river discharge, and atmospheric circulation is a well-known fact (Zillén et al., 2008). The south–north transect of Baltic Sea sites for Expedition 347 will allow detailed reconstruction of Holocene hydrologic and climatic changes influencing the whole BSB, as well as a detailed exploration of the underlying mechanisms of change.

Theme-specific scientific objectives

Scientific objectives specific to this theme are as follows:

- To understand the details of the climate evolution and associated forcing mechanisms in northwestern Europe during the deglacial phase and the Holocene (MIS 2–MIS 1), as deduced from a north–south transect of Baltic subbasins with ultrahigh time resolution.
- To determine the main mechanisms behind hypoxia-driving processes in the Baltic and to what degree human activities have played a role.
- To investigate how Baltic inflow and outflow have varied over time and how this variation is related to changes in large-scale atmospheric circulation and changing sea levels (threshold depths).
- To detect more specifically whether there is a solar forcing signal in the melting record of a shrinking ice sheet (glacial varves at Site M0063) or in the precipitation-related fluvial system (postglacial varves at Sites M0061 and M0062).
- To reconstruct the river discharge (and thereby also precipitation), with annual resolution, several millennia back in time.
- To understand how the general precipitation pattern, which is linked to the dominating AO/NAO system over the North Atlantic and circum-Arctic region, changes over the Holocene (Sites M0061 and M0062).
- To check whether there are periodicities in these changes and, if so, how they are linked to the large-scale isolation trends.

Theme 4: the deep biosphere in Baltic Sea Basin sediments

The discovery of microorganisms in deep subsurface sedimentary deposits, and even in basement rock, has profoundly changed our perspective on the limits of living organisms on our planet (Parkes et al., 1994, 2005; D'Hondt et al., 2004; Jørgensen et al., 2006). Although concealed in the subsurface, the

deep biosphere is an important global component in the long-term biological cycling of carbon and nutrients and for the chemistry of the oceans and atmosphere. The current database on prokaryotic cells in deep sediment cores indicates that the marine deep biosphere may comprise half of all microorganisms in the ocean (Kallmeyer et al., 2012). Population densities in the oceanic seabed are 10^4–10^7 cells/cm^3 to >1500 m sediment depth (Roussel et al., 2008), densities that are greater than those found in ocean water. Understanding the minimum energy requirements for growth and survival may offer a means of interpreting the distribution, composition, and activity of these deeply buried communities (cf. Hoehler, 2004; Jackson and McInerney, 2002; Hoehler and Jørgensen, 2013). With increasing depth and age of marine sediments, microbial cells become increasingly energy limited (D'Hondt et al., 2002, 2004; Schippers et al., 2005; Biddle et al., 2006). However, they maintain complex functions at an energy flux that barely allows cell growth over many years. It has been proposed that these deeply buried communities are relics of a time when the sediment was originally deposited (Inagaki et al., 2005). If this is the case, then they may still reflect the past oceanographic conditions, in particular whether the sediment was deposited under marine or limnic conditions, high or low burial rates of organic material, or high or low concentrations of oxygen.

Theme-specific scientific objectives

Scientific objectives specific to this theme are as follows:

- To understand how the environmental and depositional history of the Baltic Sea system through glacial–interglacial transitions has altered microbial communities.
- To analyze microbiological and biogeochemical responses to major shifts (1) between limnic, brackish, and marine phases and (2) between high and low deposition of terrestrial versus marine organic and clastic material.
- To understand how microbial processes in subsurface sediments control the mineralization of buried organic matter, the release of nutrients, and the formation of methane.

Site summaries

Little Belt (Sites M0059 and M0067)

Site M0059 (proposed Site BSB-3B; 55°0.29′N, 10°6.49′E) is situated in the southern Little Belt at a water depth of 35 m, and Site M0067 (proposed Site BSB-4B; 55°08.14′N,09°48.03′E) is situated farther north in the Little Belt at a water depth of 23 m (Fig. F1). Seismic studies of the western BSB, east of Als, have revealed an exceptionally thick accumulation of Quaternary sediments in deep valleys and basins running parallel to the coast. It was proposed that the almost complete Eemian interglacial succession found exposed at Mommark on Als may have been originally related to the deposit found within a deep Quaternary channel that runs along the eastern coast of Als. Subsequent glacial activity may have transported this sequence to the west-northwest.

The kilometer-wide incised valley, which in places reaches 200 mbsf, expresses an erosional unconformity. It was suggested that the valley infill included a thick MIS 5e (Eemian interglacial) succession. This interpretation was partly based on the occurrence of slices of dislocated MIS 5e sediments in the coastal areas around the western BSB and partly on direct evidence from wells penetrating a similar valley infill. One example of such a well is located close to the end of an incised valley in the Åbenrå Fjord, northwest of Als.

The aim of drilling in the central part of one of the deep incised valleys east of Als was to obtain an extremely high resolution MIS 5e record, providing a similar sequence to the Mommark section but thicker, more complete, and still in situ.

To ensure an undisturbed sediment sequence from the Eemian, two sites were proposed at this location. Both were identified as primary sites, as there was a risk that methane gas would occur in parts of the Quaternary sediment sequence, possibly preventing coring reaching the target depth at one of the sites. Of these two sites, Site M0059 was the primary objective (Figs. F8, F9).

Site M0067 (Figs. F10, F11), located north of Site M0059 in the same deep valley, was expected to contain a similar stratigraphy as a nearby terrestrial site studied by well drilling at Ensted, which indicated the presence of Eemian deposits (Eiríksson et al., 2006).

Anholt Loch (Site M0060)

Site M0060 (proposed Site BSB-1; 56°37.21′N, 11°40.24′E) is situated in the Kattegat at a water depth of 34 m (Figs. F12, F13). On the basis of a rather coarse grid of seismic lines (Fig. F14), an erosional valley was mapped southeast of Anholt Island in the Kattegat Sea (Fig. F15). The valley is ~25 km long and ~2 km wide, is oriented northwest to southeast, and was probably formed by subglacial meltwater erosion during repeated glaciations in the early and middle Quaternary. The distance from the seafloor to the valley bottom is 200–300 m. The stra-

tigraphy from a well boring on Anholt in the vicinity of the proposed drill site suggests that the valley was infilled by a sequence from MIS 6, MIS 5e, and MIS 3 (Lykke-Andersen et al., 1993). Based on later Boomer profiles and shallow cores, the younger parts of the infill were referred to as late glacial and Holocene age (MIS 2–MIS 1; Jensen et al., 2002). The area was inundated by the SIS during the LGM, but according to the most recent seismic profiles, this inundation did not lead to disturbances of the sequence in the Anholt region. Therefore, because the valley acted as a sediment trap and later disturbance was minimal, it was expected to contain an unusually complete sequence of sediments from the last interglacial–glacial cycle (Fig. F16), as well as a deglacial–Holocene sequence that would be valuable in establishing linkage between the BSB and the open Atlantic oceanic systems.

Ångermanälven River estuary (Sites M0061 and M0062)

Site M0061 (proposed Site BSB-10; 62°46.70′N, 18°02.95′E) is situated near the mouth of the estuary at a water depth of 86 m, and Site M0062 (proposed Site BSB-11; 62°57.35′N, 17°47.70′E) is situated farther into the estuary at a water depth of 68 m. In the Ångermanälven River estuary, it has been proposed that varves have been deposited during the last 10,000 y and that they are still being deposited. Varve thicknesses in open sections along the river valley have been measured, and varve diagrams have been cross-correlated to a local varve chronology, which is in turn correlated to the Swedish late glacial varve chronology, together constituting the so-called Swedish Time Scale (STS). No scientific drilling has been performed previously in the estuary, but short piston cores indicated a sediment accumulation rate of 5–10 mm/y during the early Holocene.

The target area for Site M0061 was surveyed north of Härnösand in the easternmost part of Ångermanälven (Figs. F17, F18). The surveyed area contains a suitable location for drilling where an apparently undisturbed sediment section fills a trough and reaches a thickness of >40 ms two-way traveltime (>30 m assuming a sound velocity of 1500 m/s) (Fig. F19). The sediment thickness appears to exceed the limit of the CHIRP sonar used in the survey. The proposed site is located on Profile 71021235, which ends 34 m southwest of the proposed site and provides a proximal perpendicular view of the proposed site geometry (Fig. F17).

Site M0062 is located close to the town of Kramfors and has the purpose of connecting the clay varve series from Site M0061 with the modern varves in Ångermanälven (Figs. F20, F21). Cross-correlation between this site and Site M0061 should further strengthen the varve chronology, as some varves may be missing when analyzing only one site. It should also strengthen the correlation of the varve records to the STS, which is needed in order to achieve true calendar-year accuracy in the dating. This site was moved ~50 m along Profile 71021706 in order to avoid some apparent undulations in the acoustic stratigraphy at the exact location of the crossing between this profile and Profile 71021606 (Figs. F20, F22).

Landsort Deep (Site M0063)

Site M0063 (proposed Site BSB-9; 58°37.34′N, 18°15.25′E) is situated in the central part of the Landsort Deep at a water depth of 451 m. The Landsort Deep is the deepest basin in the BSB, and its geometry makes it an excellent "sediment trap," protecting the sediments from subsequent glacial erosion. Furthermore, its location just south of the postulated margins of the early Weichselian glacial advances (MIS 5d and MIS 5b) made it particularly promising for registering the early Weichselian development of the BSB. It also displays an expanded late Weichselian and Holocene sediment sequence.

A 20 inch^3 par air gun was used together with a 50 m long single-channel streamer to collect Profiles 68170648 and 68161201, which run along the axis of (Fig. F23) or cross (Fig. F24) the Landsort Deep. The seismic reflection data acquired clearly show the most suitable drilling target selected for the purpose of recovering the longest undisturbed postglacial (possibly partly deglacial) sequence. From Profile 68161201 (Fig. F25), it is evident that the uppermost horizontally stratified sediment layer thickens toward the center of the depression. Assuming a sediment sound speed of 1500 m/s, the sediment section is ~122 m thick at the thickest part in Profile 68170648. This profile is intersected by Profile 68161201. This intersection provides an acoustically well constrained drilling target at a location in the Landsort Deep where the sediment section appears to reach the maximum thickness in the area and where there are no signs of erosion or other disturbances in the acoustic data.

Hanö Bay and Bornholm Basin (Sites M0064, M0065, and M0066)

Site M0064 (proposed Site BSB-5; 55°43.27′N, 15°13.59′E) is situated in the Hanö Bay off the south coast of Sweden at a water depth of 61 m (Figs. F26, F27). Based on information from a short piston core and the radiocarbon age of its lowermost part (26 k.y. uncorrected radiocarbon years; T. Andrén, un-

publ. data), Site M0064 was included in the presite survey. The seismic profiles around Site M0064 indicated the possible occurrence of a thick, relatively transparent sequence of sediments with some internal reflectors below a relatively thin till cover of late Weichselian age (Fig. F28). Previous offshore studies in the southern Baltic have documented the presence of marine brackish sediments, dated to MIS 3 or older, that were overridden by a glacier (Klingberg, 1998) at Kriegers Flak, along with two varved clay sequences—the upper one dating from the last deglaciation—separated by an organic-rich layer dated to older than 35 k.y. ^{14}C BP (bulk date) in Hanö Bay (Björck et al., 1990). The lower unit could therefore be of Eemian or early or mid-Weichselian age.

In the Bornholm Basin, Site M0065 (proposed Site BSB-7C; 55°28.09′N, 15°28.63′E) is situated northeast of the island Bornholm at a water depth of 87 m, and nearby Site M0066 (proposed Site BSB-7D; 55°27.77′N, 15°29.56′E) is situated at a water depth of 87 m (Fig. F29). The area of Site M0065 is covered by ~10 m of Holocene mud and clay (Fig. F30), whereas the area of Site M0066 has no distinct Holocene sequence. During the seismic survey, pockets of sediments below late Weichselian till and Holocene mud were discovered in the deeper part of the Bornholm Basin. These sediments were probably deposited in the lake that occupied the southern Baltic Basin from the Eemian interglacial up to the last Weichselian ice advance over the area. We included the two sites (Figs. F29, F30, F31) in the proposal because they could give a unique opportunity to study the development of this lake in two different types of settings, the shallow coastal setting in the Hanö Bay area (Site M0064) at a water depth of 61 m and the deep lake setting at a water depth of 87 m in the Bornholm Basin at Site M0065.

Operational strategy

Based on seismic and bathymetric data acquired during the site survey process and historical data from previous research in the BSB, seven primary drill sites and six alternate sites were proposed for paleoenvironmental objectives. Four of the primary sites were also proposed for deep biosphere investigations (Sites M0059, M0060, M0063, and M0065). Following assessment by the IODP Environmental Protection and Safety Panel, one of the primary sites (proposed Site BSB-8) was rejected because of a risk of contamination from dumped WWII chemical munitions. Instead, the alternates for this location (proposed Sites BSB-7C and BSB-7D) were approved, with the proviso that the closest alternate (Site M0065, proposed Site BSB-7C) did not core the upper 2 m of sediment to avoid any munitions residue that might have been spread by trawling activity. It was also stipulated that additional personal protective equipment be worn by those on the drill floor for the first core run following the open hole interval. For the primary site in the Ångermanälven River estuary (Site M0062, proposed Site BSB-11), an assessment of heavy metal and other contaminants was also made. As a consequence of this, restrictions on coring the upper 50 cm were put in place, although the site was given approval. Rumohr cores acquired at this location were also subject to more intensive cleaning of the outer liner and coring equipment itself prior to being brought onboard.

At Site M0060 (proposed Site BSB-1), a downpipe camera survey was conducted to assess the seabed for dumped WWII munitions prior to approving the beginning of coring operations. At Sites M0064, M0065 and M0066 (proposed Sites BSB-5, BSB-7C, and BSB-7D, respectively), a remotely operated vehicle survey was conducted at all proposed drilling locations to again survey the seabed for possible dumped munitions and chemical warfare agents from WWII prior to approving coring operations.

All holes were sited within a 20 m radius of the proposed drilling sites approved by the Environmental Protection and Safety Panel. The general locations of the sites cored are shown in Figure F1. As with all Mission Specific Plan expeditions, no cores were split during the offshore phase; therefore, a comprehensive onshore phase complements the offshore phase. Table T3 summarizes the descriptions and measurements made during Expedition 347 and indicates whether these were taken offshore or onshore.

Offshore operations

The following coring tools were carried during Expedition 347:

- Extended coring system (ECS),
- Hammer sampler (HS),
- Noncoring assembly (NCA),
- Nonrotating core barrel (NRCB),
- Rotating core barrel (RCB),
- Push coring assembly (PCA),
- Piston corer system (PCS), and
- A third-party gravity coring system known as a Rumohr Corer.

Mobilization of the vessel began on 30 August 2013 in Falmouth, UK, with the *Greatship Manisha* sailing for Kiel, Germany, on 8 September. The offshore phase ran from 12 September to 1 November, with embarkation/disembarkation of the science party.

The vessel then transited back to Falmouth, with European Consortium for Ocean Research Drilling (ECORD) Science Operator (ESO) staff demobilizing the ESO containerized laboratories and offices en route. The vessel arrived at Falmouth on 5 November, and all ESO staff departed on 6 November.

In total, 37.12 days of Expedition 347 were spent operational on station, 8.5 days in transit between sites, 1.3 days in port, 1.3 days on standby at station because of weather, and 1.8 days on equipment related downtime. See Table **T4** for a summary of the offshore operations and recovery. Please refer to the **"Methods"** chapter (Andrén et al., 2015) for a detailed description of the coring technology and operational methodology and to the "Operations" section at the beginning of each site chapter for a detailed breakdown of operations. Shipboard generated recovery plots are available on the ECORD Baltic Sea Paleoenvironment website under weekly summaries (**www.eso.ecord.org/expeditions/347/daily.php**).

In order to prevent degradation of living microbial samples acquired during the offshore phase, shipment of these samples was organized following completion of drilling operations in Holes M0059C, M0060B, M0063E, and M0065C, with all frozen and +4°C samples being offloaded via small boat and shipped to the scientists' laboratories (via Aarhus University, who kindly collected the samples from the small boat transfers) in Denmark, Germany, Japan, China, and the USA. Frozen (–80°C) and +4°C microbiology samples collected in Hole M0059E were shipped from Kiel to the scientists' laboratories at the end of the expedition.

Onshore Science Party

The cores, core catcher samples, headspace gas samples and interstitial water splits collected offshore were transported under refrigeration to the IODP Bremen Core Repository at the Center for Marine Environmental Sciences (MARUM), University of Bremen (Germany). Natural gamma radiation and thermal conductivity measurements were conducted on cores before the start of the Onshore Science Party (OSP) (see the **"Methods"** chapter [Andrén et al., 2015]).

Further analytical laboratories were accessed at MARUM (nondestructive core logging, marine geotechnics, inorganic geochemistry, and microscope laboratories) and the Department of Geosciences at the University of Bremen (paleomagnetism and hydrofluoric acid laboratories and the carbon/sulfur analysis system).

During the Expedition 347 OSP, from 22 January–20 February 2014, the cores were described in detail and the IODP minimum and some standard measurements were made (Table **T3**). In addition, sampling for postcruise scientific research was also undertaken.

Principal site results

Lithostratigraphy

At Site M0060 in the Anholt Loch, in the Kattegat area, we recovered the thickest stratigraphic succession to 229.5 mbsf. The lowermost stratigraphic units are dominated by clast-poor sandy diamicton with charcoal clasts deposited through mass-transport processes, overlain by fluvial or deltaic sands and a poorly recovered marine mollusk–bearing silty clay with dispersed clasts. The upper part of the succession comprises interbedded sand, silt, clay, and diamicton, as well as laminated clay with dispersed clasts, deposited in an ice-influenced depositional environment. These strata are covered by a thin sand unit containing marine mollusk beds in fining-upward sequences deposited near wave base.

Sites M0059, M0067, M0063, M0064, M0065, and M0066 in the Baltic Sea recovered different thicknesses of a deglacial sequence. This sequence comprises a diamicton or sand unit at the base, overlain by up to 45 m of both massive and laminated glacial lake clays with rhythmic laminations, convolute bedding, and intraclasts. The clays are unaffected by bioturbation, and the rhythmic laminae are interpreted as varves. Between 2 and 35 m of greenish black clay was deposited at the top at each site. Some intervals of greenish black clay have characteristic "mat-like" laminations interpreted to represent accumulations of algae through lake-dump events. Other intervals contain marine mollusk fragments and probably represent a brackish-marine depositional environment. Black, presumably iron sulfide intervals are common in this upper part of the succession, and variable intensities of bioturbation were observed.

Sites M0061 and M0062 were cored in the Ångermanälven River estuary. Each site terminated in a sand unit that gradually changes uphole from interbedded sand and silt to rhythmically laminated silty clays with upward-decreasing lamina thickness. Lamina couplet characteristics suggest that rhythmites could be interpreted as varves. At the top of the succession at each site is 8–11 m of greenish black laminated organic clay with meter-scale beds of black iron sulfide concentrations. The stratigraphy

at these sites represents a change from a fluvial or glaciofluvial dominated setting to a glacial lake and finally to an estuarine environment.

The intervals of iron sulfide concentrations in the greenish black clays of the Baltic Sea and the Ångermanälven River estuary are laminated and lack evidence of bioturbation. These sedimentary properties are consistent with sediments deposited in a protected basin with periods of low oxygen to account for the lack of evidence for macrobenthic life and high organic matter deposition as a precursor to iron sulfide formation.

Biostratigraphy

Siliceous microfossils

Site M0059

Diatoms, silicoflagellates, ebridians, and chrysophycean cysts were identified in Hole M0059A. The lowermost samples from Core 347-M0059A-26H (~82.7–83.2 mbsf) contain a mixed freshwater/brackish diatom assemblage. This assemblage is overlain by a series of barren samples, to Core 16H (~50–53 mbsf). Cores 16H and 15H contain a freshwater assemblage dominated by *Aulacoseira* and *Stephanodiscus* taxa. Cores 14H through 1H (~46–0 mbsf) contain a brackish-marine assemblage containing *Chaetoceros*, *Thalassionema*, and *Thalassiosira*. Preservation of opal at Site M0059 is considered to be moderate to good, pending quantitative preservational analysis, based on the presence of lightly silicified taxa and fine structures (i.e., vella) in many intervals.

Site M0060

Diatoms and chrysophycean cysts were identified in Hole M0060A. Cores 347-M0060A-82H through 9H (~203–12 mbsf) contain only rare fragmentary diatom valves and rare chrysophycean cysts. Many of these cores are completely barren. Cores 8H through 6H (~12–6 mbsf) contain a low abundance mixed freshwater/brackish diatom assemblage. Chrysophyte cysts are found only in Core 6H. All samples analyzed from Core 6H were barren. Opal preservation is considered to be moderate, pending further analysis. Diatoms are generally fragmentary, and gracile species are rare.

Site M0061

Diatoms, ebridians, and chrysophycean cysts were identified in Hole M0061A. Cores 347-M0061A-10H through 5H (~25–11 mbsf) are barren of siliceous microfossils, with the exception of Core 6H. Core 6H contains rare diatom valves in one sample. The upper parts of Core 4H and lower sections of Core 3H (~9–7 mbsf) contain a freshwater diatom assemblage, primarily containing *Aulacoseira* and *Stephanodiscus*, as well as epiphytic *Gomphonema* species. This assemblage is overlain by a brackish diatom assemblage in Core 3H containing *Chaetoceros* and *Thalassiosira* species. Cores 2H and 1H contain an estuarine diatom assemblage. This assemblage is diverse, containing *Aulacoseira*, *Cyclotella*, and *Thalassiosira*. Influence of the Ångermanälven River is noted in the diatom assemblage present at Site M0061, especially in Cores 2H and 1H (~4.8–1.5 mbsf), by the presence of periphytic taxa. Sea ice diatoms are noted throughout the diatom-bearing interval. Chrysophycean cysts are found below the diatom-bearing cores, in Cores 7H and 6H (~17.6–11 mbsf). Additional samples were analyzed from Cores 347-M0061B-2H and 3H. A very similar brackish/estuarine assemblage is found in Hole M0061B. Opal preservation is generally considered to be good, pending quantitative analysis, based on the presence of lightly silicified taxa and fine structures.

Site M0062

The siliceous microfossil record from Site M0062 strongly resembles that of Site M0061. One key difference is the lack of ebridians at Site M0062. Hole M0062A, however, shows a stronger influence of the Ångermanälven River. Specifically, Core 347-M0062-13H through the lowermost sections of Core 4H (~35.9–9 mbsf) are barren of siliceous microfossils. Diatoms and chrysophycean cysts are present for the remainder of the analyzed material, from Core 4H to the top of Core 2H (~10–0.5 mbsf). The upper portions of Core 4H and the lower portions of Core 3H contain a freshwater assemblage, which is overlain by a brackish assemblage in Cores 3H and 2H (~7–0.5 mbsf). The upper portions of Core 2H contain a freshwater assemblage strongly influenced by the Ångermanälven River. The diatom taxa seen at Site M0062 are very similar to those recorded at Site M0061.

Site M0063

Sediment samples from Site M0063 contain diatoms, chrysophytes, ebridians, and silicoflagellates. The lower samples analyzed in Hole M0063A, from Core 347-M0063A-36H to the lower sections of Core 15H (~102–42.5 mbsf), are barren of siliceous microfossils. The upper sections of Core 15H contain a low-diversity brackish water assemblage, dominated by *Thalassiosira*. This is overlain by another barren interval from Core 14H through Core 10H (~42.5–26 mbsf). Core 10H contains a freshwater diatom (*Aulacoseira* and *Stephanodiscus*) and chrysophyte-bearing assemblage. This freshwater assemblage is overlain by diverse siliceous microfossil flora containing sili-

coflagellates, chrysophycean cysts, ebridians, and brackish water diatoms, principally from *Chaetoceros*, *Cyclotella*, and *Thalassiosira*. Sea ice–related diatom taxa are common throughout this uppermost brackish interval. Additional samples were analyzed from Holes M0063C and M0063E. In Hole M0063C, samples were analyzed from Core 347-M0063C-22H (42–44 mbsf), and both the lowermost barren interval and the lower brackish *Thalassiosira* interval were identified. In Hole M0063E, samples were analyzed from Cores 347-M0063E-22H through 13H (~44–24 mbsf). The lower barren interval and freshwater interval were identified. Opal preservation is considered to be excellent, pending quantitative analysis, based on the presence of lightly silicified taxa and fine structures.

Site M0064

Only the uppermost sample from Site M0064 from Core 347-M0064A-1H (0–3 mbsf) contained siliceous microfossils. A typical Baltic brackish water diatom assemblage, consisting of diatom taxa primarily from the genera *Chaetoceros*, *Cocconeis*, *Cyclotella*, and *Thalassiosira* was identified. Chrysophycean cysts were also present. The remaining cores were barren of siliceous microfossils.

Site M0065

The siliceous microfossil record from Site M0065 is very similar to that of Site M0063. The lowermost samples analyzed from Hole M0065A were barren of siliceous microfossils, from Cores 347-M0065A-15H through 5H (~46–12 mbsf). The uppermost intervals of Core 5H contain a brackish-freshwater assemblage composed of *Aulacoseira*, *Fragilaria*, *Navicula*, *Stephanodiscus*, and *Thalassiosira*. This is overlain immediately by a low-diversity freshwater flora composed of diatoms from *Aulacosiera* and *Stephanodiscus* and chrysophytes in Core 4H (~12–8.5 mbsf). Cores 3H and 2H (~8.5–2 mbsf) contain a subrecent diatom, silicoflagellate, ebridian, and chrysophyte assemblage typical of the Baltic Sea. This assemblage is composed primarily of *Chaetoceros*, *Dimeregramma*, *Grammatophora*, *Paralia*, and *Thalassiosira* species. Diatom preservation is considered to be generally poor in the brackish interval sections, based on the level of visible corrosion and fragmentation of diatom valves. Preservation is of higher quality in the freshwater sections. Quantitative analysis will follow.

Site M0066

No siliceous microfossils were found in any samples from Site M0066.

Site M0067

Diatoms and silicoflagellates were identified in Hole M0067B. Chrysophytes were also present in Core 347-M0067B-2H only (3–5 mbsf). A typical subrecent Baltic Sea diatom assemblage was recorded from the lower portions of Core 2H to the top of Core 1H. This assemblage contained primarily diatoms from the genera *Actinoptychus*, *Chaetoceros*, *Dimeregramma*, *Diploneis*, *Grammatophora*, *Opephora*, and *Thalassiosira*. Cores 347-M0067A-2H and 1H (4–0 mbsf) were also analyzed, yielding a nearly identical assemblage, which is lacking in chrysophytes. Opal preservation is considered to be good, pending quantitative analysis, based on the preservation of gracile diatom species and fine structures.

Palynology

Sites M0059 and M0067

At Site M0059, the uppermost samples contain well-preserved palynomorphs, whereas samples from greater depths show signs of degradation/oxygenation and contain reworked (partly Tertiary) palynomorphs. Pollen spectra from the uppermost interval reveal a broad-leaf tree pollen succession, known from terrestrial pollen records from the southern Baltic region. High percentages of *Fagus* in the uppermost samples indicate an age younger than ~2.5 ka BP. Mass occurrences of *Gymnodinium* cysts in the uppermost 38 mbsf also imply sub-Atlantic age. High abundances of dinoflagellate cysts point to a marine environment. Between ~35 and 50 mbsf, high percentages of *Ulmus* pollen indicate ages between 9.5 and 6.0 ka BP. A decline in freshwater algae at 49.16 mbsf implies the transition from the Ancylus Lake stage of Baltic Sea history to marine conditions. Samples from lower intervals contain limited in situ pollen and high amounts of reworked Tertiary pollen. Numerous freshwater algae and aquatic insect larvae remains are present at greater depths. Combined, these findings indicate meltwater inflow with redeposition of Tertiary sediments. Results for Site M0067 are similar to those for Site M0059.

Site M0060

Twenty-five sediment samples from Site M0060 were analyzed, but except for the uppermost sample (0.75 mbsf), all analyzed samples indicate a high degree of oxygenation and are characterized by high percentages of bisaccate pollen grains and high amounts of reworked Tertiary pollen. The uppermost sample revealed high pollen concentration and no reworked pollen. The pollen association indicates an early Holocene age for this sample.

Sites M0061 and M0062

A total of 25 samples have been analyzed for the northernmost Sites M0061 and M0062. The uppermost samples contained enough palynomorphs to generate statistically relevant results, whereas samples from greater depths (from silty/sandy sediments) were almost barren of palynomorphs. Pine and birch pollen dominate the assemblages in all samples from the upper parts of the sites. The youngest samples contain spruce pollen in significant amounts, indicating an age of ~3.0 ka BP. The rarity of marine taxa in the upper parts points to a strong terrestrial influence. Nonpollen palynomorphs (algae and insect remains) indicate strong freshwater input or lacustrine conditions for the samples from the upper part of Site M0062. Some samples also contain *Thecamoeba* remains. An older phase is indicated by a pollen spectrum from Site M0062, which may be provisionally ascribed to the onset of the Holocene.

Site M0063

The pollen record from the interval from 0.06 to 39.45 mbsf at Site M0063 indicates a late to mid-Holocene age. Palynomorph frequency and preservation diminishes toward the bottom part of this interval. Analyses of two samples from the lower part resulted in reliable pollen spectra. One sample (56.80 mbsf) may reflect a late glacial interstadial. A pollen assemblage at 66.18 mbsf may point to a late glacial age and suggests a transition from colder, steppe-like landscape to a landscape with pine-birch type of forest.

Site M0064

Most of the palynomorphs in all samples analyzed for Site M0064 have been degraded/oxygenated to a high degree. No sample contained enough palynomorphs in situ to yield statistically relevant data. Reworked dinoflagellate cysts in samples from the lower part are of Paleogene origin.

Sites M0065 and M0066

Among the four examined sediment samples from Sites M0065 and M0066, only the two shallowest, at 2.17 and 8.82 mbsf, are characterized by high pollen concentrations. Relatively high *Quercus*, together with *Picea* percentages, imply a late Atlantic/Subboreal age for these spectra. There may, however, be pollen-transportation bias due to the offshore position of the site.

Foraminifers

Foraminifers in the BSB almost exclusively occur as benthic foraminifers. Planktonic foraminifers are only rarely found in the Kattegat because of a combination of very shallow water depths (average Baltic Sea depth = 54 m) and low salinity. Bottom water salinity is an important factor controlling benthic foraminifer distribution; salinity declines along a transect from the marine Kattegat (salinity ~32) to the brackish Landsort Deep (salinity ~12) and the fresher Ångermanälven River estuary in the Gulf of Bothnia (salinity ~5) (Samuelsson, 1996). Additionally, low oxygen concentrations in the bottom waters of many of the Baltic basins, especially Landsort Deep, may limit the survival of benthic organisms. In general, it seems that higher diversity of benthic foraminiferal species occurring in the sediments corresponds to higher bottom water salinity.

Site M0059

Foraminifers commonly occur at Site M0059 in the Little Belt from the seafloor to 50 mbsf. The assemblage diversity is low with *Elphidium excavatum* dominant and other *Elphidium* species occurring occasionally. This low faunal diversity suggests salinities lower than in the Kattegat but higher than in the Bornholm Basin and the Landsort Deep. A second interval with abundant foraminifers occurs from 80 to 85 mbsf. In addition to the dominant *Elphidium* spp., other species like *Bucella frigida* and *Ammonia beccari* are present, possibly suggesting colder conditions.

Site M0060

Site M0060, located near the island of Anholt in the Kattegat, is the most marine of the sites cored during this expedition, with modern bottom water salinity as high as 32 (Samuelsson, 1996). Very diverse fauna was present in some deeper intervals of Site M0060. The upper part, to ~21 mbsf at Site M0060, however, contains a moderate diversity faunal assemblage often dominated by the genus *Elphidium* (particularly *Elphidium excavatum* f. *clavata*), with *Cassidulina* sp., *Bulimina marginata*, and *Quinqueloculina* sp. occurring in low abundances. The limited diversity and lack of warmer boreal species compared to modern Kattegat fauna (Nordberg and Bergsten, 1988) in all but the uppermost core suggests that only a thin Holocene interval is present. Between 21 and 75 mbsf, low diversity together with the dominance of *E. excavatum* f. *clavata* and *Cassidulina* sp. suggest that a potentially continuous deglacial sequence is present. Below 75 mbsf, two intervals between 2 and 10 m thick occur with diverse faunal assemblages, though they are generally poorly recovered. These assemblages are dominated by *B. marginata* and *Hyalinea balthica*, indicating warmer and more marine conditions possibly similar to today. Although absolute

age determinations have not been established to date, these intervals might be linked to previous interstadials or interglacials.

Site M0061

The occurrence of foraminifers at Site M0061 in the Ångermanälven River estuary is the first record of foraminifers from the Bothnian Bay. Foraminifers were found in an interval between 1.5 and 6 mbsf, and all belonged to the species *Elphidium albiumbilicatum*, which is known for its tolerance of very low salinity conditions (<10; Lutze, 1965). The absence of foraminifers in the most recent part of the record, which has a present-day bottom water salinity of just 5 (Samuelsson, 1996), suggests that conditions were slightly more saline at the time when *E. albiumbilicatum* occurred and can possibly be attributed to the middle Holocene (Widerland and Andersson, 2011).

Site M0062

Foraminifers do not occur at Site M0062, presumably because of the low salinity in this estuarine site today and in the past.

Site M0063

Site M0063 in the Landsort Deep today is characterized by low bottom water oxygen concentrations, which also have occurred to varying degrees throughout the Littorina stage of Baltic Sea history during the Holocene. Foraminifers occur continuously downcore to ~30 mbsf and are often common to abundant to 20 mbsf, suggesting that oxygen levels were generally high enough for subsistence. The harsh conditions are nevertheless reflected in the low diversity of the fauna, which is dominated by opportunistic and stress-tolerant *Elphidium* spp., especially *E. excavatum* f. *clavata* and sometimes *Elphidium excavatum* f. *selseyensis*. The absence of more marine species during the middle Holocene suggests that bottom water salinity likely did not exceed 20 (Miettinen et al., 2014).

Sites M0064–M0066

In the Bornholm Basin and Hanö Bay (Sites M0064–M0066), foraminifers were only present at Site M0065. *Elphidium* spp. is dominant in the upper 12 m of Site M0065 (primarily *Elphidium excavatum clavatum*), but the absolute number of specimens is generally low. As modern conditions in the Bornholm Basin and Hanö Bay are more saline than in the Landsort Deep, the similarity between fauna at Sites M0065 and M0063 suggests that a full Holocene sequence may not have been recovered. This lack of recovery is most likely related to the operational need to open hole the upper 2 m of sediment because of the risk of contamination from dumped chemical munitions.

Site M0067

Site M0067, like Site M0059, is located in Little Belt. The two short holes drilled here contained an interesting foraminiferal assemblage in the upper 4.5 mbsf. Although the sites are located near each other, the assemblage at Site M0067 is significantly different from the one at Site M0059. The uppermost core at this site is dominated by the agglutinated foraminifer *Eggerelloides scaber* (Frenzel et al., 2005), whereas several *Elphidium* spp. and *A. beccarii* dominate the fauna of the lowermost samples.

Ostracods

Ostracods are poorly represented in records from the Baltic Sea, mainly because of significant dissolution of calcareous carapaces in the organic-rich sediments (Frenzel et al., 2010). At the same time, abundant data are available on ostracod assemblages living in the Baltic Sea and on the ecology of the ostracod species (e.g., Elofson, 1941; Rosenfeld, 1977; Frenzel et al., 2010). Baltic Sea bottom water salinity varies greatly from 31 in the Kattegat to values of 7–8 in the southeastern part and 10–12 in the central Baltic (Samuelsson, 1996). The presence of ostracod taxa is dependent on a specific range of environmental parameters such as salinity, temperature, and oxygen, making ostracod assemblage analysis a good instrument for reconstructions of the Baltic Sea paleoenvironments (e.g., Viehberg et al., 2008; Kristensen and Knudsen, 2006).

Site M0059

Ostracods occur at Site M0059 and are most abundant and diverse in the upper 60 mbsf. Variations in composition of ostracod assemblages suggest bottom water salinity changes from freshwater (*Candona* spp.) to brackish-marine conditions with the following characteristic taxa: *Leptocythere* spp., *Palmoconcha* spp., *Cytheropteron latissimum*, and *Sarsicytheridea bradii*. Around 80 mbsf, a different assemblage was recorded, comprising different ecological groups from freshwater to shallow-water marine together with redeposited pre-Quaternary valves, suggesting a high-energy shallow environment.

Site M0060

Site M0060 contains an abundant ostracod assemblage down to ~20 mbsf. Below this level only scattered juvenile and redeposited valves were recorded. The interval 6–20 mbsf is characterized by a diverse marine assemblage with *Elofsonella concinna*, *Sarsicytheridea punctillata*, *Roundstonia globulifera*, and *Het-*

erocyprideis sorbyana, with some of the marine taxa typical of North Atlantic waters and high salinity ≥26–30 such as *Bythocythere constricta*, *Cytheropteron biconvexa*, and *Cytheropteron arcuatum* occurring in the lower part of this interval. At ~6 mbsf, shallow brackish-marine and freshwater ostracods (*Ilyocypris* sp.) were identified, suggesting a shallow brackish environment.

Site M0061

At Site M0061, ostracods occur in low abundance to 6 mbsf. The assemblage is dominated by *Paracyprideis fennica*. Low abundance and taxonomic diversity implies harsh environments for ostracods. Similarity between ostracod and foraminifer records implies that salinity decreases uphole.

Site M0063

Site M0063 contains a very limited ostracod assemblage. Ostracods occur in low abundance in the upper 18 mbsf and at ~26 and ~39 mbsf. Low abundance and poor preservation prevented paleoenvironmental interpretation of the ostracod data.

Site M0065

Site M0065 is characterized by a low-diversity ostracod assemblage from the surface to 9 mbsf. Predominance of brackish water taxa (*Palmoconcha* spp.) in the lower part of the interval and brackish-marine (*Cytheropteron latissimum* and *Sarsicytheridea bradii*) in the upper part suggests increasing salinity uphole.

Site M0067

Site M0067 contained ostracods in the interval between 0.2 and 4.2 mbsf. Significant variations in abundance were observed. The highest abundances were recorded at ~3.2–3.5 mbsf, reaching 50–130 valves/20 cm^3 sample. All taxa identified from this site are shallow-water marine, with the following species being the most abundant: *E. concinna*, *S. punctillata*, *S. bradii*, and *Robertsonites tuberculatus*. A relatively low ratio of juvenile valves suggests a high-energy environment where some redeposition took place.

Sites M0062, M0064, and M0066

Sites M0062, M0064, and M0066 were barren with respect to ostracods.

Geochemistry

For the analysis of interstitial waters, a total of 789 samples were collected offshore using either Rhizon samplers or squeezers. An additional 876 sediment samples were collected for analysis of headspace gas, from which 161 samples were taken at the four microbiology sites and measured for methane concentrations during the offshore phase. Pore water analyses onboard the ship included measurements of salinity, pH, sulfide, alkalinity, and ammonium. An additional 23 chemical pore water species were analyzed during the OSP, including chloride, bromide, and sulfate by ion chromatography and aluminum, barium, boron, calcium, iron, magnesium, manganese, potassium, phosphorus, silica, sodium, strontium, sulfur, titanium, lithium, molybdenum, rubidium, vanadium, zinc, and zirconium by inductively coupled plasma–optical emission spectrometry (ICP-OES). We also analyzed 657 sediment samples for total carbon, total organic carbon, and total sulfur using a carbon sulfur analyzer at the University of Bremen.

The pore water composition at most sites reflects the rise in salinity associated with the transition from a freshwater environment to the modern brackish-marine Baltic Sea. The length of the sediment column impacted by the salinity change in the bottom water strongly depends on the sediment accumulation rate and diffusion. At Site M0059 in the Little Belt, for example, the brackish-marine sediment deposit is exceptionally thick at ~47 m. Concentrations of chloride, a conservative element in seawater, are high and relatively constant at ~380 mM throughout the upper 15 m of the sediment, before declining to 100 mM at depth. In contrast, at Site M0066 in the Bornholm Basin, the brackish-marine deposit is <2 m thick. Here, chloride concentrations display a comparatively moderate decline from near 170 mM near the seafloor, largely reflecting diffusive transport into the sediment. Evidence for fresher water at depth at Site M0060 may reflect flow through high-porosity sand units.

Differences in pore water salinity also reflect the position of each site within the BSB. Sites located a greater distance from the Danish Straits and the connection with the North Sea are generally characterized by lower salinity in the pore water in the upper part of the sediment column. Thus, although the surface sediment salinity is ~33 at Site M0060 near Anholt, salinities of ~6 were observed at Sites M0061 and M0062 in the Ångermanälven River estuary.

The chemical composition of the interstitial waters also records large spatial and temporal differences in the input and degradation of organic matter in the sediment. Key indicators for high rates of organic matter degradation include high alkalinities, elevated concentrations of ammonium and phosphate, and lack of sulfate in the pore water. Exceptionally high alkalinities of ~200 and 55 meq/L are observed

at Sites M0059 and M0063, respectively. Alkalinities are at least an order of magnitude lower at most other sites, indicating lower rates of organic matter degradation.

Methane was detected in the sediment at all microbiology sites (i.e., Sites M0059, M0060, M0063, and M0065), indicating an important role for methanogenesis in the degradation of organic matter at depth in the sediments. However, because of extensive degassing during coring, most of the values indicate presence or absence of methane only and cannot be used as a quantitative measure. Sediment total organic carbon and total sulfur profiles support the spatial and temporal variations in organic matter input and degradation as deduced from pore water profiles.

Physical properties

Physical property data obtained during the offshore, pre-onshore, and onshore phases of Expedition 347 vary in quality at each drill site, but several parameters are of constantly high quality and generally reflect the different lithologic and in many cases seismic units identified within each hole (see **"Lithostratigraphy"** and **"Stratigraphic correlation"**). Natural gamma ray (NGR) data obtained during the pre-onshore phase were of particular importance for preliminary interpretations and predominantly reflect variations in clay, water, and organic content at all sites. Noncontact resistivity, magnetic susceptibility (MS), and gamma density obtained with the shipboard multisensor core logger (MSCL) also commonly aided downhole interpretation. At a number of sites, bulk density (i.e., wet density) obtained during onshore analyses corresponded very well to the shipboard MSCL gamma density data. Shipboard Fast-track MS, together with standard MSCL MS, allowed construction of composite stratigraphic splices at most sites (see **"Stratigraphic correlation"**). These splices proved to be very useful, especially for microbiology holes/cores that were heavily whole-round core subsampled onboard. Interpreted together, the above physical property parameters also reflect the disturbance common in the uppermost intervals of cores.

Shipboard MSCL *P*-wave velocity and onshore color reflectance data exhibit greater variation in quality and were of limited utility at most sites. Problems with these two parameters may result from coring and postcoring disturbance, such as cracking due to expansion and undersized cores. Additional processing of the color reflectance data, aided by examination of line scanner images, is likely necessary to identify and remove intervals characterized by spurious values.

Downhole logging

Downhole geophysical logs provide continuous information on physical, chemical, textural, and structural properties of geological formations penetrated by a borehole. Offshore downhole logging operations for Expedition 347 were provided by Weatherford Wireline Service and managed by the European Petrophysics Consortium (EPC). The set of downhole geophysical instruments utilized during Expedition 347 was constrained by the scientific objectives, the coring technique, and the hole conditions at the nine sites. The suite of downhole geophysical methods was chosen to obtain high-resolution resistivity images of the borehole wall, to measure borehole size, and to measure or derive petrophysical or geochemical properties of the formation such as porosity, electrical resistivity, acoustic velocities, and natural gamma radioactivity. No nuclear tools were deployed during Expedition 347.

The Weatherford Compact suite comprised the following tools:

- The gamma ray tool (MCG) measures natural gamma radiation.
- The spectral gamma ray tool (SGS) allows identification of individual elements that emit gamma rays (e.g., potassium, uranium, and thorium).
- The array induction tool (MAI) measures electrical conductivity of the geological formation. The output of the tool comprises three logs: induction electrical conductivity of shallow, medium, and deep investigation depth.
- The sonic sonde (MSS) measures formation compressional slowness (inverse velocity).
- The Compact microimager (CMI) is a memory capable resistivity microimaging tool. The eight arms in two planes of the CMI also provide four independent radii measurements, which can be used to identify near-borehole stress regimes.

A total of nine boreholes (Holes M0059B, M0059E, M0060B, M0062D, M0063A, M0064A, M0064D, M0065A, and M0065C) were prepared for downhole logging measurements. Measurements were performed in open borehole conditions (no casing). Despite difficult borehole conditions (nonconsolidated formations, risk of collapse, etc.), the recovery and overall quality of the downhole logging data are good. The gamma ray tool was used at the top of every tool string as a communication tool and for correlation between the different runs. The choice of tool string was based on borehole conditions and drilled depth. Because of borehole conditions, it was not possible to log with all tools in every borehole or to reach total drilled depth in most of the holes. Natural gamma ray measurements performed on unsplit

cores will enable core-log correlation. Comparison of downhole logging units with petrophysical properties boundaries and lithologic unit boundaries showed generally good correlation.

Holes M0059B and M0059E

Hole M0059B was drilled to 204.03 m drilling depth below seafloor (DSF). In preparation for logging, the hole was circulated and the drill string was pulled back in the hole to 20 m wireline log depth below seafloor (WSF). The MCG/MAI was the first tool string to be run, and it reached 72.5 m WSF from where an uplog was started. Then the drill pipe was run again to 204 m DSF and set to 87 m WSF, and the MCG/MAI tool string was deployed again in order to log the bottom part of the hole. The tool string reached 186.4 m WSF from where an uplog was started. Pulling out of the hole, overpull was observed and the decision was taken to set the pipe again to ~20 m DSF and deploy the MCG/SGS/MSS tool string. This tool string was run to 72.5 m WSF, and an uplog was started.

Hole M0059E was drilled from seafloor to 100.8 m DSF. In preparation for logging, the hole was circulated and the drill string was pulled back in the hole to 15 m WSF. The first tool string was the MCG/MAI tool string, which reached ~70 m WSF from where an uplog was performed. The second tool string was the MCG/CMI tool string, which reached 59 m WSF. The last tool string (MCG/SGS/MSS), with total gamma, spectral gamma, and sonic, reached the same depth from where an uplog was started.

Hole M0060B

Hole M0060B was drilled from seafloor to 85.7 m DSF. In preparation for logging, the hole was circulated and the drill string was pulled back in the hole to 17.5 m WSF. The first tool string deployed included the gamma and induction tools, followed by the gamma, spectral gamma, and sonic tool string. The first tool string reached a maximum depth of 67 m WSF. The second tool string (MCG/SGS/MSS) reached 61 m WSF, where an uplog was started. The last tool string deployed was the MCG/CMI. A maximum depth of 56 m WSF was reached.

Hole M0062D

Downhole logging measurements in Hole M0062D were made after completion of coring to a total depth of 21 m DSF. In preparation for logging, the hole was circulated with seawater and the pipe was pulled back to 2 m WSF. Two tool strings were deployed. The MCG/MAI was run from seafloor to 10.4 m WSF from where an uplog was started. The MCG/SGS tool string, measuring total gamma ray and spectral gamma ray, was run from seafloor to 10.4 m WSF, and an uplog was started.

Hole M0063A

Hole M0063A was drilled from seafloor to 115.8 m DSF. In preparation for logging, the hole was circulated with seawater and the drill string was pulled back in the hole to 17.55 m WSF. Three tool strings were deployed. The MCG/MAI tool string was run from seafloor to 108.5 m WSF from where an upload was started. The MCG/SGS/MSS tool string was run from seafloor to 108.5 m WSF, and an uplog was started. The MCG/CMI tool string was run down to the same depth, and a high-resolution uplog was started.

Holes M0064A and M0064D

Hole M0064A was drilled from seafloor to 41.5 m DSF. In preparation for logging, the hole was circulated with seawater and the drill string was pulled back in the hole to 2 m WSF. The MCG/MAI tool string was run into hole, and a downlog was started. The seafloor was picked up by the gamma ray, and the tool string came out of the pipe. Immediately, a sudden drop in tension indicated that the tool string set up at ~5 m WSF. Logging operation was abandoned after this unsuccessful attempt.

Downhole logging measurements in Hole M0064D were made after completion of coring to a total depth of 41.2 m DSF. In preparation for logging, the hole was circulated with seawater and the pipe was pulled back to 7.6 m WSF. Two tool strings were deployed. The MCG/MAI was run from seafloor to 31 m WSF, and the MCG/SGS was run from seafloor to 26.4 m WSF.

Holes M0065A and M0065C

Hole M0065A was drilled from seafloor to 73.9 m DSF. In preparation for logging, the hole was circulated with seawater and the drill string was pulled back in the hole to 14 m WSF. Two tool strings were deployed. The MCG/MAI was run from seafloor to 41 m WSF, and the MCG/SGS was run from seafloor to 16 m WSF. As the borehole was closing and an attempt to do a wiper trip of the borehole was unsuccessful, logging was abandoned at this hole.

Hole M0065C was drilled from seafloor to 47.9 m DSF. In preparation for logging, the hole was circulated with seawater and the drill string was pulled back in the hole to 13.2 m WSF. Two tool strings were deployed. The MCG/SGS/MSS was run from seafloor to 40 m WSF, and the MCG/CMI was run from seafloor to the same depth.

Paleomagnetism

The magnetic susceptibility (χ) and natural remanent magnetization (NRM) of a total of 1779 discrete cubic (volume = 7.6 or 1 cm^3) samples were measured during the OSP. Sixteen U-channel samples (~1.5 m long) were taken from cores recovered at Sites M0061 and M0062 to complement the discrete sample data. Forty-three minicubes (volume = 1 cm^3) were included in the suite of paleomagnetic samples from Site M0066, where the restricted diameter of the split cores did not allow for standard paleomagnetic boxes to be taken in addition to the requested U-channel samples.

The range of χ, which was normalized to the wet mass of each discrete sample, spans across four orders of magnitude and included one negative sample from the Cretaceous limestone recovered from 204 meters composite depth (mcd) at Site M0059. The highest magnetic susceptibilities of 8×10^{-6} m^3/kg (discounting samples that showed signs of contamination) were displayed by samples from a unit of well-sorted sand at 122 mcd at Site M0059. In general, χ was $<1 \times 10^{-6}$ m^3/kg, with values $<0.4 \times 10^{-6}$ m^3/kg restricted to the relatively organic rich postglacial brackish and marine sediments that characterize the Littorina Sea stage of Baltic Sea history. Units of varved clays, including those with silty and sandy components characteristic of the BIL of the Baltic Sea, have intermediate to high χ values between 0.4×10^{-6} and 1×10^{-6} m^3/kg. It was noted that enhanced χ values were frequently associated with lithologic boundaries considered to reflect the transition from the Ancylus Lake stage to the Littorina Sea stage of the Baltic Sea and were frequently connected to observations of iron sulfide precipitates.

A viscous component of the NRM in the vast majority of discrete paleomagnetic pilot samples was effectively randomized by the application of an alternating field of 5 mT. The subsequently determined inclinations and declinations of all the discrete samples are shown projected as polar (stereoplots) in Figure **F32.** Cores were not oriented with respect to an azimuth, and the relatively few number of sample points per core section limits the usefulness of the declination data. This data set shows a distinct cluster of data points that vary a few degrees from the predictions of a geocentric axial dipole (GAD) model. There are, however, many samples with shallow and reversed inclinations, and these were almost entirely restricted to coarse-grained units (including some varved clays with silt) that were deposited during early stages of Baltic Sea history (Baltic Ice Lake, Yoldia Sea, and Ancylus Lake). No convincing evidence of known late Quaternary geomagnetic field excursions is present in the data set, and the shallow and reversed directions are ascribed to deposition in high-energy environments. Paleomagnetic samples recovered from units that were formed during the Littorina Sea stage of the Baltic Sea history (approximately the last 3000–8000 y) show no sign of mechanically induced inclination shallowing. Core disturbance caused by gas (methane) expansion physically disturbed the between-sample fidelity of the paleomagnetic record in the Littorina Sea stage sediments recovered from Landsort Deep (Site M0063), although it was noted that the NRM intensity of laminated units of Littorina Sea stage age was higher than nonlaminated units. A biplot of χ versus NRM intensity is shown in Figure **F33.** Evidence of the most distinct regional feature in Holocene paleomagnetic secular variation, which occurred ~2600 y ago and is defined by a peak in inclination and a relative east to west swing in declination, was identified at 5 mbsf at Site M0062, in a varved sequence from Ångermanälven.

Microbiology

Site M0059

Two holes, M0059C and M0059E, were drilled for microbiology, interstitial water chemistry, and ephemeral geochemical parameters. Counts of microbial cells were made by fluorescence microscopy using the acridine orange direct count (AODC) method and by flow cytometry (FCM) using SYBR green stain. Microbial cell abundances in the deep Holocene clay are very high and decrease gradually with depth, from $\geq 10^9$ cells/cm^3 near the sediment surface to ~10^8 cells/cm^3 at 50 mbsf. The high cell counts are in accordance with the high rates of organic matter mineralization, as indicated by extraordinary high alkalinity and ammonium concentrations. Interestingly, there is no abrupt change in cell abundance between the Holocene sequence and the underlying glacial clay in spite of a strong shift in organic carbon content and, expectedly, in the availability of organic substrates and energy. Whether there is a shift in the phylogenetic or functional composition of the microbial community may be revealed by later DNA-based analyses.

Cell counts made by the two approaches of fluorescence staining, using microscopy or FCM, yielded very similar data with a 1:1 relationship and no significant difference by a paired sample t-test. This is the first successful offshore comparison between cell

counts by FCM and standard AODC, and the result is therefore also important for future IODP deep biosphere expeditions. The results show that the techniques used for FCM quantitatively extracted and identified microbial cells.

Perfluorocarbon (PFC) tracer was used while drilling the microbiology holes in order to evaluate potential contamination of microbiology samples with cells from the drilling fluid. There were initial problems with the delivery of the PFC to Hole M0059C that were partly resolved when drilling the second microbiology hole toward the end of the expedition. Furthermore, the PFC contamination test was significantly improved between the first and second hole after the drilling fluid samples were taken directly from the core liner upon retrieval of each piston core. The average contamination level corresponds to the potential introduction of 10–100 cells/cm^3 of sediment. In comparison to the in situ cell abundance of 10^8–10^9 cells/cm^3, this is still less than a millionth of the indigenous community.

Site M0060

Hole M0060B was drilled for microbiology, interstitial water chemistry, and ephemeral geochemical parameters. Counts of microbial cells were made by fluorescence microscopy using the AODC method and by FCM using SYBR green stain. A paired sample t-test shows that the cell numbers estimated by the two methods do not differ significantly when applied to samples from the same core depths. Cell counts are relatively low in the upper 6 m of well-sorted sand. In the deep sequence of glacial clay below the sand, cell counts are high, 10^8–10^9 cells/cm^3. Although a broad peak of alkalinity and ammonium indicates a higher rate of organic carbon mineralization in the upper 0–30 mbsf than below, cell counts do not change significantly with depth to ~85 mbsf, where the clay shifts to sand and where uncontaminated sediment could no longer be sampled for microbiology.

PFC contamination tests show a high level of potential contamination in the uppermost sandy cores (347-M0060B-1H through 3H), where PFC concentrations are as high in the interior of the core as on the exterior. In the glacial clay, the calculated potential contamination ranges from 10^2–10^3 cells/cm^3 in some cores to <1 cell/cm^3 in others. Compared to the in situ cell abundance of 10^8–10^9 cells/cm^3, contamination is thus <1:10^5 of the indigenous cells.

Site M0063

Hole M0063E was drilled for microbiology, interstitial water chemistry, and ephemeral geochemical parameters. Microbial cells were counted by fluorescence microscopy using the AODC method and by FCM using SYBR green stain. In accordance with high rates of organic matter mineralization, as indicated by a broad peak of alkalinity and ammonium concentration, fluorescence microscopy yielded very high cell counts, approaching 10^{10} cells/cm^3 near the sediment surface and decreasing steeply to ~10^8 cells/cm^3 at ~40 mbsf. From this depth, which marks the transition from Holocene, organic-rich clay to glacial, low-organic clay, cell counts decrease with depth at a significantly lower rate.

In contrast to Sites M0059 and M0060, FCM counts are similar to AODC counts only in the lower, organic-poor clay below 41 mbsf at Site M0063, whereas FCM counts are significantly lower than the AODC counts in the overlying Holocene, organic-rich sediment, with samples taken near the sediment surface showing the largest deviation (>10-fold). This discrepancy may derive from the difficulty of counting individual cells in samples from this interval because of the presence of large clumps of cells and very small cells (~0.1 µm in diameter) that escape detection by FCM. An improved sample preparation technique will need to be developed to deal with these samples.

Based on PFC data, Cores 347-M0063E-3H, 4H, 30H, 31H, and 42H show the highest calculated contamination levels, with potentially as many as 10^4 drilling fluid-derived cells/cm^3 in their interiors. On the other hand, Cores 1H, 2H, and 17H have no detectable PFC in the interior, and Cores 5H, 10H, 12H, 25H, and 41H have only moderate contamination (<100 cells/cm^3) and are therefore suitable for microbiological analyses. No clear depth- or lithology-related trend in the level of contamination could be observed.

Site M0065

Hole M0065C was drilled for microbiology, interstitial water chemistry, and ephemeral geochemical parameters. Microbial cells were counted by fluorescence microscopy using the AODC method and by FCM using SYBR green stain.

Cell densities obtained by AODC are among the highest observed in all marine sediments examined by scientific drilling, with a sample at 3.53 mbsf yielding a cell count of 1.23×10^{10} cells/cm^3. Similar to Site M0063, AODC counts decrease steeply through the upper 14 m of marine, high-organic sediment. Below this depth, which marks the transition to late glacial clay, cell counts decrease at a significantly lower rate. High cell densities in the organic-rich sediments above 14 mbsf coincide with the in-

terval of high degradation rate of organic matter, as indicated by a broad maximum in alkalinity and ammonium concentrations at this depth interval. Salinity decreases linearly to ~30 mbsf and therefore does not appear to be directly related to the cell profile.

FCM counts are significantly lower than those of AODC in the upper, high-organic section of Hole M0065C. In this same interval, and similar to what was observed at Site M0063, the occurrence of large clumps of cells made individual cell counting problematic, likely resulting in underestimation of the real microbial densities. No significant deviation between FCM and AODC counts was observed in samples from the glacial clay deeper than 14 mbsf.

PFC contamination tests indicate that most cores bear very limited contamination in their interiors (<100 contaminating cells/cm^3), with Cores 347-M0065C-3H, 6H, and 7H potentially having <10 contaminating cells/cm^3 in their inner part. Compared to the other sites, M0065 has the highest fraction of cores that are suitable for microbiological analyses.

Stratigraphic correlation

Site M0059

At Site M0059, it was possible to correlate five holes and create one continuous splice from 0 to ~87 mcd (bottom of glacial clays). Comparison of seismic boundaries (calculated with a simple velocity-depth equation, using seismic velocity values measured onshore from each unit) with lithologic unit boundaries and physical property boundaries showed good results. Below 87 mcd, sediment recovery was sporadic, and splicing beyond that point was not possible.

Site M0060

At Site M0060, sandy intervals and noncontinuous recovery presented some difficulties in correlation. From seismic images, it was possible to find good matches for lithologic unit boundaries, using a simple velocity-depth equation and discrete velocity values measured for each unit. Lithologic unit boundaries were also easily identifiable from physical parameters data. As Hole M0060B was a microbiology hole, it was not possible to construct a splice on this site, as most of the material from the second hole was consumed by microbiological sampling and recovery was from one hole only below ~90 mcd.

Sites M0061 and M0062

Site M0061 provided material for good correlation to ~26 mcd, where rhythmically variable silt and clay changed into sand. Within the sand unit, reliability of correlation was difficult to check. Data integration suggests a possible unconformity/erosion approximately between a sulfide-rich clay unit and clay and silt rhythmite units at both sites. Good correspondence between two-way traveltime values was calculated for lithologic unit boundaries, physical properties, and features in seismic data. It was possible to construct an almost continuous splice to ~35 mcd. Site M0062 was very similar to Site M0061.

Site M0063

Site M0063 provided many challenges to correlation. Similar larger scale trends are visible in all physical properties in all holes (microbiology Hole M0063E was an exception, as only Fast-track magnetic susceptibility data were available from the entire length). Hole-to-hole correlation remains at a relatively approximate level (0.5–1.0 m) because of large nonlinear sediment expansion and coring disturbances. Sediment expansion (uppermost 40 mcd) made it difficult to precisely align prominent lithologic features between adjacent holes. Strong noise in the physical property data in each core top (coring disturbances) had to be cleaned. Based on lithologic information (see **"Lithostratigraphy"**) and seismic profiles, it is also possible that some type of gravity flows have occurred in the area, deforming sediment. A comparison of NGR data and downhole log gamma data suggests that despite sediment expansion and coring disturbances, combined sediment record recovery from Holes M0063A, M0063C, and M0063D was nearly continuous.

Site M0064

Site M0064 provided some variation in soft-sediment unit thickness. Correlation between holes was possible because lithologic changes (different types of clay sediments and diamicton) were clearly visible in the physical property data and slabbed core scan images. However, within the diamicton unit, correlation between holes could not be checked; therefore, splicing was restricted to the uppermost ~10 mcd.

Site M0065

At Site M0065, correlation and splicing was possible to ~48 mcd. Sediment recovery was nearly continuous, with some small gaps between 19 and 35 mcd. Seismic units could be connected well to major lithologic changes, although some finer unit boundary details were difficult to detect.

Site M0066

Correlation for Site M0066 was relatively good for the uppermost ~2–15 mcd, and it was possible to

construct a splice. Below that point, sediment recovery was poor, and it was not possible to connect holes accurately with any physical parameters or a lithologic feature. Lithologic unit boundaries could be detected from the seismic image fairly well.

Site M0067

Two holes at Site M0067 were very shallow, with a thin organic-rich sediment blanket covering sandy and gravelly, and a possible diamicton-like material. Correspondence with seismic units was relatively good, although no measured velocity data were available from the diamicton unit. Correlation and splicing were possible only for the uppermost 3.10 mcd.

Preliminary scientific assessment

Paleoenvironmental evolution of the Baltic Sea Basin through the latest glacial cycle

The overarching objective of Expedition 347 was to gain a deeper understanding of the paleoenvironmental evolution of the BSB through the latest glacial cycle. The expedition set out to recover sediment sequences covering the time from MIS 5 to the present at as high resolution as possible. In order to meet this aim, nine sites were drilled during the expedition, selected on the basis of thorough seismic pre-site surveys and with a geographic distribution aimed to register the in- and outflows from the BSB, as well as the sediments deposited within the basin itself.

After the expedition, the following OSP carried out visual inspection and description of the >1600 m of core retrieved, measurements of physical properties, and intense sampling of the cores. Initial biostratigraphic and lithologic analyses provided a preliminary chronology that, together with the visual appearance of the sediment, was used as a guide for further sampling.

The original proposal for Expedition 347 stated four major research themes, listed below. To explore these four themes, further laboratory work will be carried out during the coming year.

In general, the expedition was very successful and many of the research questions formulated in the original proposal will be explored and the objectives met. In the following, we give a brief overview of the preliminary results.

Climate and sea level dynamics of MIS 5, including onsets and terminations

The lowermost part of the cored sequences from Sites M0059 and M0060 revealed biostratigraphic indications of possible MIS 5 age, and sufficient material was collected to perform OSL dating. The stratigraphic complexity of the two sites calls for intense laboratory investigations and dating, both by the OSL method and by pollen stratigraphy, before more conclusions can be drawn regarding dating. At this point, however, we conclude that the prospect of a deeper understanding of MIS 5 will be provided by the cored material.

Complexities of the latest glacial (MIS 4–MIS 2)

The sediments recovered between ~80 and 120 mbsf at Site M0059 and between ~90 and 150 mbsf at Site M0060 display intriguingly complex lithologies that, together with the preliminary biostratigraphic and geochemical data, hold important environmental information about the latest glacial stages, MIS 4–MIS 2. Sediments were recovered at Sites M0064, M0065, and M0066 that are older than late glacial and will provide very specific information, especially on conditions within the BSB during parts of MIS 4–MIS 2.

Deglacial and Holocene (MIS 2–MIS 1) climate forcing

The glacial varve sequences recovered at Sites M0063, M0064, and M0065 will greatly improve knowledge of the deglaciation of the southern and central BSB and will provide new general understanding of the behavior of the ice sheet during MIS 2. The varved sequences from Sites M0059 and M0060 may also contribute to this knowledge, although they can probably not be directly correlated to the existing Swedish glacial varve chronology and thus not used for any age determination. The cored varved sequences from Sites M0061 and M0062 will give new insights into the late Holocene history of the northern part of the BSB.

An unexpected long Holocene sequence from Site M0059, together with an extremely expanded Holocene sequence from Site M0063, will allow reconstructions of, for example, climate response and other external forcing mechanisms with a resolution that was previously not possible. The prospect of reconstructing Holocene environmental variations with such high resolution as provided by these sediment archives will give unique new knowledge on how the anthropogenically unaffected BSB ecosystem responded.

Deep biosphere responses to glacial–interglacial cycles

Four of the drilled sites were selected for the study of the deep biosphere and how the buried microbial

communities responded to major shifts in the Baltic Sea environment in the past and to varying lithologies and geochemical stratification in the present. Separate holes were drilled at Sites M0059, M0060, M0063, and M0065 to sample for microbiology, interstitial water chemistry, and ephemeral geochemical parameters such as organic biomarkers.

For the first time during IODP, two different methods were used offshore for cell counts, both using fluorescent staining. The IODP standard AODC method was compared to an FCM method that relied on a quantitative extraction of cells from the sediment. It was an important result that the two methods gave very similar results in the majority of sediments. Microbial cell counts are generally extremely high, particularly in the organic-rich Holocene deposits younger than ~8000 y that yielded the highest microbial abundances yet recorded by IODP.

A perfluorocarbon tracer was used while drilling the microbiology holes to evaluate potential contamination with cells from the drill fluid. A new application of this technique with sampling of liner fluid from each drilled piston core and a modified preparation of samples for gas chromatography improved the standard approach significantly and helped guide the selection of samples for subsequent microbiological analyses.

A large number of samples were taken offshore from the microbiology holes, using microbiological techniques. These were shipped during and after the expedition to requesting laboratories around the world and, based on the many novel ideas and techniques that will be applied, important new information on microbial life in the deep biosphere is expected.

References

Alley, R.B., Mayewski, P.A., Sowers, T., Stuiver, M., Taylor, K.C., and Clark, P.U., 1997. Holocene climatic instability: a prominent, widespread event 8200 years ago. *Geology,* 25(6):483–486. **doi:10.1130/0091-7613(1997)025<0483:HCIAPW>2.3.CO;2**

Andrén, E., Andrén, T., and Kunzendorf, H., 2000a. Holocene history of the Baltic Sea as a background for assessing records of human impact in the sediments of the Gotland Basin. *Holocene,* 10(6):687–702. **doi:10.1191/09596830094944**

Andrén, E., Andrén, T., and Sohlenius, G., 2000b. The Holocene history of the southwestern Baltic Sea as reflected in a sediment core from the Bornholm Basin. *Boreas,* 29(3):233–250. **doi:10.1111/j.1502-3885.2000.tb00981.x**

Andrén, T., and Andrén, E., 2001. Did the second Storegga slide affect the Baltic Sea? *Baltica,* 14:115–121.

Andrén, T., Andrén, E., Berglund, B.E., and Yu, S.-Y., 2007. New insights on the Yoldia Sea low stand in the Blekinge archipelago, southern Baltic Sea. *GFF,* 129(4):277–285. **doi:10.1080/11035890701294277**

Andrén, T., Björck, J., and Johnsen, S., 1999. Correlation of Swedish glacial varves with the Greenland (GRIP) oxygen isotope record. *J. Quat. Sci.,* 14(4):361–371. **doi:10.1002/(SICI)1099-1417(199907)14:4<361::AID-JQS446>3.0.CO;2-R**

Andrén, T., Jørgensen, B.B., and Cotterill, C., 2012. Baltic Sea Basin Paleoenvironment: paleoenvironmental evolution of the Baltic Sea Basin through the last glacial cycle. *IODP Sci. Prosp.,* 347. **doi:10.2204/iodp.sp.347.2012**

Andrén, T., Lindeberg, G., and Andrén, E., 2002. Evidence of the final drainage of the Baltic Ice Lake and the brackish phase of the Yoldia Sea in glacial varves from the Baltic Sea. *Boreas,* 31(3):226–238. **doi:10.1111/j.1502-3885.2002.tb01069.x**

Andrén, T., and Sohlenius, G., 1995. Late Quaternary development of the north-western Baltic proper—results from the clay-varve investigation. *Quat. Int.,* 27:5–10. **doi:10.1016/1040-6182(94)00055-A**

Anjar, J., Larsen, N.K., Björck, S., Adrielsson, L., and Filipsson, H.L., 2010. MIS 3 marine and lacustrine sediments at Kriegers Flak, southwestern Baltic Sea. *Boreas,* 39(2):360–366. **doi:10.1111/j.1502-3885.2010.00139.x**

Bennike, O., Jensen, J.B., Lemke, W., Kuijpers, A., and Lomholt, S., 2004. Late- and postglacial history of the Great Belt, Denmark. *Boreas,* 33(1):18–33. **doi:10.1111/j.1502-3885.2004.tb00993.x**

Berglund, B.E., Sandgren, P., Barnekow, L., Hannon, G., Jiang, H., Skog, G., and Yu, S.-Y., 2005. Early Holocene history of the Baltic Sea, as reflected in coastal sediments in Blekinge, southeastern Sweden. *Quat. Int.,* 130(1):111–139. **doi:10.1016/j.quaint.2004.04.036**

Bianchi, T.S., Engelhaupt, E., Westman, P., Andren, T., Rolff, C., and Elmgren, R., 2000. Cyanobacterial blooms in the Baltic Sea: natural or human-induced? *Limnol. Oceanogr.,* 45(3):716–726. **doi:10.4319/lo.2000.45.3.0716**

Biddle, J.F., Lipp, J.S., Lever, M.A., Lloyd, K.G., Sørensen, K.B., Anderson, R., Fredricks, H.F., Elvert, M., Kelly, T.J., Schrag, D.P., Sogin, M.L., Brenchley, J.E., Teske, A., House, C.H., and Hinrichs, K.-U., 2006. Heterotrophic Archaea dominate sedimentary subsurface ecosystems off Peru. *Proc. Natl. Acad. Sci. U. S. A.,* 103(10):3846–3851. **doi:10.1073/pnas.0600035103**

Björck, S., 1995. A review of the history of the Baltic Sea, 13.0–8.0 ka BP. *Quat. Int.,* 27:19–40. **doi:10.1016/1040-6182(94)00057-C**

Björck, S., Andrén, T., and Jensen, J.B., 2008. An attempt to resolve the partly conflicting data and ideas on the Ancylus–Litorina transition. *Pol. Geol. Inst. Spec. Pap.,* 23:21–26.

Björck, S., Dennegård, B., and Sandgren, P., 1990. The marine stratigraphy of the Hanö Bay, SE Sweden, based on different sediment stratigraphic methods. *Geol. Foeren. Stockholm Foerh.,* 112(3):265–280. **doi:10.1080/11035899009454774**

Björck, S., Kromer, B., Johnsen, S., Bennike, O., Hammarlund, D., Lemdahl, G., Possnert, G., Rasmussen, T.L.,

Wohlfarth, B., Hammer, C.U., and Spurk, M., 1996. Synchronized terrestrial-atmospheric deglacial records around the North Atlantic. *Science,* 274(5290):1155–1160. **doi:10.1126/science.274.5290.1155**

Bond, G., Kromer, B., Beer, J., Muscheler, R., Evans, M.N., Showers, W., Hoffmann, S., Lotti-Bond, R., Hajdas, I., and Bonani, G., 2001. Persistent solar influence on North Atlantic climate during the Holocene. *Science,* 294(5549):2130–2136. **doi:10.1126/science.1065680**

Borgendahl, J., and Westman, P., 2007. Cyanobacteria as a trigger for increased primary productivity during sapropel formation in the Baltic Sea—a study of the Ancylus/Litorina transition. *J. Paleolimnol.,* 38(1):1–12. **doi:10.1007/s10933-006-9055-0**

Cato, I., 1985. The definitive connection of the Swedish geochronological time scale with the present, and the new date of the zero year in Döviken, northern Sweden. *Boreas,* 14(2):117–122. **doi:10.1111/j.1502-3885.1985.tb00901.x**

Conley, D.J., Humborg, C., Rahm, L., Savchuk, O.P., and Wulff, F., 2002. Hypoxia in the Baltic Sea and basin-scale changes in phosphorus biogeochemistry. *Environ. Sci. Technol.,* 36(24):5315–5320. **doi:10.1021/es025763w**

D'Hondt, S.L., Jørgensen, B.B., Miller, D.J., et al., 2003. *Proc. ODP, Init. Repts.,* 201: College Station, TX (Ocean Drilling Program). **doi:10.2973/odp.proc.ir.201.2003**

D'Hondt, S., Jørgensen, B.B., Miller, D.J., Batzke, A., Blake, R., Cragg, B.A., Cypionka, H., Dickens, G.R., Ferdelman, T., Hinrichs, K.-U., Holm, N.G., Mitterer, R., Spivack, A., Wang, G., Bekins, B., Engelen, B., Ford, K., Gettemy, G., Rutherford, S.D., Sass, H., Skilbeck, C.G., Aiello, I.W., Guerin, G., House, C.H., Inagaki, F., Meister, P., Naehr, T., Niitsuma, S., Parkes, R.J., Schippers, A., Smith, D.C., Teske, A., Wiegel, J., Naranjo Padillo, C., and Solis Acosta, J.L., 2004. Distributions of microbial activities in deep subseafloor sediments. *Science,* 306(5705):2216–2221. **doi:10.1126/science.1101155**

D'Hondt, S., Rutherford, S., and Spivack., A.J., 2002. Metabolic activity of the subsurface life in deep-sea sediments. *Science,* 295(5562):2067–2070. **doi:10.1126/science.1064878**

D'Hondt, S., Spivack, A.J., Pockalny, R., Ferdelman, T.G., Fischer, J.P., Kallmeyer, J., Abrams, L.J., Smith, D.C., Graham, D., Hasiuk, F., Schrum, H., and Stancine, A.M., 2009. Subseafloor sedimentary life in the South Pacific Gyre. *Proc. Natl. Acad. Sci. U. S. A.,* 106(28):11651–11656. **doi:10.1073/pnas.0811793106**

Dickson, A.J., Austin, W.E.N., Hall, I.R., Maslin, M.A., and Kucera, M., 2008. Centennial-scale evolution of Dansgaard–Oeschger events in the northeast Atlantic Ocean between 39.5 and 56.5 ka BP. *Paleoceanography,* 23(3):PA3206. **doi:10.1029/2008PA001595**

Dokken, T., Andrews, J., Hemming, S., Stokes, C., and Jansen, E., 2003. Researchers discuss abrupt climate change: ice sheets and oceans in action. *Eos, Trans. Am. Geophys. Union,* 84(20):189. **doi:10.1029/2003EO200006**

Donner, J., Kankainen, T., and Karhu, J.A., 1999. Radiocarbon ages and stable isotope composition of Holocene shells in Finland. *Quat. Ser. A,* 7:31–38.

Eiríksson, J., Kristensen, P.H., Lykke-Andersen, H., Brooks, K., Murray, A., Knudsen, K.L., and Glaister, C., 2006. A sedimentary record from a deep Quaternary valley in the southern Lillebælt area, Denmark: Eemian and early Weichselian lithology and chronology at Mommark. *Boreas,* 35(2):320–331. **doi:10.1111/j.1502-3885.2006.tb01161.x**

Elmgren, R., 1989. Man's impact on the ecosystem of the Baltic Sea: energy flows today and at the turn of the century. *Ambio,* 18(6):326–332. **http://www.jstor.org/stable/4313603**

Elmgren, R., 2001. Understanding human impact on the Baltic ecosystem: changing views in recent decades. *Ambio,* 30(4):222–231. **doi:10.1579/0044-7447-30.4.222**

Elofson, O., 1941. Zur Kenntnis der marinen Ostracoden Schwedens, mit besonderer Berücksichtigung des Skagerraks. *Zool. Bidr. Uppsala,* 19:215–234.

Emeis, K.-C., Struck, U., Blanz, T., Kohly, A., and Voß, M., 2003. Salinity changes in the central Baltic Sea (NW Europe) over the last 10000 years. *Holocene,* 13(3):411–421. **doi:10.1191/0959683603hl634rp**

Frenzel, P., Keyser, D., and Viehberg, F.A., 2010. An illustrated key and (palaeo)ecological primer for postglacial to Recent Ostracoda (Crustacea) of the Baltic Sea. *Boreas,* 39(3):567–575. **doi:10.1111/j.1502-3885.2009.00135.x**

Frenzel, P., Tech, T., and Bartholdy, J., 2005. Checklist and annotated bibliography of recent Foraminiferida from the German Baltic Sea coast. *Stud. Geol. Pol.,* 124:67–86. **http://sgp.ing.pan.pl/124_pdf/SGP124_067-086.pdf**

Fronval, T., and Jansen, E., 1996. Rapid changes in ocean circulation and heat flux in the Nordic seas during the last interglacial period. *Nature,* 383:806–810. **doi:10.1038/383806a0**

Funder, S., Demidov, I., and Yelovicheva, Y., 2002. Hydrography and mollusc faunas of the Baltic and the White Sea–North Sea seaway in the Eemian. *Palaeogeogr., Palaeoclimatol., Palaeoecol.,* 184(3–4):275–304. **doi:10.1016/S0031-0182(02)00256-0**

Gibbard, P., and Glaister, C., 2006. Pollen stratigraphy of the late Pleistocene sediments at Mommark, Als, South Denmark. *Boreas,* 35(2):332–348. **doi:10.1111/j.1502-3885.2006.tb01162.x**

Grimm, E.C., Watts, W.A., Jacobson, G.L., Jr., Hansen, B.C.S., Almquist, H.R., and Dieffenbacher-Krall, A.C., 2006. Evidence for warm wet Heinrich events in Florida. *Quat. Sci. Rev.,* 25(17–18):2197–2211. **doi:10.1016/j.quascirev.2006.04.008**

Grootes, P.M., Stuiver, M., White, J.W.C., Johnsen, S., and Jouzel, J., 1993. Comparison of oxygen isotope records from the GISP2 and GRIP Greenland ice cores. *Nature,* 366(6455):552–554. **doi:10.1038/366552a0**

Gustafsson, B.G., and Westman, P., 2002. On the causes for salinity variations in the Baltic Sea during the last 8500 years. *Paleoceanography,* 17(3):12.1–12.14. **doi:10.1029/2000PA000572**

Gyldenholm, K.G., Lykke-Andersen, H., and Lind, G., 1993. Seismic stratigraphy of the Quaternary and its substratum in southeastern Kattegat, Scandinavia. *Boreas,* 22(4):319–327. **doi:10.1111/j.1502-3885.1993.tb00192.x**

Hald, M., and Hagen, S., 1998. Early Preboreal cooling in the Nordic seas region triggered by meltwater. *Geology,* 26(7):615–618. **doi:10.1130/0091-7613(1998)026<0615:EPCITN>2.3.CO;2**

Hille, S., Leipe, T., and Seifert, T., 2006. Spatial variability of recent sedimentation rates in the Eastern Gotland Basin (Baltic Sea). *Oceanologia,* 48(2):297–317. **http://www.iopan.gda.pl/oceanologia/48_2.html#A8**

Hoehler, T.M., 2004. Biological energy requirements as quantitative boundary conditions for life in the subsurface. *Geobiology,* 2(4):205–215. **doi:10.1111/j.1472-4677.2004.00033.x**

Hoehler, T.M., and Jørgensen, B.B., 2013. Microbial life under extreme energy limitation. *Nat. Rev. Microbiol.,* 11(2):83–94. **doi:10.1038/nrmicro2939**

Houmark-Nielsen, M., 2007. Extent and age of middle and late Pleistocene glaciations and periglacial episodes in southern Jylland, Denmark. *Bull. Geol. Soc. Den.,* 55:9–35. **http://2dgf.dk/publikationer/bulletin/197bull55.html#houmark**

Houmark-Nielsen, M., 2008. Testing OSL failures against a regional Weichselian glaciation chronology from southern Scandinavia. *Boreas,* 37(4):660–677. **doi:10.1111/j.1502-3885.2008.00053.x**

Houmark-Nielsen, M., and Kjær, K.H., 2003. Southwest Scandinavia, 40–15 kyr BP: palaeogeography and environmental change. *J. Quat. Sci.,* 18(8):769–786. **doi:10.1002/jqs.802**

Houmark-Nielsen, M., Krüger, J., and Kjær, K., 2005. De seneste 150.000 år i Danmark: istidslandskabet og naturens udvikling. *Geoviden—Geol. Geog.,* 2:1–20. **http://geocenter.dk/xpdf/geoviden-2-2005.pdf**

Inagaki, F., Okada, H., Tsapin, A.I., and Nealson, K.H., 2005. Microbial survivial: the Paleome: a sedimentary genetic record of past microbial communities. *Astrobiology,* 5(2):141–153. **doi:10.1089/ast.2005.5.141**

Jackson, B.E., and McInerney, M.J., 2002. Anaerobic microbial metabolism can proceed close to thermodynamic limits. *Nature,* 415(6870):454–456. **doi:10.1038/415454a**

Jakobsson, M., Björck, S., Alm, G., Andrén, T., Lindeberg, G., and Svensson, N.-O., 2007. Reconstructing the Younger Dryas ice dammed lake in the Baltic Basin: bathymetry, area and volume. *Global Planet. Change,* 57(3–4):355–370. **doi:10.1016/j.gloplacha.2007.01.006**

Jensen, J.B., Petersen, K.S., Konradi, P., Kuijpers, A., Bennike, O., Lemke, W., and Endler, R., 2002. Neotectonics, sea level changes, and biological evolution in the Fennoscandian border zone of the southern Kattegat Sea. *Boreas,* 31(2):133–150. **doi:10.1111/j.1502-3885.2002.tb01062.x**

Jiang, H., Svensson, N.-O., and Björck, S., 1998. Meltwater discharge to the Skagerrak–Kattegat from the Baltic Ice Lake during the Younger Dryas interval. *Quat. Res.,* 49(3):264–270. **doi:10.1006/qres.1998.1971**

Johnsen, S.J., Clausen, H.B., Dansgaard, W., Fuhrer, K., Gundestrup, N., Hammer, C.U., Iversen, P., Jouzel, J., Stauffer, B., and Steffensen, J.P., 1992. Irregular glacial interstadials recorded in a new Greenland ice core. *Nature,* 359(6393):311–313. **doi:10.1038/359311a0**

Jørgensen, B.B., 2012. Shrinking majority of the deep biosphere. *Proc. Natl. Acad. Sci. U. S. A,* 109(40):15976–15977. **doi:10.1073/pnas.1213639109**

Jørgensen, B.B., D'Hondt, S.L., and Miller, D.J., 2006. Leg 201 synthesis: controls on microbial communities in deeply buried sediments. *In* Jørgensen, B.B., D'Hondt, S.L., and Miller, D.J. (Eds.), *Proc. ODP, Sci. Results,* 201: College Station, TX (Ocean Drilling Program), 1–45. **doi:10.2973/odp.proc.sr.201.101.2006**

Kabel, K., Moros, M., Porsche, C., Neumann, T., Adolphi, F., Joest Andersen, T., Siegel, H., Gerth, M., Leipe, T., Jansen, E., and Sinninghe Damsté, J.S., 2012. Impact of climate change on the Baltic Sea ecosystem over the past 1,000 years. *Nat. Clim. Change,* 2:871–874. **doi:10.1038/nclimate1595**

Kallmeyer, J., Pockalny, R., Adhikari, R.R., Smith, D.C., and D'Hondt, S., 2012. Global distribution of microbial abundance and biomass in subseafloor sediment. *Proc. Natl. Acad. Sci. U. S. A.,* 109(40):16213–16216. **doi:10.1073/pnas.1203849109**

Kjellström, E., Brandefelt, J., Näslund, J.-O., Smith, B., Strandberg, G., Voelker, A.H.L., and Wohlfarth, B., 2010. Simulated climate conditions in Europe during the marine isotope Stage 3 stadial. *Boreas,* 39(2):436–456. **doi:10.1111/j.1502-3885.2010.00143.x**

Klingberg, F., 1998. A late Pleistocene marine clay succession at Kriegers Flak, westernmost Baltic, southern Scandinavia. *J. Quat. Sci.,* 13(3):245–253. **doi:10.1002/(SICI)1099-1417(199805/06)13:3<245::AID-JQS358>3.0.CO;2-G**

Klitgaard-Kristensen, D., Sejrup, H.P., Haflidason, H., Johnsen, S., and Spurk, M., 1998. A regional 8200 cal. yr BP cooling event in northwest Europe, induced by final stages of the Laurentide Ice Sheet deglaciation? *J. Quat. Sci.,* 13(2):165–169. **doi:10.1002/(SICI)1099-1417(199803/04)13:2<165::AID-JQS365>3.3.CO;2-R**

Kortekaas, M., Murray, A.S., Sandgren, P., and Björck, S., 2007. OSL chronology for a sediment core from the southern Baltic Sea: a continuous sedimentation record since deglaciation. *Quat. Geochronol.,* 2(1–4):95–101. **doi:10.1016/j.quageo.2006.05.036**

Kristensen, P.H., and Knudsen, K.L., 2006. Palaeoenvironments of a complete Eemian sequence at Mommark, South Denmark: foraminifera, ostracods and stable isotopes. *Boreas,* 35(2):349–366. **doi:10.1111/j.1502-3885.2006.tb01163.x**

Kukla, G.J., Bender, M.L., de Beaulieu, J.-L., Bond, G., Broecker, W.S., Cleveringa, P., Gavin, J.E., Herbert, T.D., Imbrie, J., Jouzel, J., Keigwin, L.D., Knudsen, K.-L., McManus, J.F., Merkt, J., Muhs, D.R., Müller, H., Poore, R.Z., Porter, S.C., Seret, G., Shackleton, N.J., Turner, C., Tzedakis, P.C., and Winograd, I.J., 2002. Last interglacial

climates. *Quat. Res.,* 58(1):2–13. doi:10.1006/qres.2001.2316

Kunzendorf, H., Voss, M., Brenner, W., Andrén, T., and Vallius, H., 2001. Molybdenum in sediments of the central Baltic Sea as an indicator for algal blooms. *Baltica,* 14:123–130.

Lambeck, K., and Chappell, J., 2001. Sea level change through the last glacial cycle. *Science,* 292(5517):679–686. doi:10.1126/science.1059549

Larsen, N.K., Knudsen, K.L., Krohn, C.F., Kronborg, C., Murray, A.S., and Nielsen, O.B., 2009. Late Quaternary ice sheet, lake and sea history of southwest Scandinavia—a synthesis. *Boreas,* 38(4):732–761. doi:10.1111/j.1502-3885.2009.00101.x

Leipe, T., Dippner, J.W., Hille, S., Voss, M., Christiansen, C., and Bartholdy, J., 2008. Environmental changes in the central Baltic Sea during the last 1000 years: inferences from sedimentary records, hydrography and climate. *Oceanologia,* 50(1):23–41. http://www.iopan.gda.pl/oceanologia/50_1.html#A3

Lemke, W., Jensen, J.B., Bennike, O., Endler, R., Witkowski, A., and Kuijpers, A., 2001. Hydrographic thresholds in the western Baltic Sea: late Quaternary geology and the Dana River concept. *Mar. Geol.,* 176(1–4):191–201. doi:10.1016/S0025-3227(01)00152-9

Levine, R.C., and Bigg, G.R., 2008. Sensitivity of the glacial ocean to Heinrich events from different iceberg sources, as modeled by a coupled atmosphere-iceberg-ocean model. *Paleoceanography,* 23(4):PA4213. doi:10.1029/2008PA001613

Lutze, G.F., 1965. Zur foraminiferen-fauna der ostsee (The distribution of foraminifera in the Baltic Sea). *Meyniana,* 15:75–142.

Lykke-Andersen, H., Seidenkrantz, M.-S., and Knudsen, K.L., 1993. Quaternary sequences and their relations to the pre-Quaternary in the vicinity of Anholt, Kattegat, Scandinavia. *Boreas,* 22(4):291–298. doi:10.1111/j.1502-3885.1993.tb00189.x

Majoran, S., and Nordberg, K., 1997. Late Weichselian ostracod assemblages from the southern Kattegat, Scandinavia: a palaeoenvironmental study. *Boreas,* 26(3):181–200. doi:10.1111/j.1502-3885.1997.tb00851.x

Mangerud, J., 2004. Ice sheet limits in Norway and on the Norwegian continental shelf. *In* Ehlers, J., and Gibbard, P.L. (Eds.), *Quaternary Glaciations—Extent and Chronology, Part 1: Europe.* Dev. Quat. Sci., 2(1):271–294. doi:10.1016/S1571-0866(04)80078-2

Marshall, S.J., and Clark, G.K.C., 1999. Modeling North American freshwater runoff through the last glacial cycle. *Quat. Res.,* 52(3):300–315. doi:10.1006/qres.1999.2079

Miettinen, A., Head, M.J., and Knudsen, K.L., 2014. Eemian sea-level highstand in the eastern Baltic Sea linked to long-duration White Sea connection. *Quat. Sci. Rev.,* 86:158–174. doi:10.1016/j.quascirev.2013.12.009

Nordberg, K., and Bergsten, H., 1988. Biostratigraphic and sedimentological evidence of hydrographic changes in the Kattegat during the later part of the Holocene. *Mar. Geol.,* 83(1–4):135–158. doi:10.1016/0025-3227(88)90056-4

North Greenland Ice Core Project Members, 2004. High-resolution record of Northern Hemisphere climate extending into the last interglacial period. *Nature,* 431(7005):147–151. doi:10.1038/nature02805

Parkes, R.J., Cragg, B.A., Bale, S.J., Getliff, J.M., Goodman, K., Rochelle, P.A., Fry, J.C., Weightman, A.J., and Harvey, S.M., 1994. Deep bacterial biosphere in Pacific Ocean sediments. *Nature,* 371(6496):410–413. doi:10.1038/371410a0

Parkes, R.J., Webster, G., Cragg, B.A., Weightman, A.J., Newberry, C.J., Ferdelman, T.G., Kallmeyer, J., Jørgensen, B.B., Aiello, I.W., and Fry, J.C., 2005. Deep subseafloor prokaryotes stimulated at interfaces over geological time. *Nature,* 436(7049):390–394. doi:10.1038/nature03796

Rasmussen, T.L., van Weering, T.C.E., and Labeyrie, L., 1997. Climatic instability, ice sheets and ocean dynamics at high northern latitudes during the last glacial period (58–10 ka BP). *Quat. Sci. Rev.,* 16(1):71–80. doi:10.1016/S0277-3791(96)00045-5

Rosenfeld, A., 1977. Die rezenten Ostracoden-Arten in der Ostsee. *Meyniana,* 29:11–49.

Roussel, E.G., Bonavita, M.-A.C., Querellou, J., Cragg, B.A., Webster, G., Prieur, D., and Parkes, R.J., 2008. Extending the subseafloor biosphere. *Science,* 320(5879):1046. doi:10.1126/science.1154545

Salonen, V.-P., Kaakinen, A., Kultti, S., Miettinen, A., Eskola, K.O., and Lunkka, J.P., 2007. Middle Weichselian glacial event in the central part of the Scandinavian Ice Sheet recorded in the Hitura pit, Ostrobothnia, Finland. *Boreas,* 37(1):38–54. doi:10.1111/j.1502-3885.2007.00009.x

Samuelsson, M., 1996. Interannual salinity variations in the Baltic Sea during the period 1954–1990. *Cont. Shelf Res.,* 16(11):1463–1477. doi:10.1016/0278-4343(95)00082-8

Sánchez Goñi, M.F., Eynaud, F., Turon, J.L., and Shackleton, N.J., 1999. High-resolution palynological record off the Iberian margin: direct land-sea correlation for the last interglacial complex. *Earth Planet. Sci. Lett.,* 171(1):123–137. doi:10.1016/S0012-821X(99)00141-7

Sander, M., Bengtsson, L., Holmquist, B., Wohlfarth, B., and Cato, I., 2002. The relationship between annual varve thickness and maximum annual discharge (1909–1971). *J. Hydrol.,* 263(1–4):23–35. doi:10.1016/S0022-1694(02)00030-6

Schippers, A., Neretin, L.N., Kallmeyer, J., Ferdelman, T.G., Cragg, B.A., Parkes R.J., and Jørgensen, B.B., 2005. Prokaryotic cells of the deep sub-seafloor biosphere identified as living bacteria. *Nature,* 433(7028):861–864. doi:10.1038/nature03302

Siddall, M., Rohling, E.J., Almogi-Labin, A., Hemleben, C., Meischner, D., Schmelzer, I., and Smeed, D.A., 2003. Sea-level fluctuations during the last glacial cycle. *Nature,* 423(6942):853–858. doi:10.1038/nature01690

Snowball, I., Korhola, A., Briffa, K.R., and Koç, N., 2004. Holocene climate dynamics in Fennoscandia and the North Atlantic. *In* Battarbee, R.W., Gasse, F., and Stick-

ley, C.E. (Eds.), *Past Climate Variability through Europe and Africa*. Dev. Paleoenviron. Res., 6:465–494. doi:10.1007/978-1-4020-2121-3_22

Snowball, I., Zillén, L., and Gaillard, M.-J., 2002. Rapid early-Holocene environmental changes in northern Sweden based on studies of two varved lake-sediment sequences. *Holocene,* 12(1):7–16. doi:10.1191/0959683602hl515rp

Sohlenius, G., Emeis, K.-C., Andrén, E., Andrén, T., and Kohly, A., 2001. Development of anoxia during the fresh–brackish water transition in the Baltic Sea. *Mar. Geol.,* 177(3–4):221–242. doi:10.1016/S0025-3227(01)00174-8

Sohlenius, G., Sternbeck, J., Andrén, E., and Westman, P., 1996. Holocene history of the Baltic Sea as recorded in a sediment core from the Gotland Deep. *Mar. Geol.,* 134(3–4):183–201. doi:10.1016/0025-3227(96)00047-3

Sohlenius, G., and Westman, P., 1998. Salinity and redox alternations in the northwestern Baltic proper during the late Holocene. *Boreas,* 27(2):101–114. doi:10.1111/j.1502-3885.1998.tb00871.x

Sternbeck, J., Sohlenius, G., and Hallberg, R.O., 2000. Sedimentary trace elements as proxies to depositional changes induced by a Holocene fresh–brackish water transition. *Aquat. Geochem.,* 6(3):325–345. doi:10.1023/A:1009680714930

Tinner, W., and Lotter, A.F., 2001. Central European vegetation response to abrupt climate change at 8.2 ka. *Geology,* 29(6):551–554. doi:10.1130/0091-7613(2001)029<0551:CEVRTA>2.0.CO;2

Viehberg, F.A., Frenzel, P., and Hoffman, G., 2008. Succession of late Pleistocene and Holocene ostracode assemblages in a transgressive environment: a study at a coastal locality of the southern Baltic Sea (Germany). *Palaeogeogr., Palaeoclimatol., Palaeoecol.,* 264(3–4):318–329. doi:10.1016/j.palaeo.2007.05.026

von Post, L., 1929. Svea, Göta och Dana älvar. *Ymer,* 49:1–33.

Walker, M., Johnsen, S., Rasmussen, S.O., Popp, T., Steffensen, J.-P., Gibbard, P., Hoek, W., Lowe, J., Andrews, J., Björck, S., Cwynar, L.C., Hughen, K., Kershaw, P., Kromer, B., Litt, T., Lowe, D.J., Nakagawa, T., Newnham, R., and Schwander, J., 2009. Formal definition and dating of the GSSP (Global Stratotype Section and Point) for the base of the Holocene using the Greenland NGRIP ice core, and selected auxiliary records. *J. Quat. Sci.,* 24(1):3–17. doi:10.1002/jqs.1227

Wang, Y.J., Cheng, H., Edwards, R.L., An, Z.S., Wu, J.Y., Shen, C.-C., and Dorale, J.A., 2001. A high-resolution absolute-dated late Pleistocene monsoon record from Hulu Cave, China. *Science,* 294(5580):2345–2348. doi:10.1126/science.1064618

Wastegård, S., Andrén, T., Sohlenius, G., and Sandgren, P., 1995. Different phases of the Yoldia Sea in the northwestern Baltic proper. *Quat. Int.,* 27:121–129. doi:10.1016/1040-6182(94)00069-H

Westman, P., and Sohlenius, G., 1999. Diatom stratigraphy in five offshore sediment cores from the northwestern Baltic proper implying large scale circulation changes during the last 8500 years. *J. Paleolimnol.,* 22(1):53–69. doi:10.1023/A:1008011511101

Widerlund, A., and Andersson, P.S., 2006. Strontium isotopic composition of modern and Holocene mollusc shells as a palaeosalinity indicator for the Baltic Sea. *Chem. Geol.,* 232(1–2):54–66. doi:10.1016/j.chemgeo.2006.02.010

Widerlund, A., and Andersson, P.S., 2011. Late Holocene freshening of the Baltic Sea derived from high-resolution strontium isotope analyses of mollusk shells. *Geology,* 39(2):187–190. doi:10.1130/G31524.1

Winterhalter, B., 1992. Late-Quaternary stratigraphy of Baltic Sea basins—a review. *Bull. Geol. Soc. Finl.,* 64:189–194.

Wohlfarth, B., Veres, D., Ampel, L., Lacourse, T., Blaauw, M., Preusser, F., Andrieu-Ponel, V., Kéravis, D., Lallier-Vergès, E., Björck, S., Davies, S.M., de Beaulieu, J.-L., Risberg, J., Hormes, A., Kasper, H.U., Possnert, G., Reille, M., Thouveny, N., and Zander, A., 2008. Rapid ecosystem response to abrupt climate changes during the last glacial period in western Europe, 40–16 ka. *Geology,* 36(5):407–410. doi:10.1130/G24600A.1

Zillén, L., and Conley, D.J., 2010. Hypoxia and cyanobacterial blooms are not natural features of the Baltic Sea. *Biogeosci. Discuss.,* 7(2):1783–1812. doi:10.5194/bgd-7-1783-2010

Zillén, L., Conley, D.J., Andrén, T., Andrén, E., and Björck, S., 2008. Past occurrences of hypoxia in the Baltic Sea and the role of climate variability, environmental change and human impact. *Earth-Sci. Rev.,* 91(1–4):77–92. doi:10.1016/j.earscirev.2008.10.001

Publication: 20 February 2015
MS 347-101

Figure F1. A. Geographic locations of local names used in text. 1 = Landsort Deep, 2 = Øresund, 3 = south central Sweden, 4 = Lake Vänern, 5 = Darss, 6 = Møn, 7 = Mecklenburger Bay, 8 = Fehmar Belt, 9 = Langeland, 10 = Great Belt, 11 = Little Belt, 12 = Anholt, 13 = Blekinge archipelago, 14 = Kriegers Flak. (Continued on next page.)

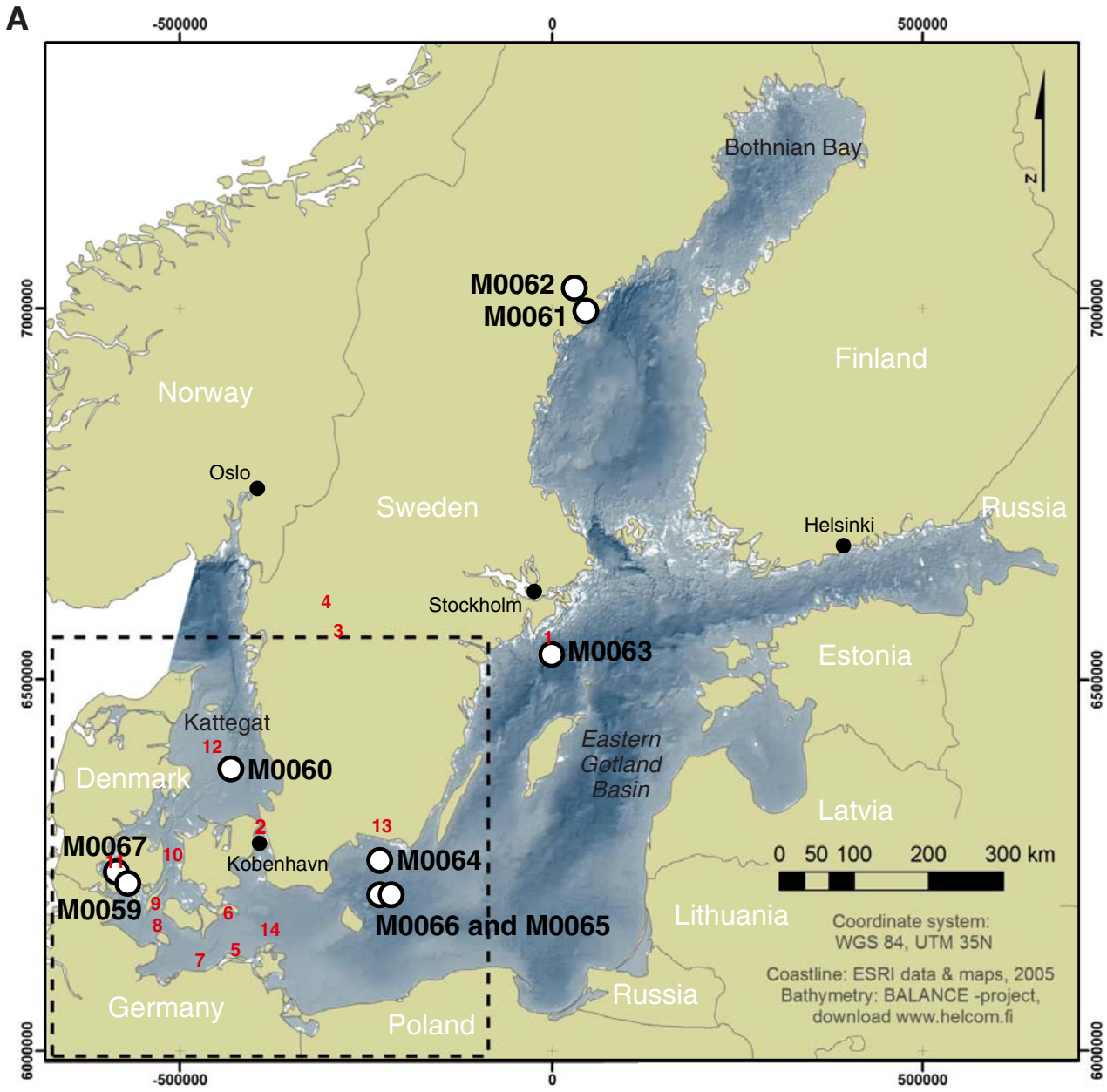

Figure F1 (continued). B. Close up.

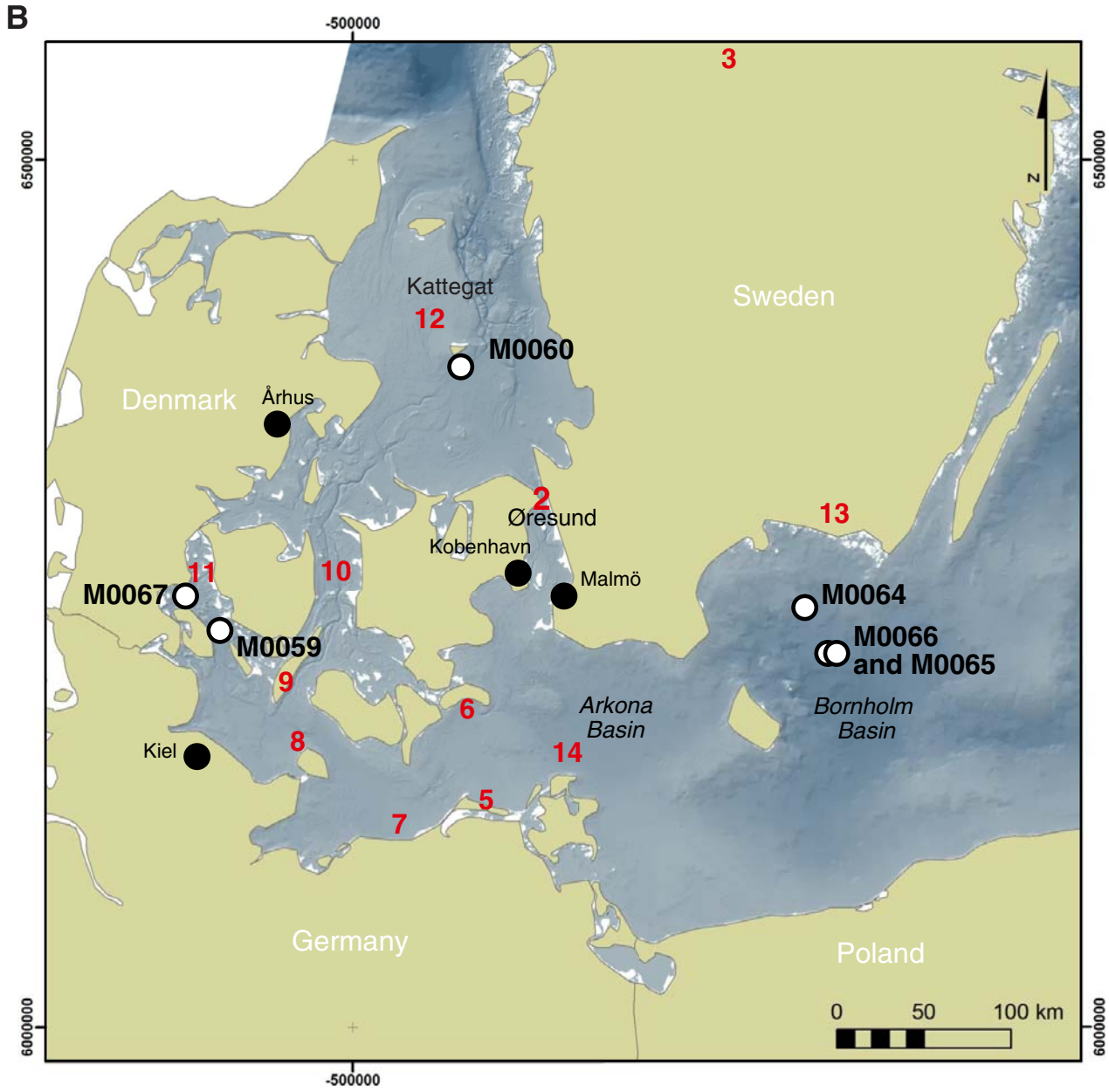

Figure F2. Paleogeographic map showing the Baltic Ice Lake stage of Baltic Sea history just prior to the maximum extension and final drainage at ~11.7 ka BP.

Figure F3. Correlation between the glacial varve record from the Baltic Sea Basin, the atmospheric $\delta^{14}C$ variation, and $\delta^{18}O$ records from the Greenland Ice Core Project (GRIP) ice core. PBO = Preboreal oscillation. BIL = Baltic Ice Lake. Redrawn from Andrén et al. (1999, 2002).

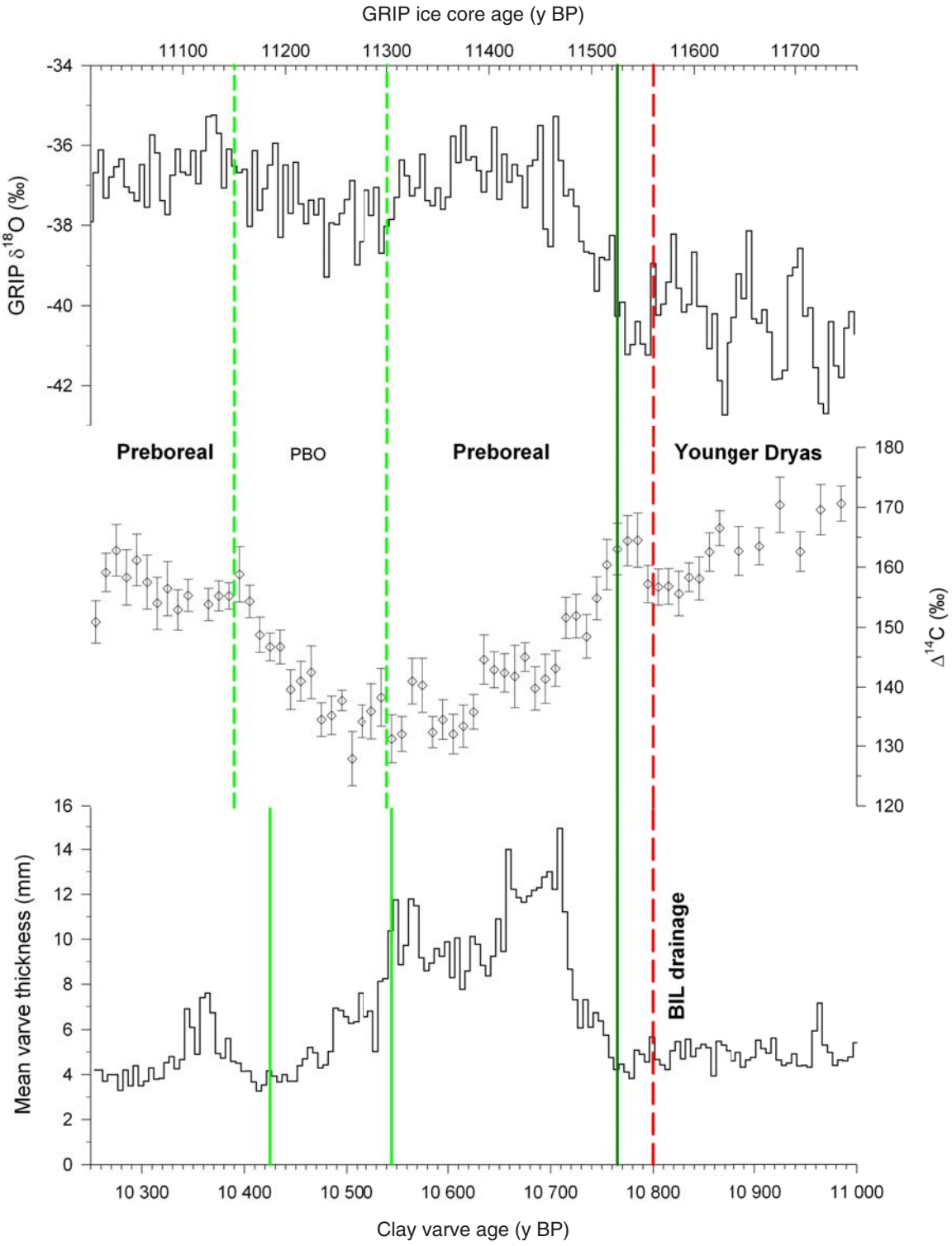

Figure F4. Paleogeographic map showing the Yoldia Sea stage of Baltic Sea history at the end of the brackish phase at ~11.1 ka BP.

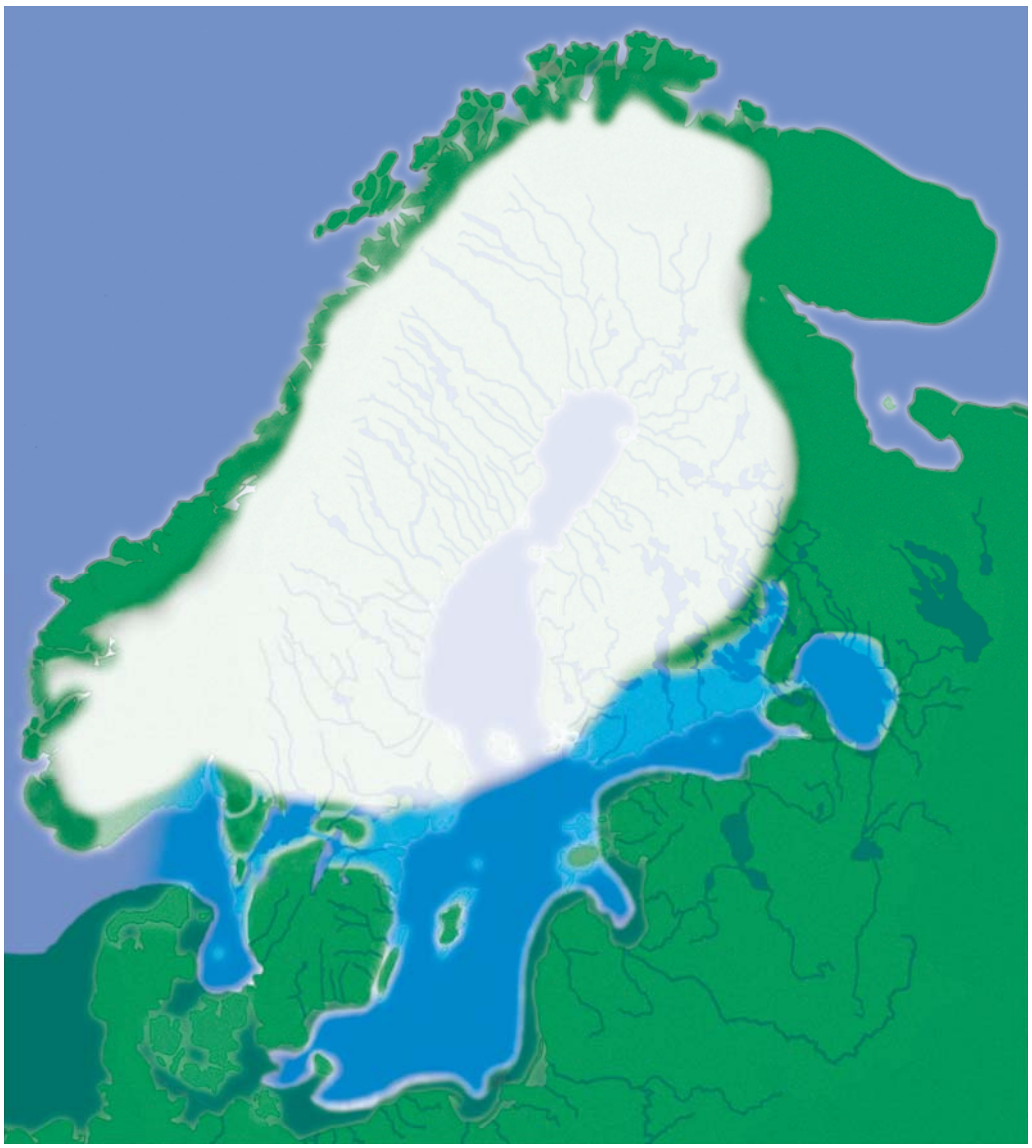

Figure F5. Paleogeographic map showing the Ancylus Lake stage of Baltic Sea history during the maximum transgression at ~10.5 ka BP.

Figure F6. Paleogeographic map showing the Littorina Sea stage of Baltic Sea history during the most saline phase at ~6.5 ka BP.

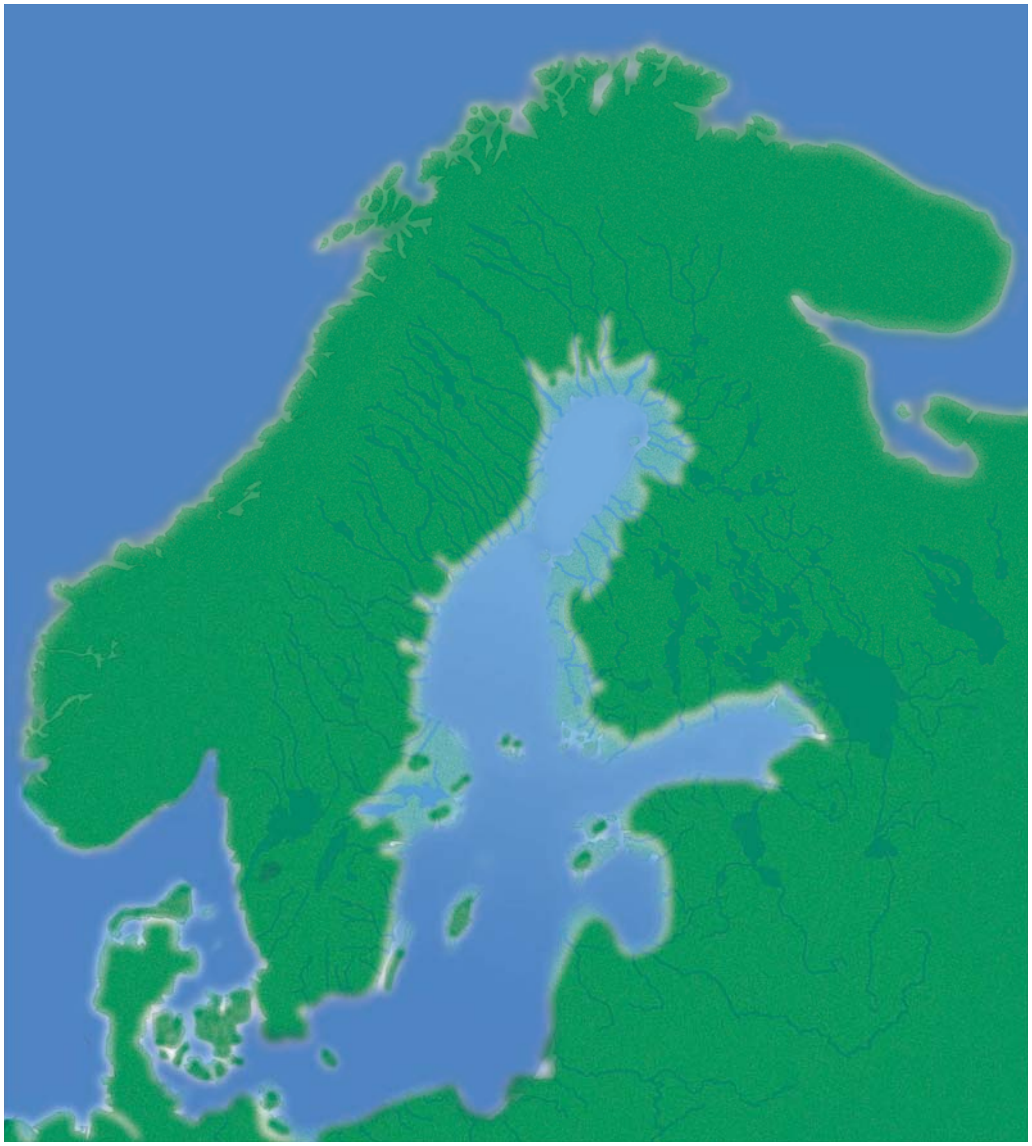

Figure F7. Distribution of microbial cells in the seabed. The double-logarithmic plot shows examples of cell numbers per cubic centimeter and how these decrease with the age of the sediment, ranging from a hundred years to a hundred million years. Cell counts from the Baltic Sea, 10^8–10^9 cells/cm^3, are compared to data from the Pacific Ocean where counts drop below 10^4 cells/cm^3 in the oldest sediments of the most nutrient poor area, the South Pacific Gyre. Data compiled from the Baltic Sea (B. Cragg and R.J. Parkes, unpubl. data), Ocean Drilling Program sites (D'Hondt et al., 2003), and the South Pacific Gyre (D'Hondt et al., 2009). Modified from Jørgensen (2012).

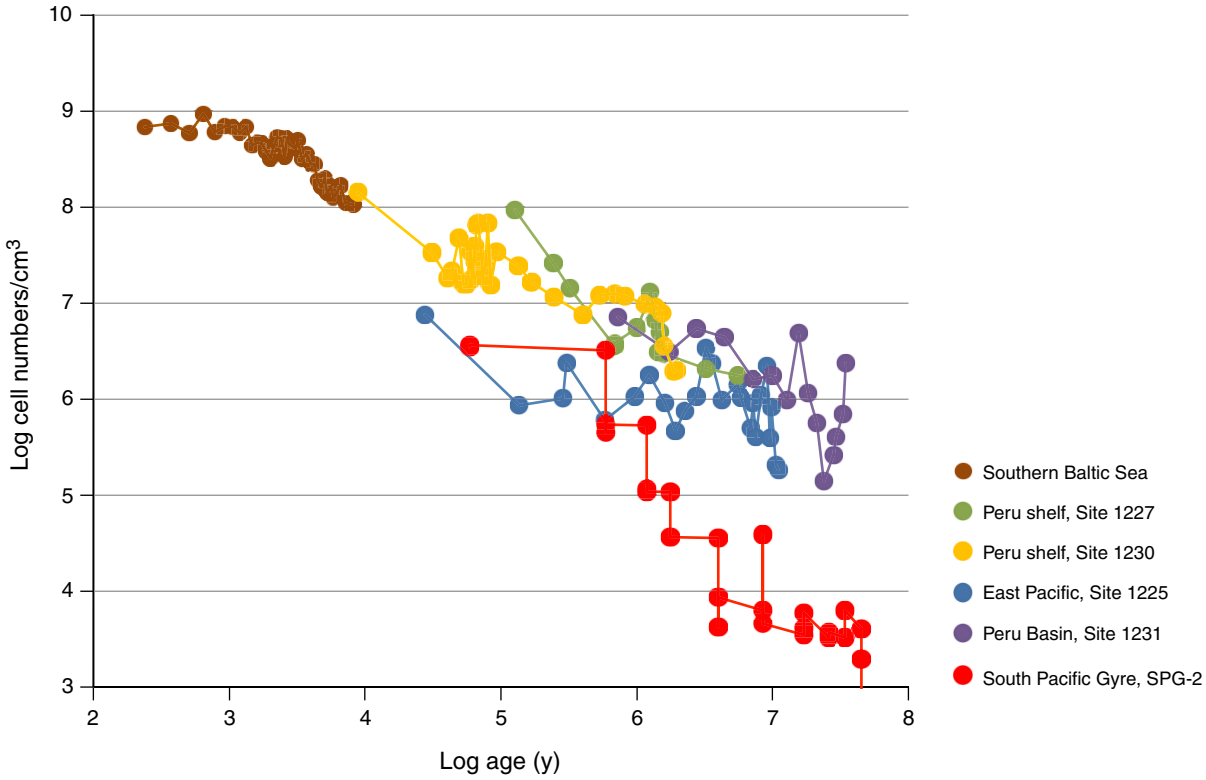

Figure F8. Single-beam bathymetry from the area around Site M0059 (red dot) in southern Little Belt. The overall depth difference across the area is ~6 m. Seismic Line DA98-31 is shown. TWT = two-way traveltime.

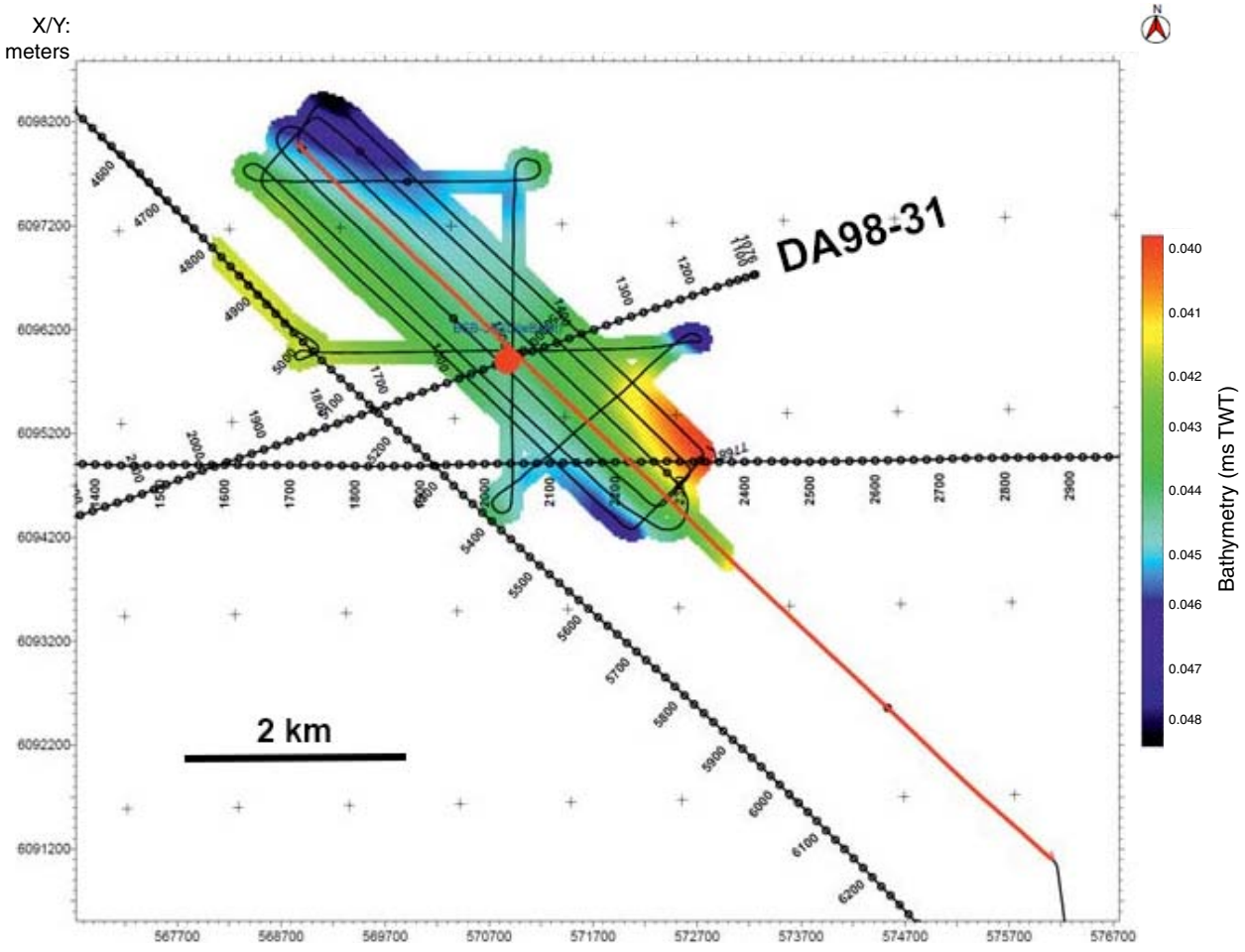

Figure F9. Seismic Line DA98-31 with location of Site M0059. Original interpretation of the seismic transect: SF = seafloor, LG2 = bottom of late glacial Unit II (varved glacial clay), BWT = bottom of Weichselian till, BR = bedrock. SP = shot point. TWT = two-way traveltime.

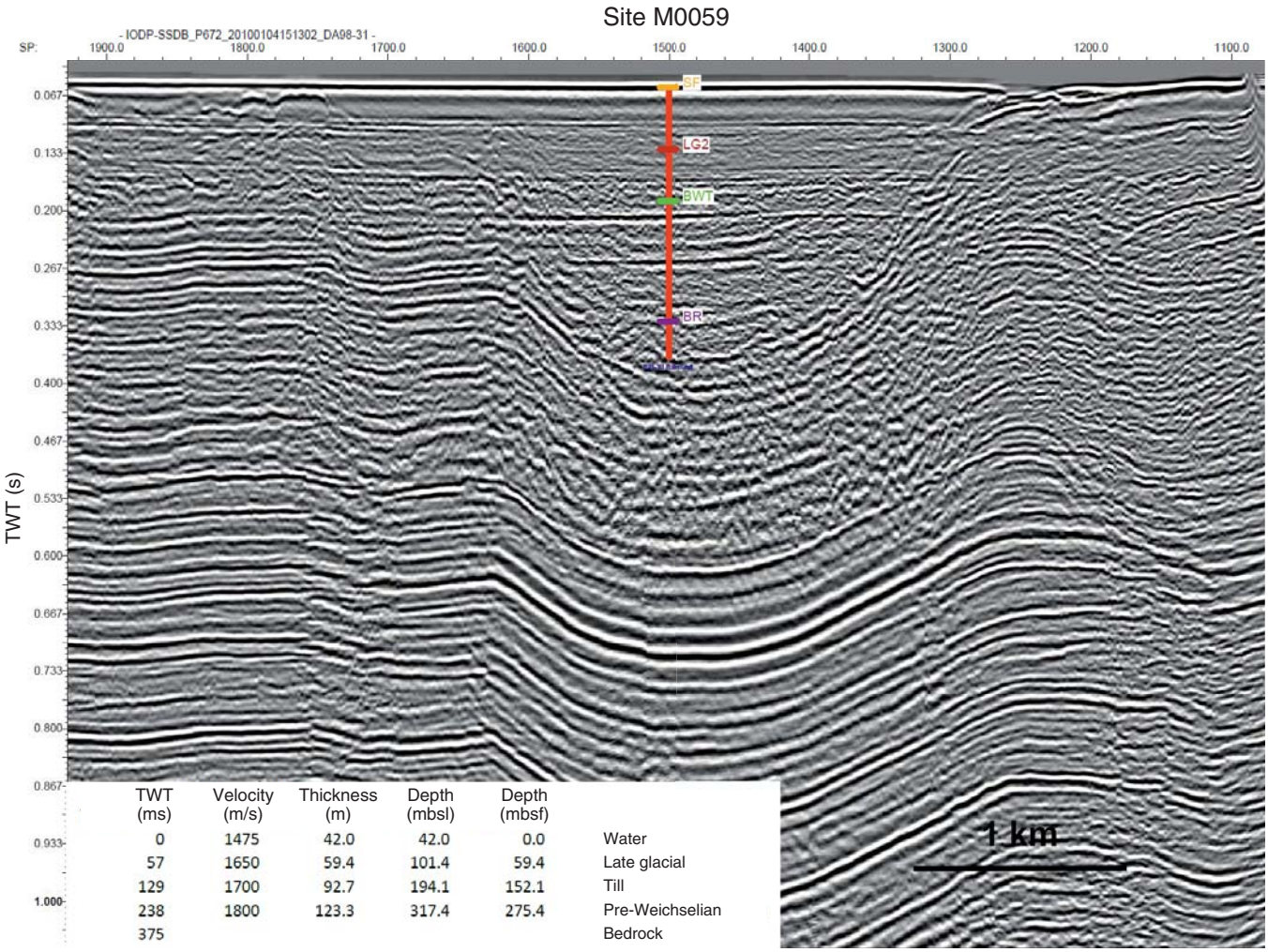

Figure F10. Seismic tracks from the area around Site M0067 (red dot). Multichannel seismic Line AL402-GeoB12-085 across proposed Site BSB-4 (green dot) is shown.

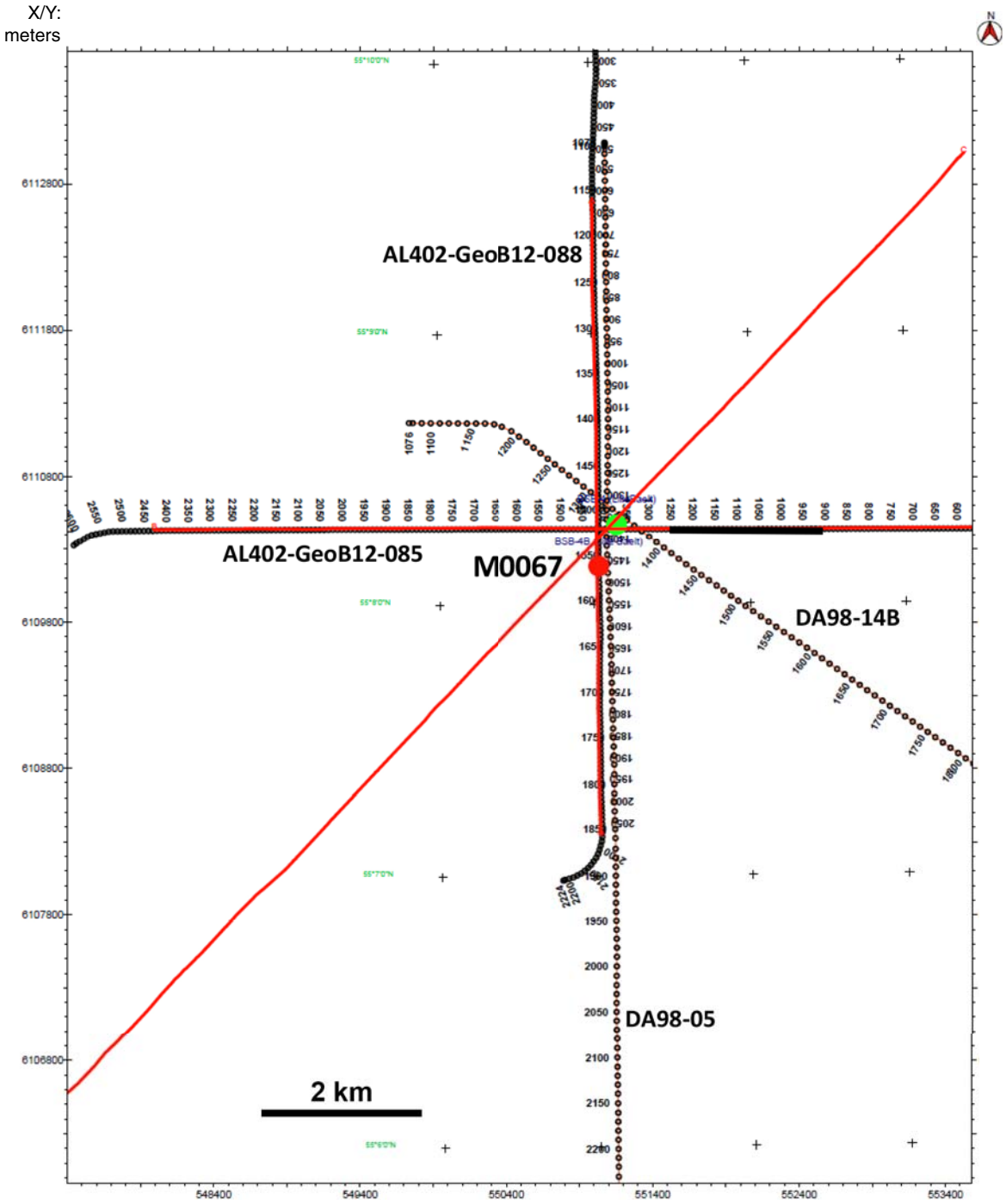

Figure F11. Seismic Line AL402-GeoB12-085 across proposed Site BSB-4 (green) and at ~250 m distance from Site M0067 (red). Original interpretation of the seismic transect: SF = seafloor, LG2 = bottom of latest glacial Unit II (varved glacial clay), BWT = bottom of Weichselian till, BR = bedrock. SP = shot point. TWT = two-way traveltime.

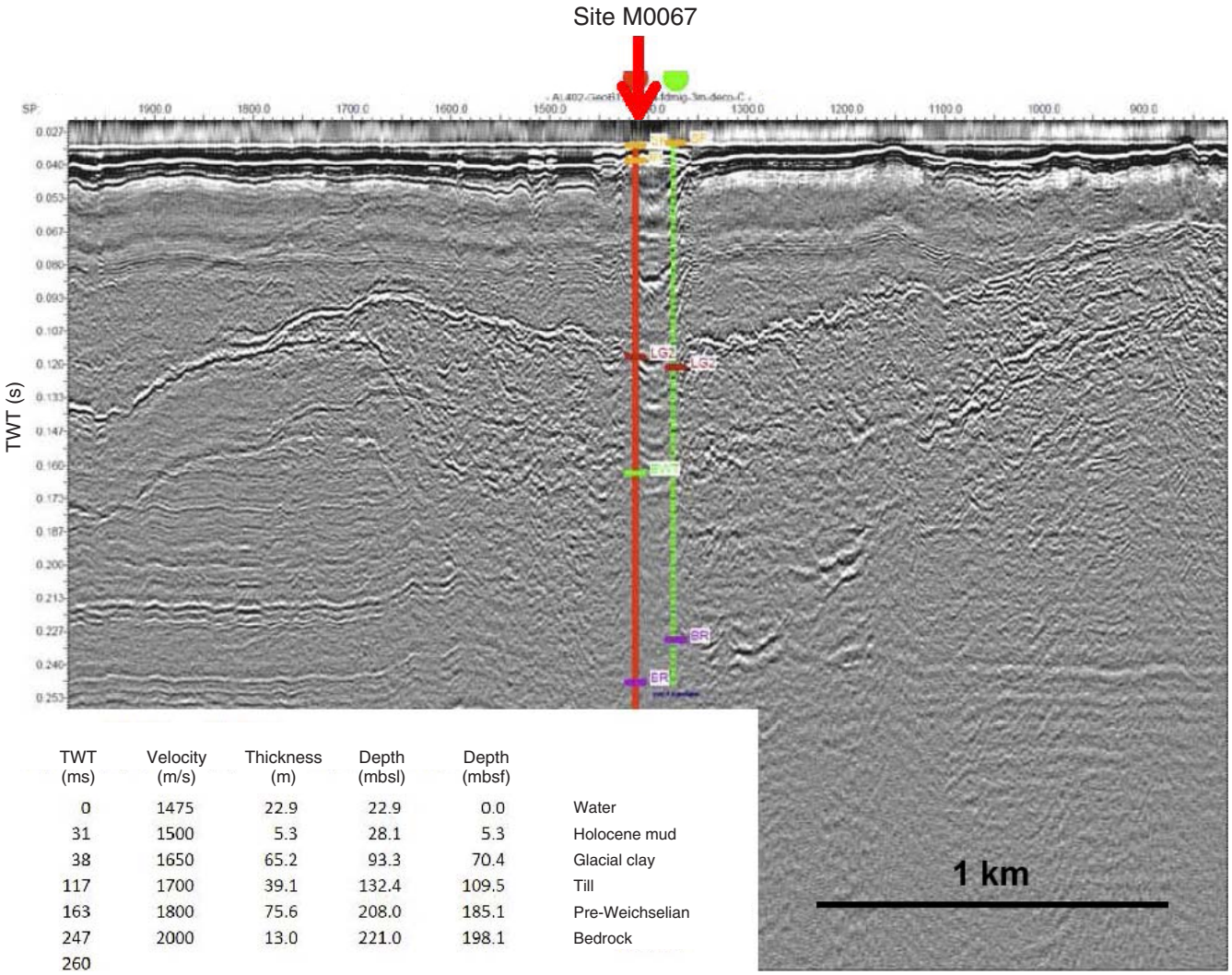

TWT (ms)	Velocity (m/s)	Thickness (m)	Depth (mbsl)	Depth (mbsf)	
0	1475	22.9	22.9	0.0	Water
31	1500	5.3	28.1	5.3	Holocene mud
38	1650	65.2	93.3	70.4	Glacial clay
117	1700	39.1	132.4	109.5	Till
163	1800	75.6	208.0	185.1	Pre-Weichselian
247	2000	13.0	221.0	198.1	Bedrock
260					

Figure F12. Pre-Quaternary surface topography (Jensen et al., 2002) across the proposed drilling area at Anholt. Detailed interpretation of the solid line (transect A–B) is shown in Figure **F13.**

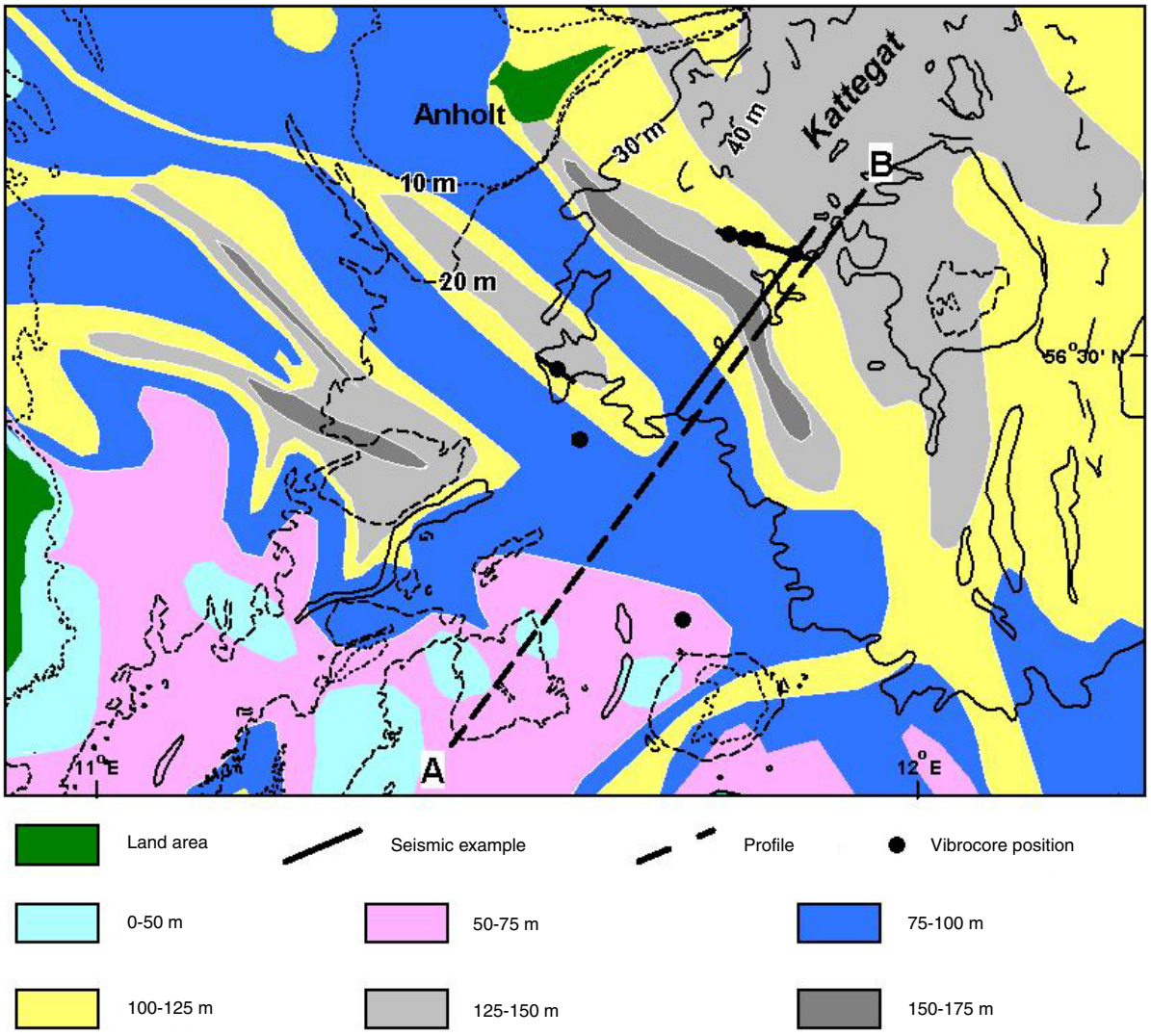

Figure F13. Interpreted cross section of a sparker profile from Jensen et al. (2002), running parallel to transect A–B (Fig. F12). Penetration is ~70 m, but the base of the depression was not imaged.

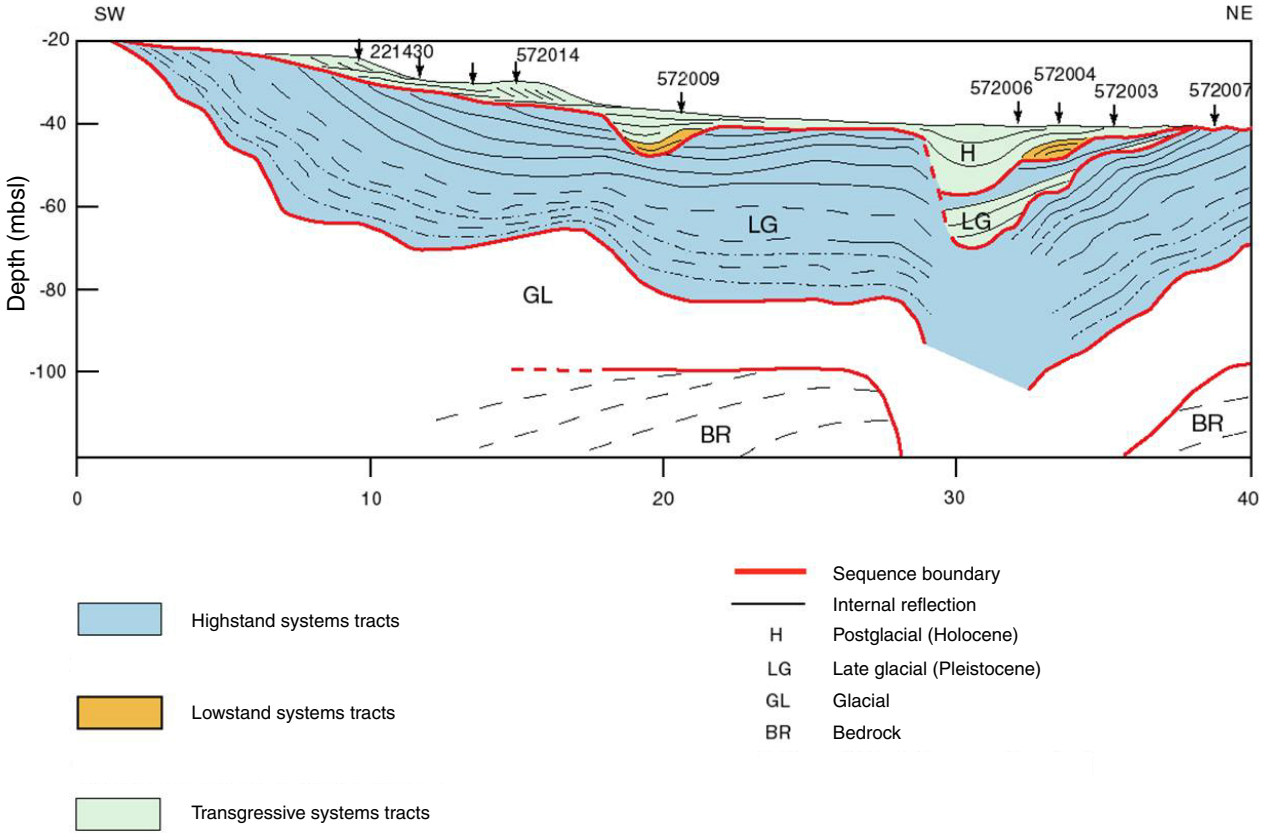

Figure F14. Chart of seismic tracks from the Anholt area. Purple lines = data from RV *Heincke* cruise He244 in 2006, light blue and black lines = data from RV *Alkor* cruise AL402 in 2012. Green dots indicate locations of originally proposed Sites BSB-1B and BSB-2B. Red dot = position of Site M0060 on seismic Line AL402-GeoB12-097.

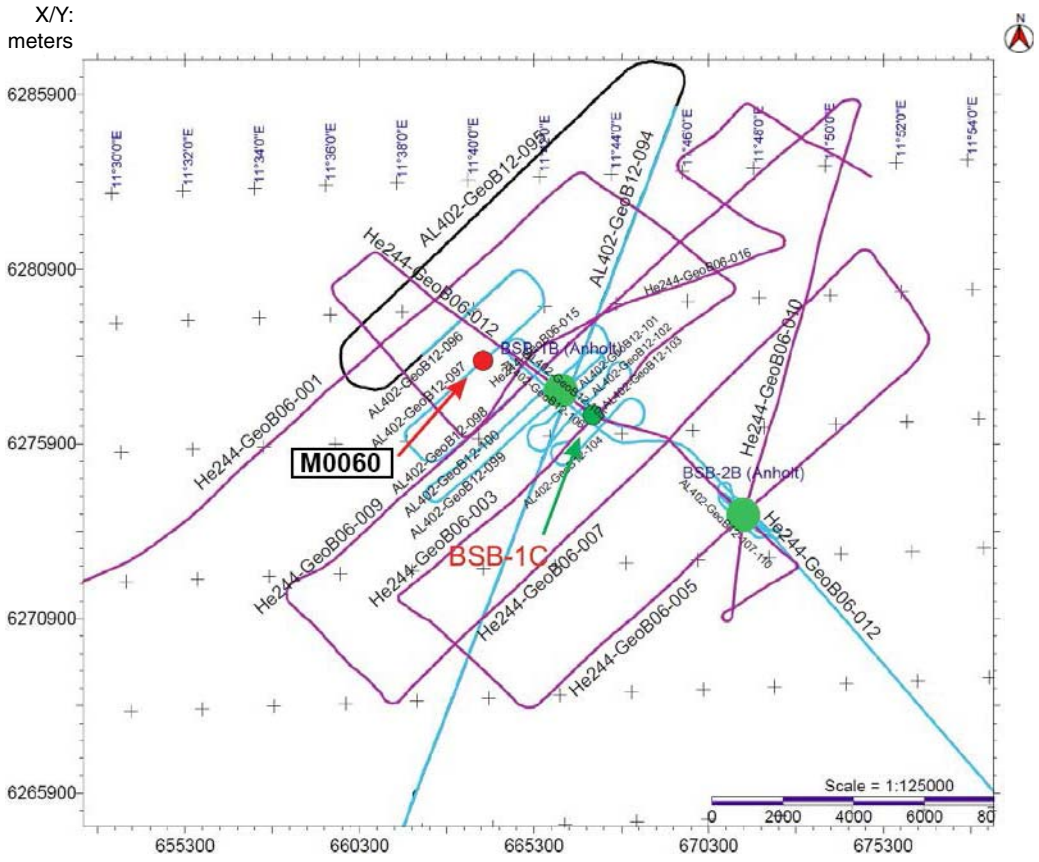

Figure F15. Seafloor reflection map in two-way traveltime (TWT), derived from SES echo sounder data from the Anholt area. Contour interval is 1 ms TWT (~0.75 m). Position of Site M0060 is shown (red dot).

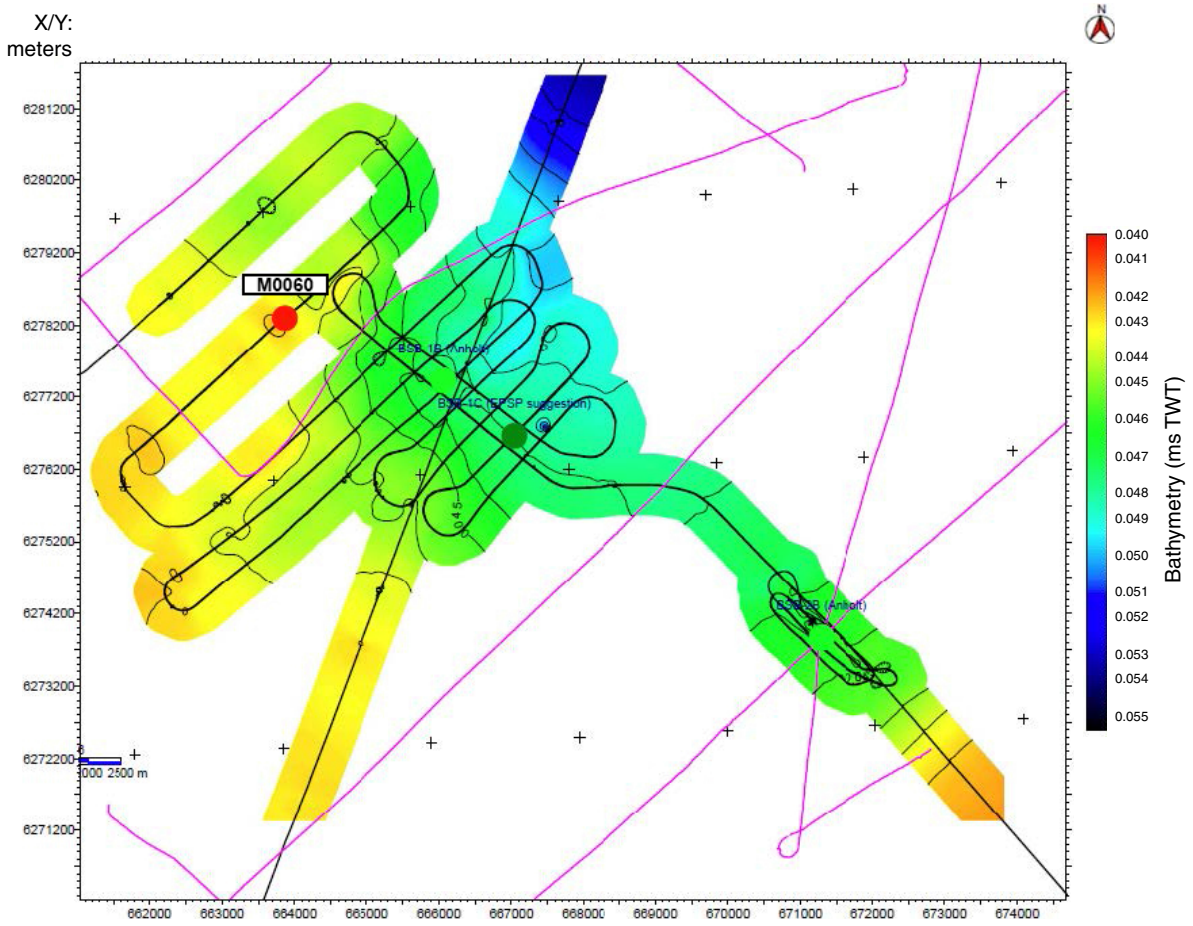

Figure F16. Seismic Line AL402-GeoB12-097 (Fig. F12) with location of Site M0060 (3 m common depth point spacing) and stratigraphic assignments. Reflectivity within the sequence is overall very low, and blanking is absent. Original interpretation of the seismic transect: SF = seafloor, LG1 = bottom of latest glacial Unit I, LG2 = bottom of latest glacial Unit II, BWT = bottom of Weichselian till, BR = bedrock. SP = shot point. TWT = two-way traveltime.

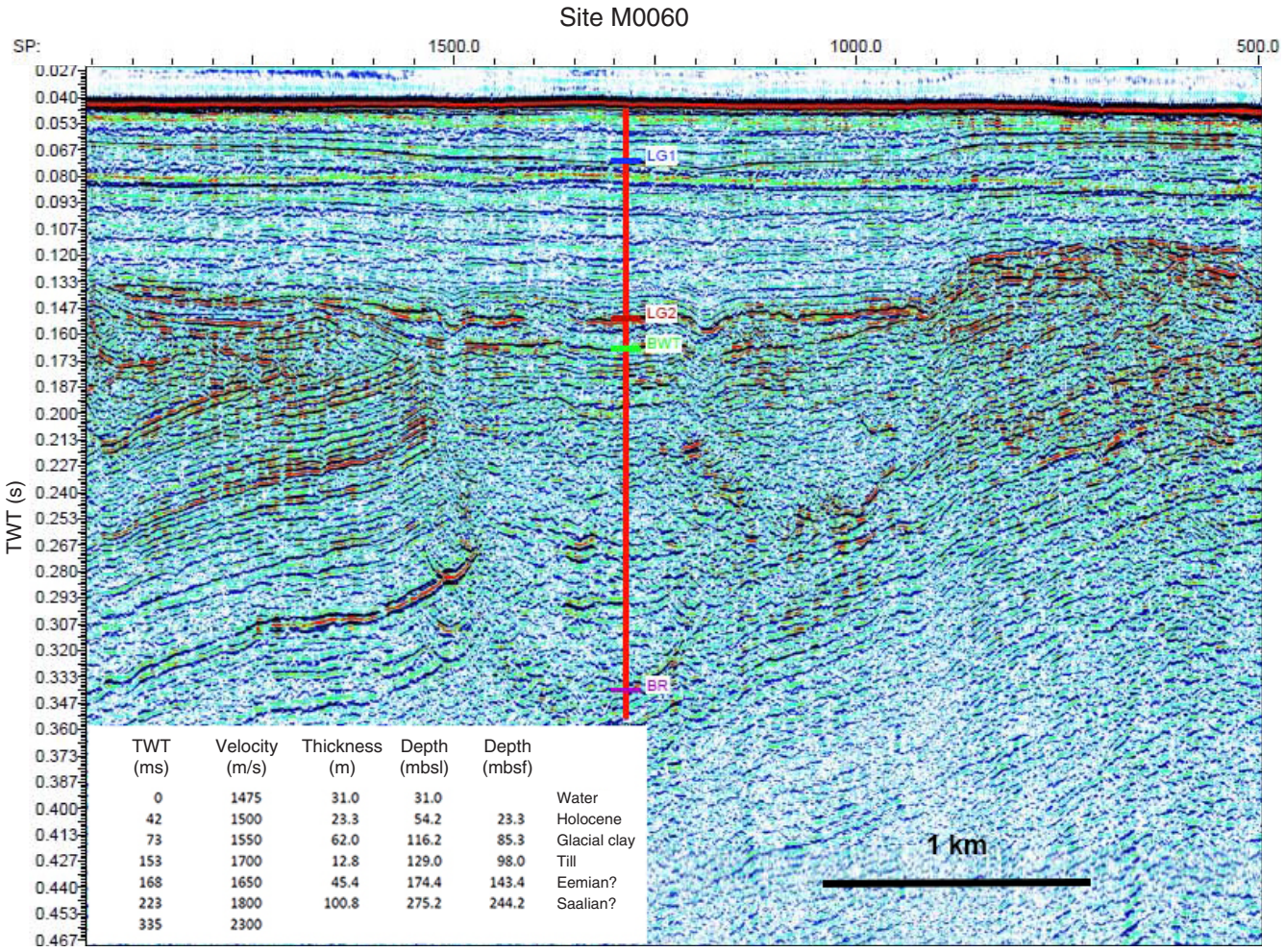

Figure F17. Seismic survey lines in the Ångermanälven River estuary around Site M0061 (yellow diamond), located at crossing Lines 71021316 and 71021335.

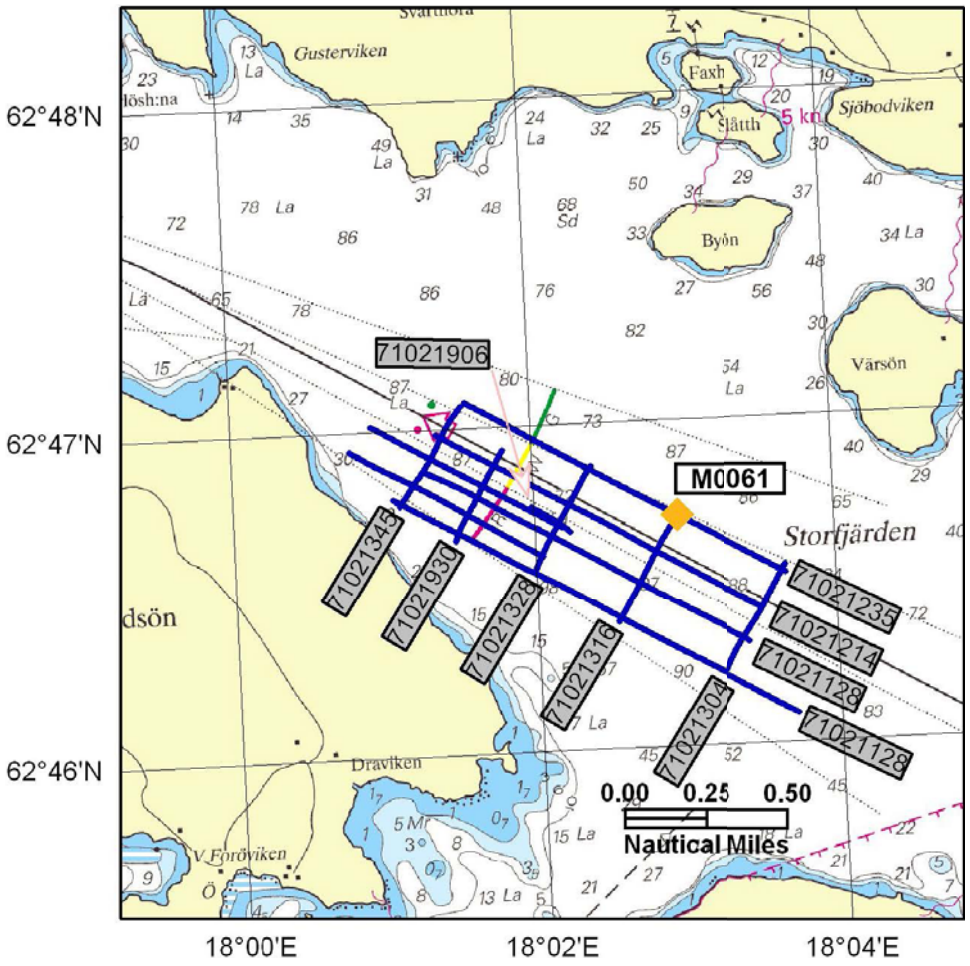

Figure F18. Bathymetry in the area surrounding Site M0061. Distance between isobaths is 5 m.

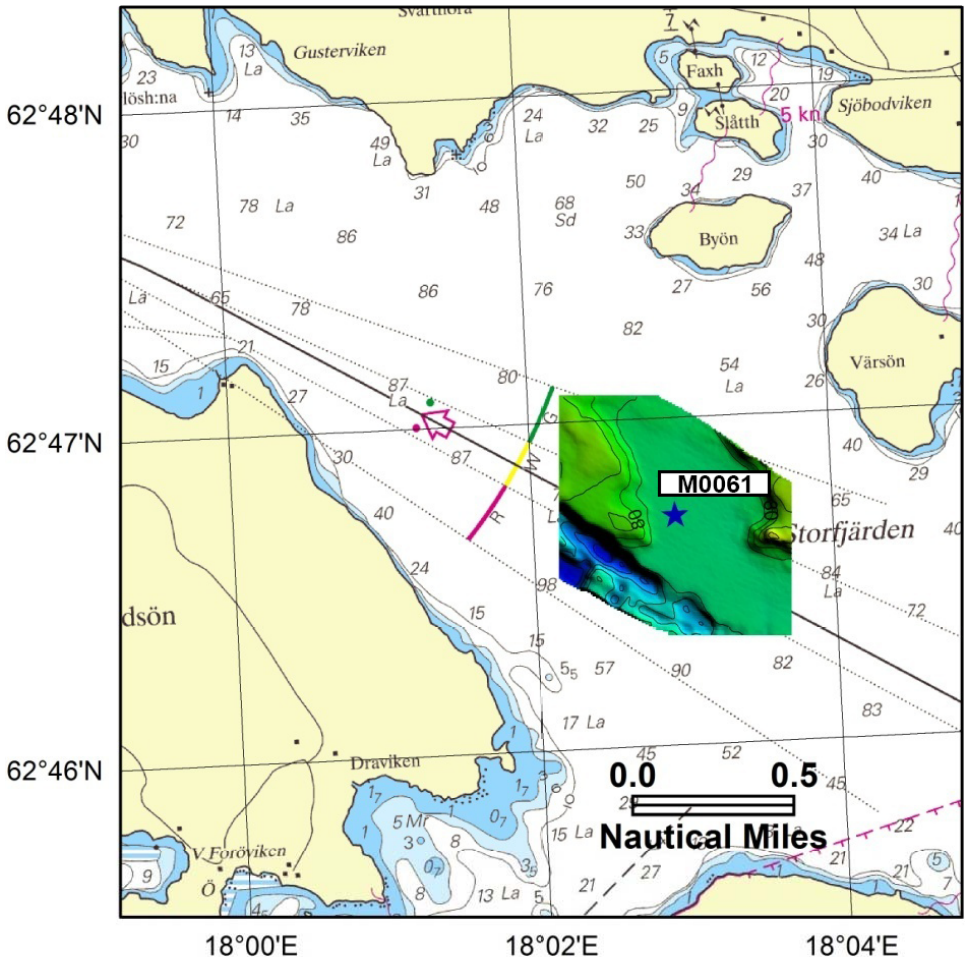

Figure F19. CHIRP sonar Profiles 71021316 and 71021235 crossing at Site M0061.

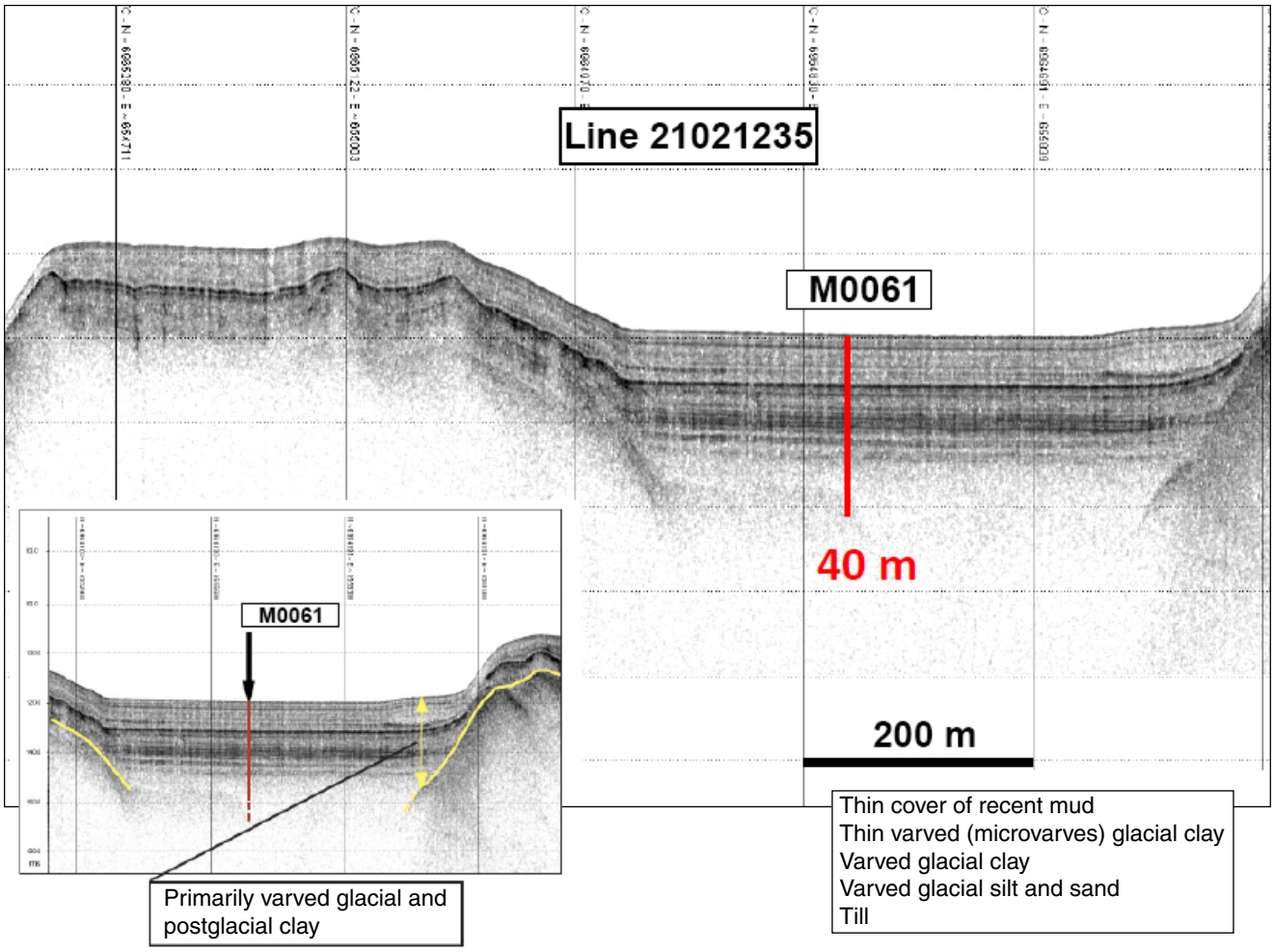

Figure F20. Seismic survey lines around Site M0062 (yellow diamond), located at crossing Lines 71021706 and 71021604.

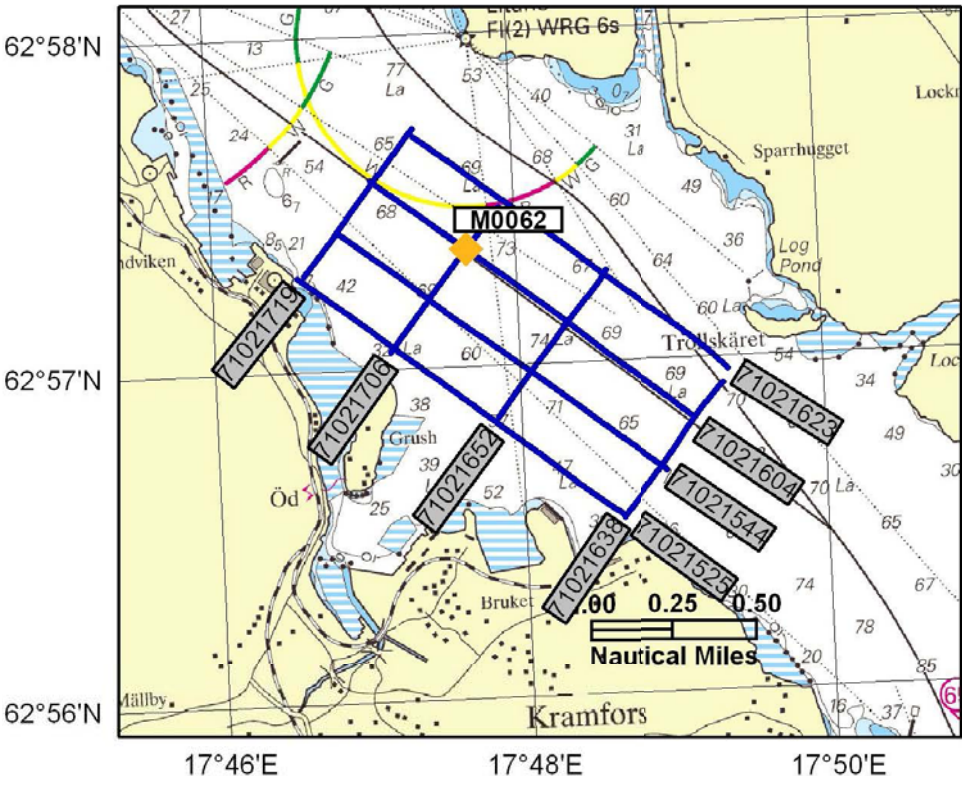

Figure F21. Bathymetry in the area surrounding Site M0062. Distance between isobaths is 5 m.

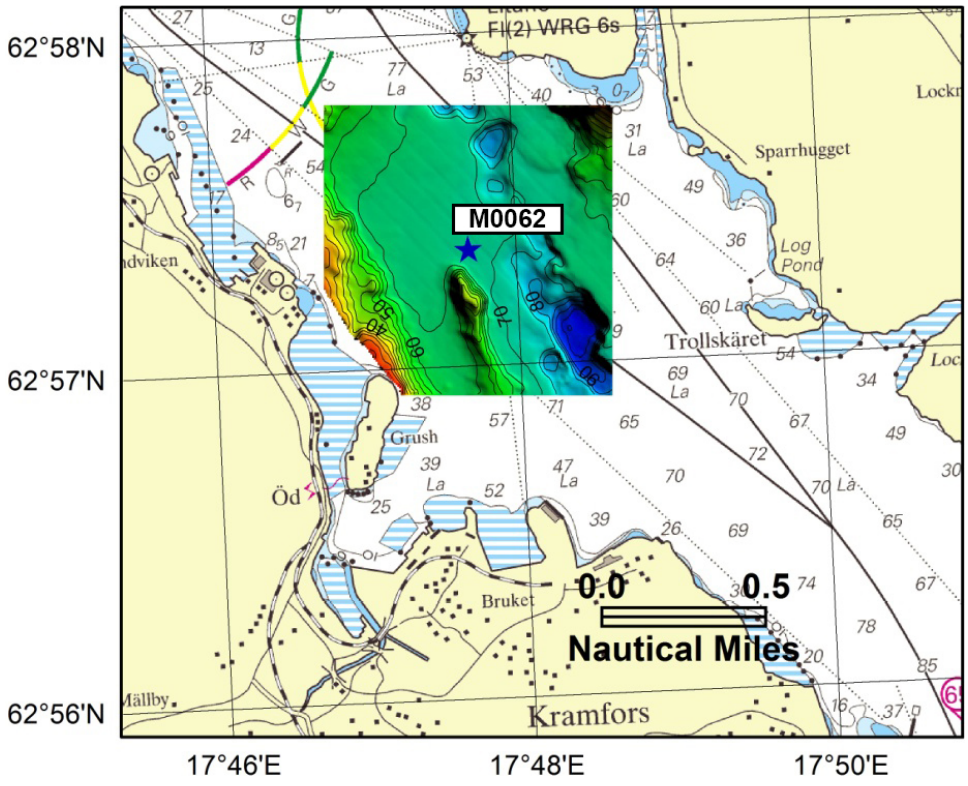

Figure F22. CHIRP sonar Profile 71021606 crossing Site M0062. TWT = two-way traveltime.

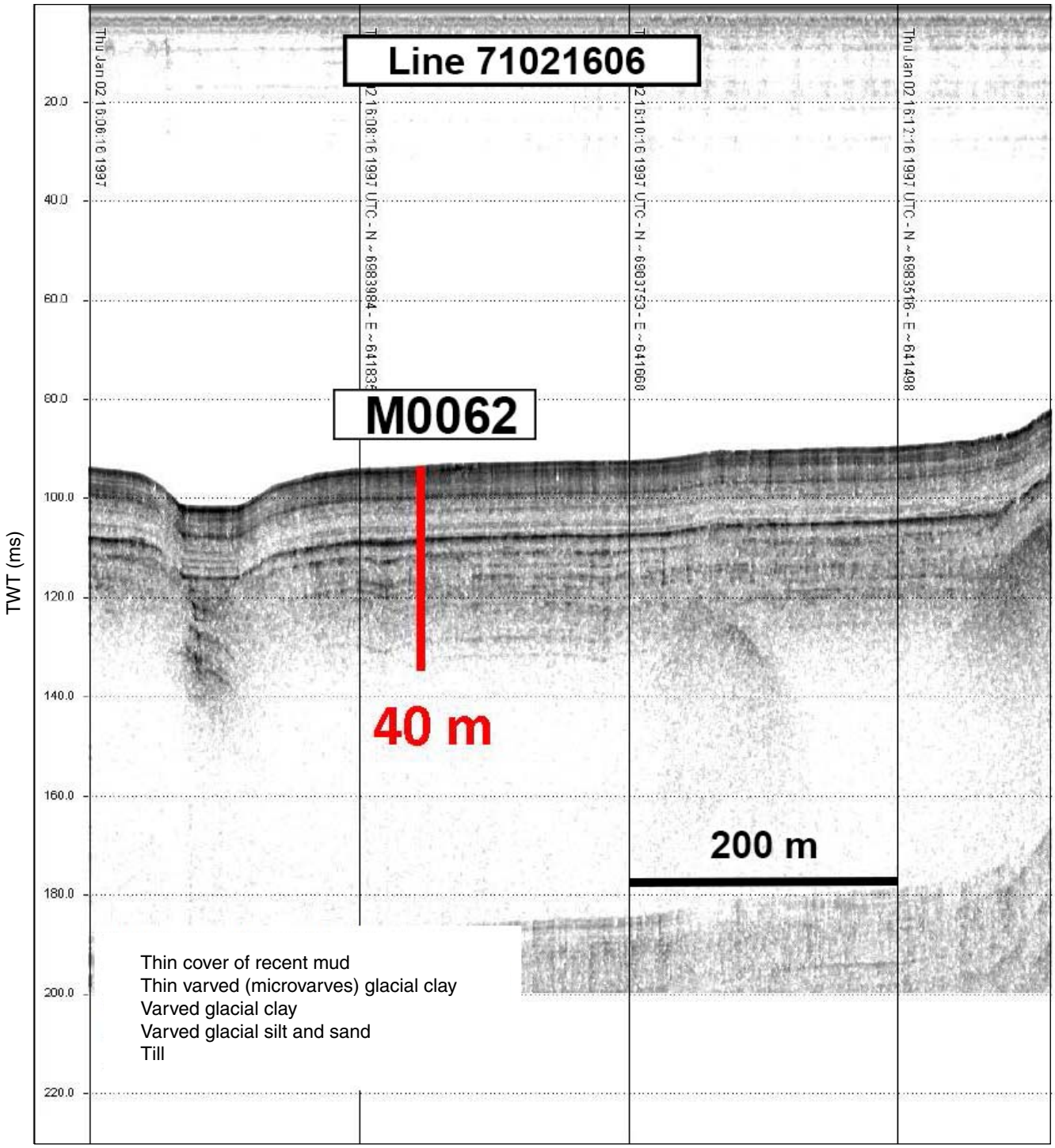

Figure F23. Map of the surface geology around Site M0063 (yellow diamond) in the Landsort Deep. Shot points are shown at even increments of 200. SGU = Geological Survey of Sweden.

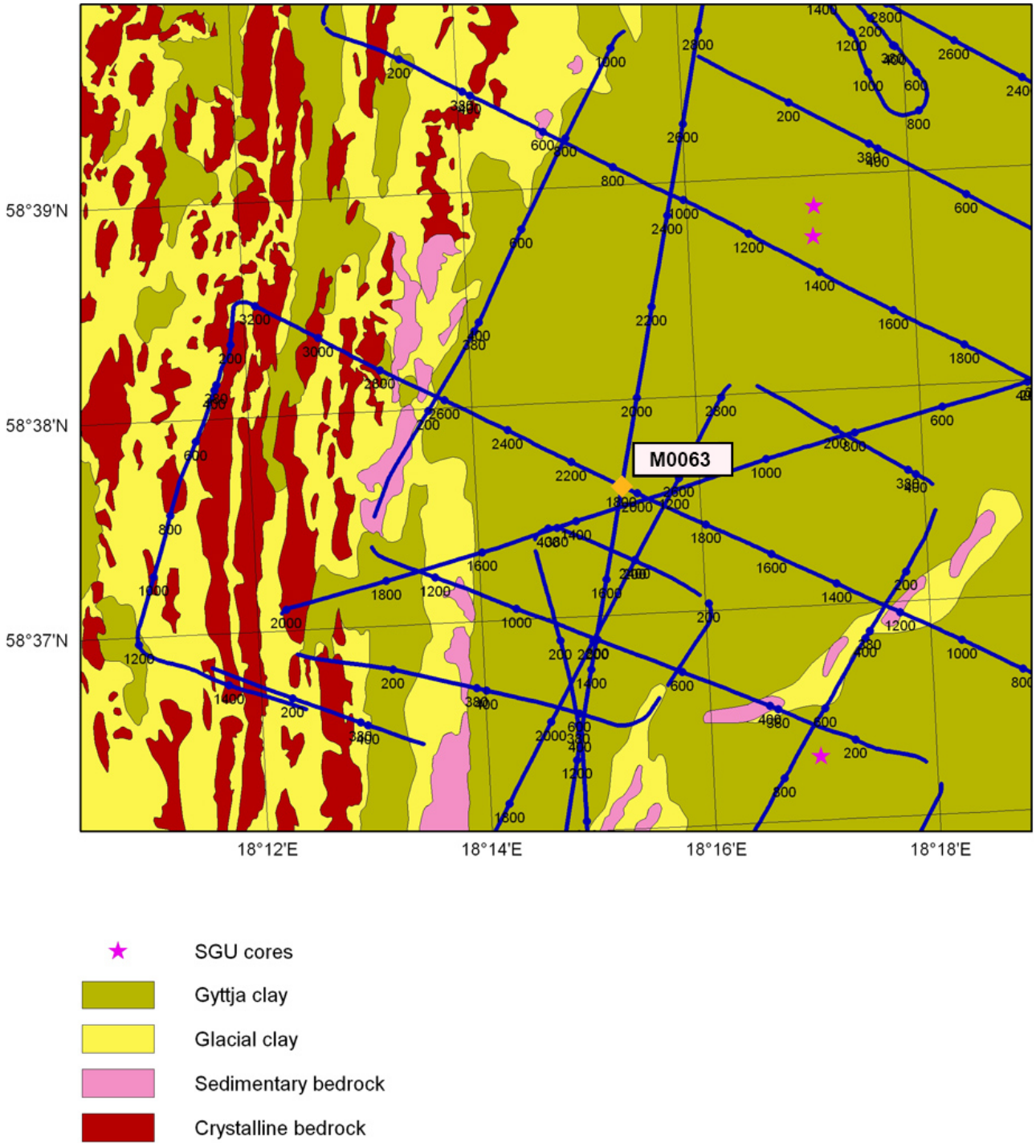

Figure F24. Track plot of seismic survey lines in the Landsort Deep around Site M0063 (yellow diamond). Distance between isobaths is 100 m. ODAS = Oceanographic Data Acquisition Systems.

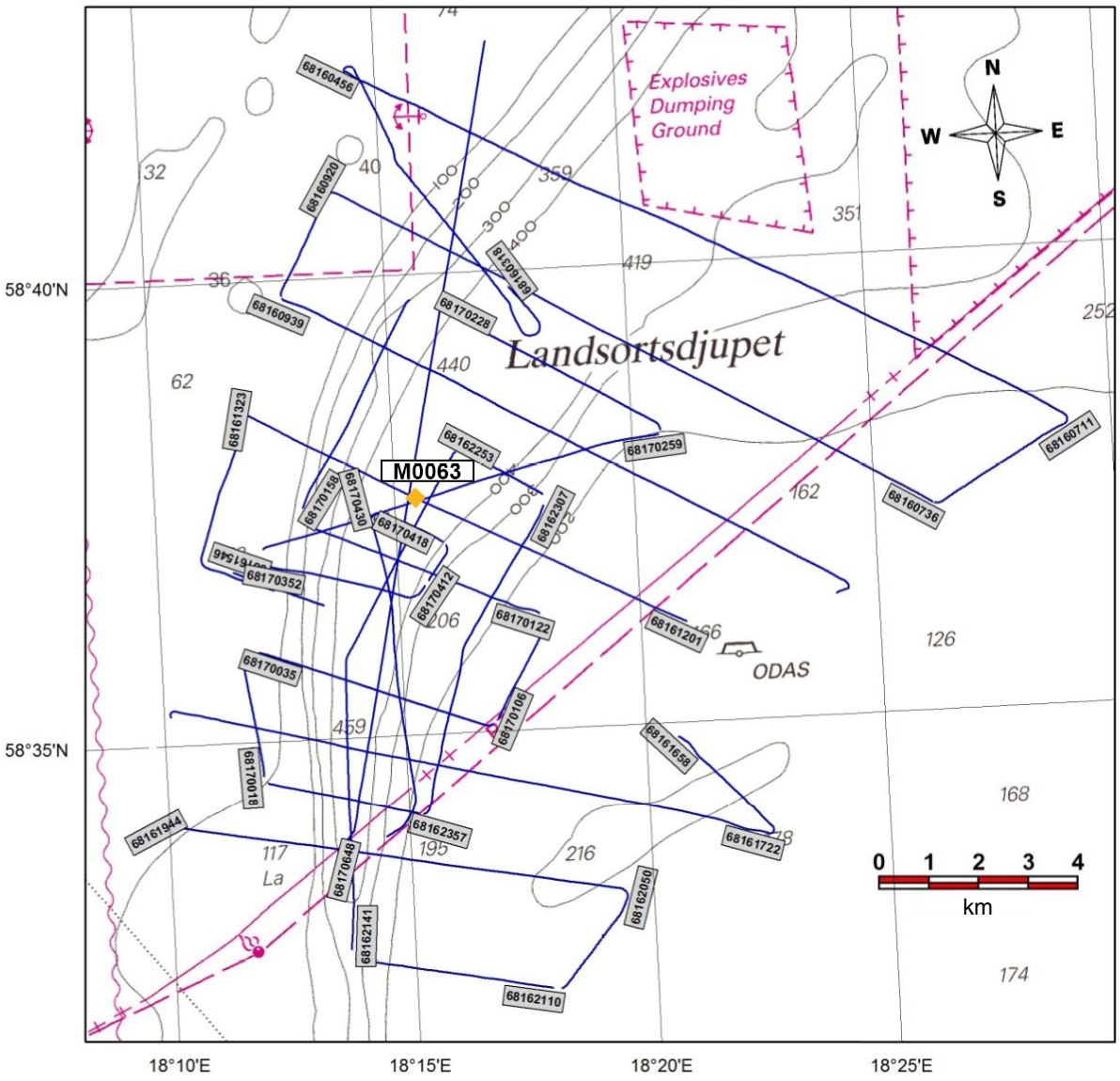

Figure F25. Close-up of transect along seismic Line 68161201, crossing Site M0063, with original interpretation of seismic signals. TWT = two-way traveltime.

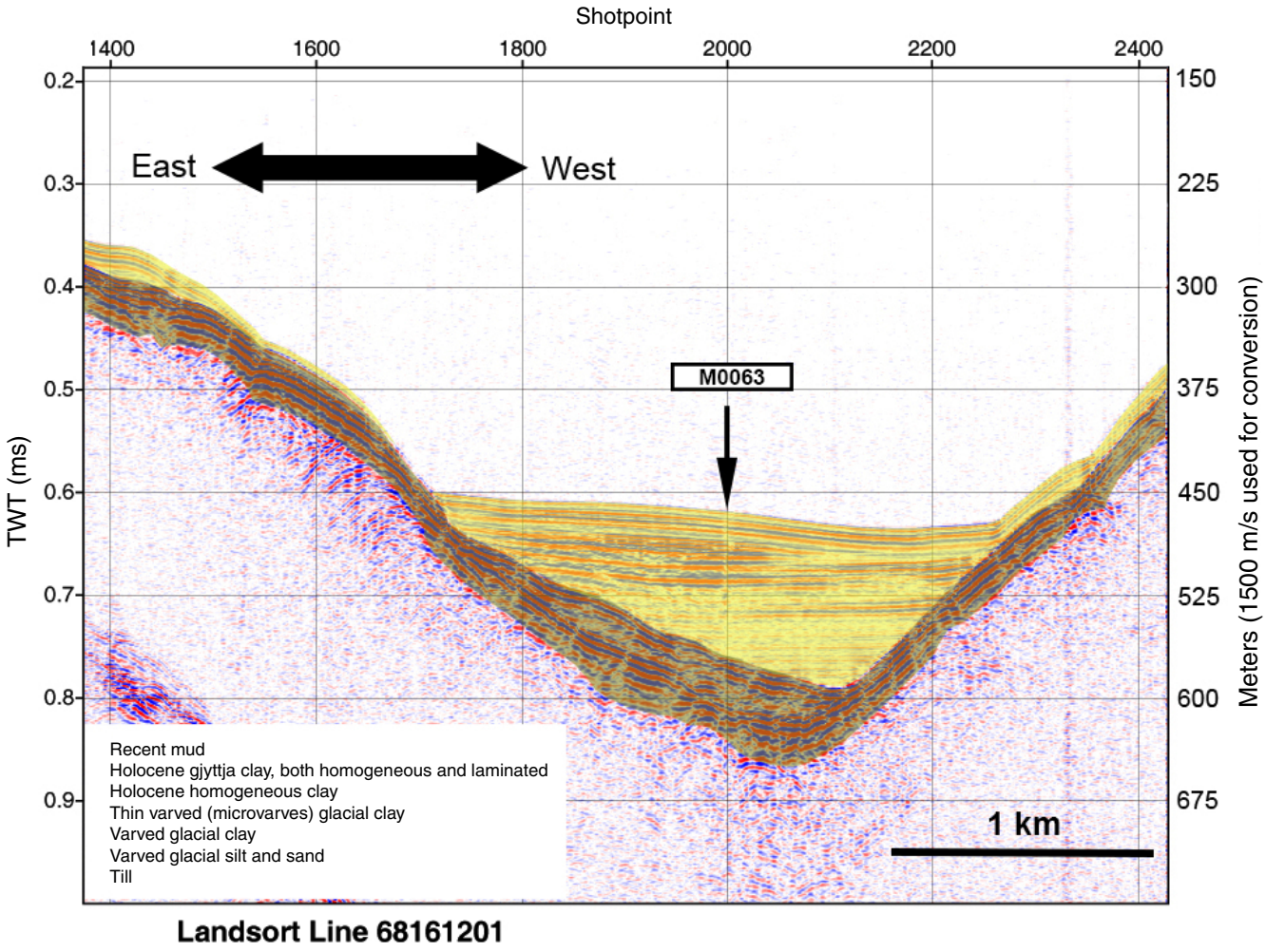

Figure F26. Bathymetry from multichannel seismic data in two-way traveltime (TWT). Terrain slopes down southward. In the vicinity of drill Site M0064 (red dot on left), no anomalous features were observed in seismic or echo sounder data. Contour interval is 10 ms TWT. Alternate Site BSB-6 (red dot on right) is also shown.

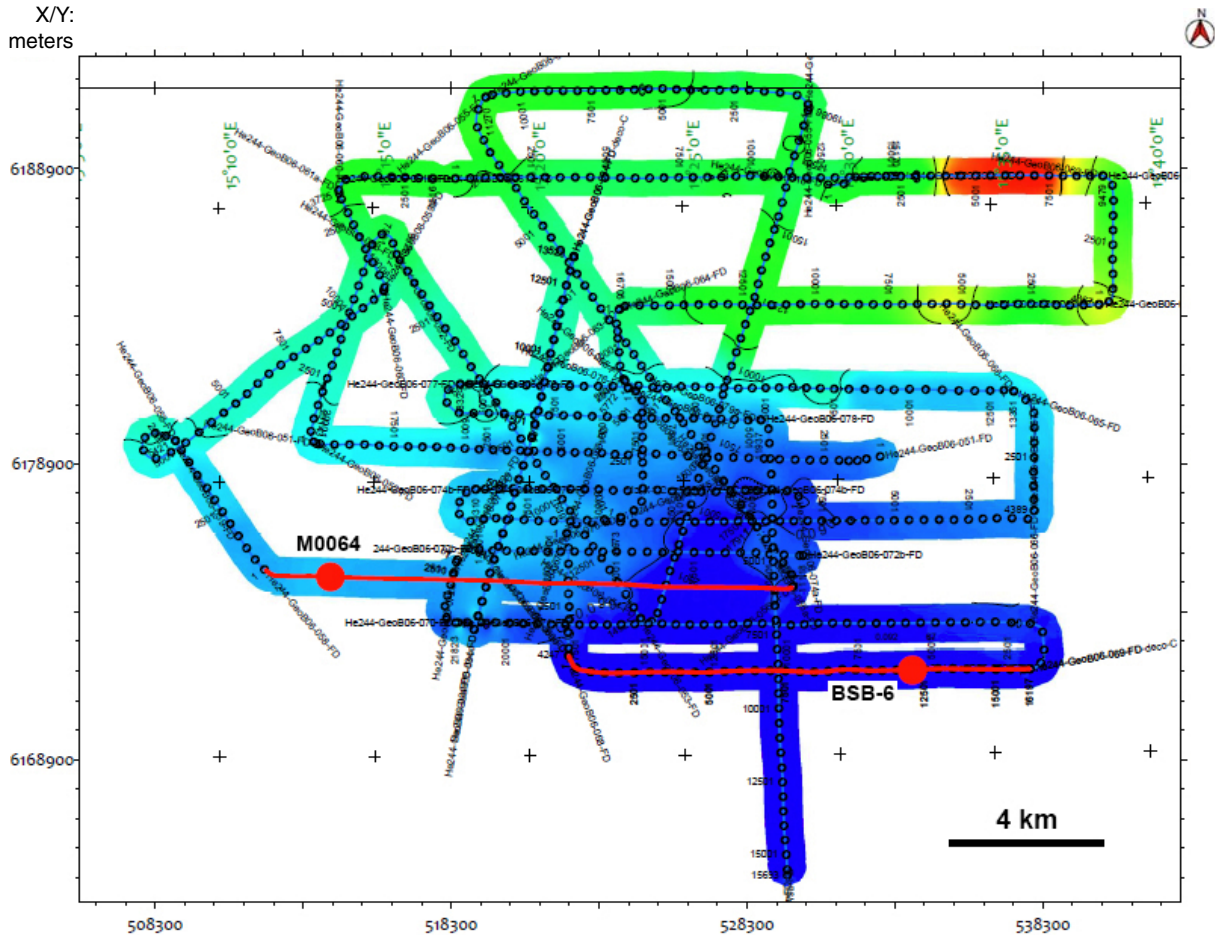

Figure F27. Multibeam bathymetry around Site M0064 (red dot).

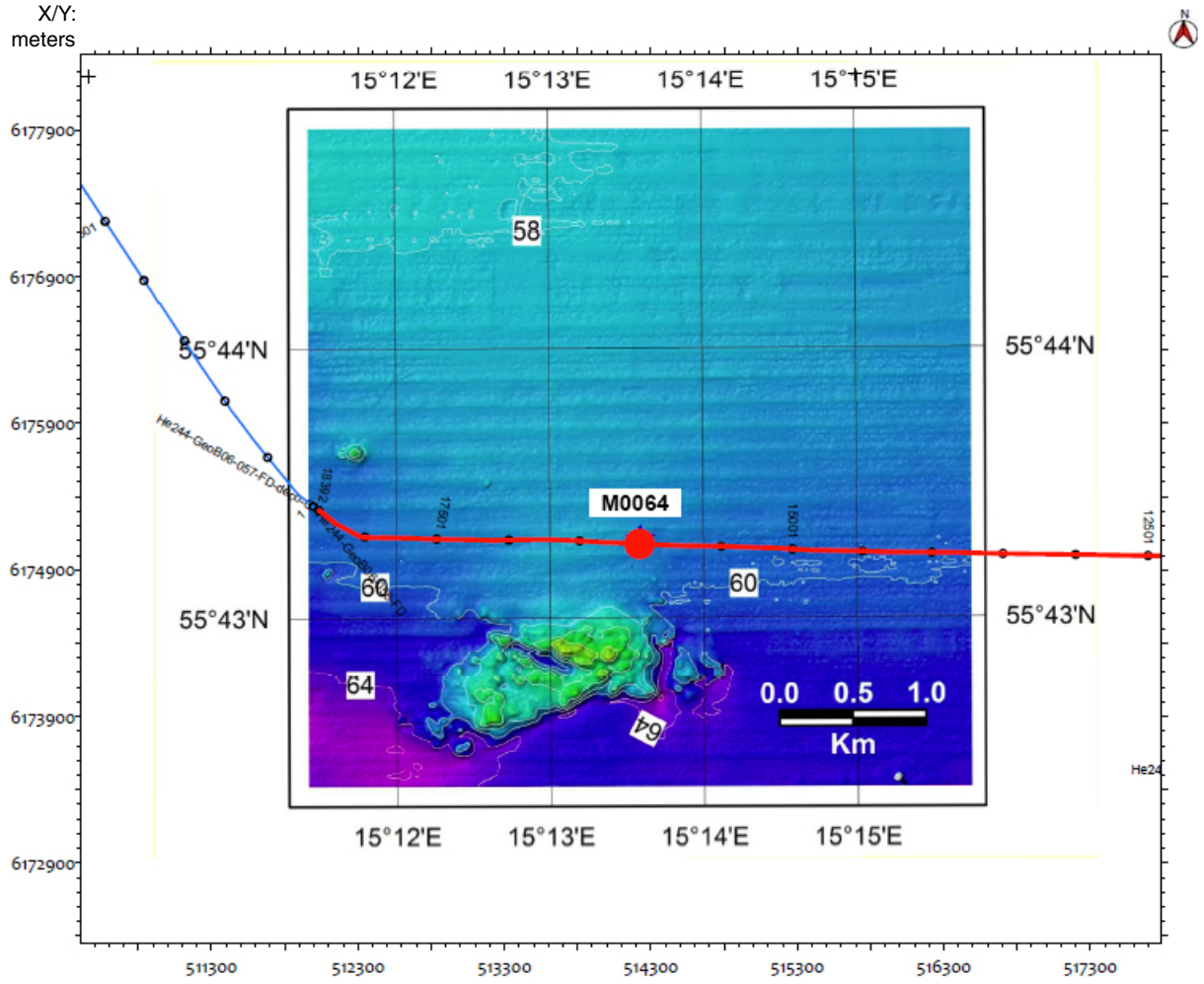

Figure F28. Close-up of seismic Line He244-GeoB06-057 across Site M0064. Original interpretation of the seismic transect: SF = seafloor, BH = bottom of Holocene, BWT = bottom of Weichselian till, BR = bedrock. SP = shot point. TWT = two-way traveltime.

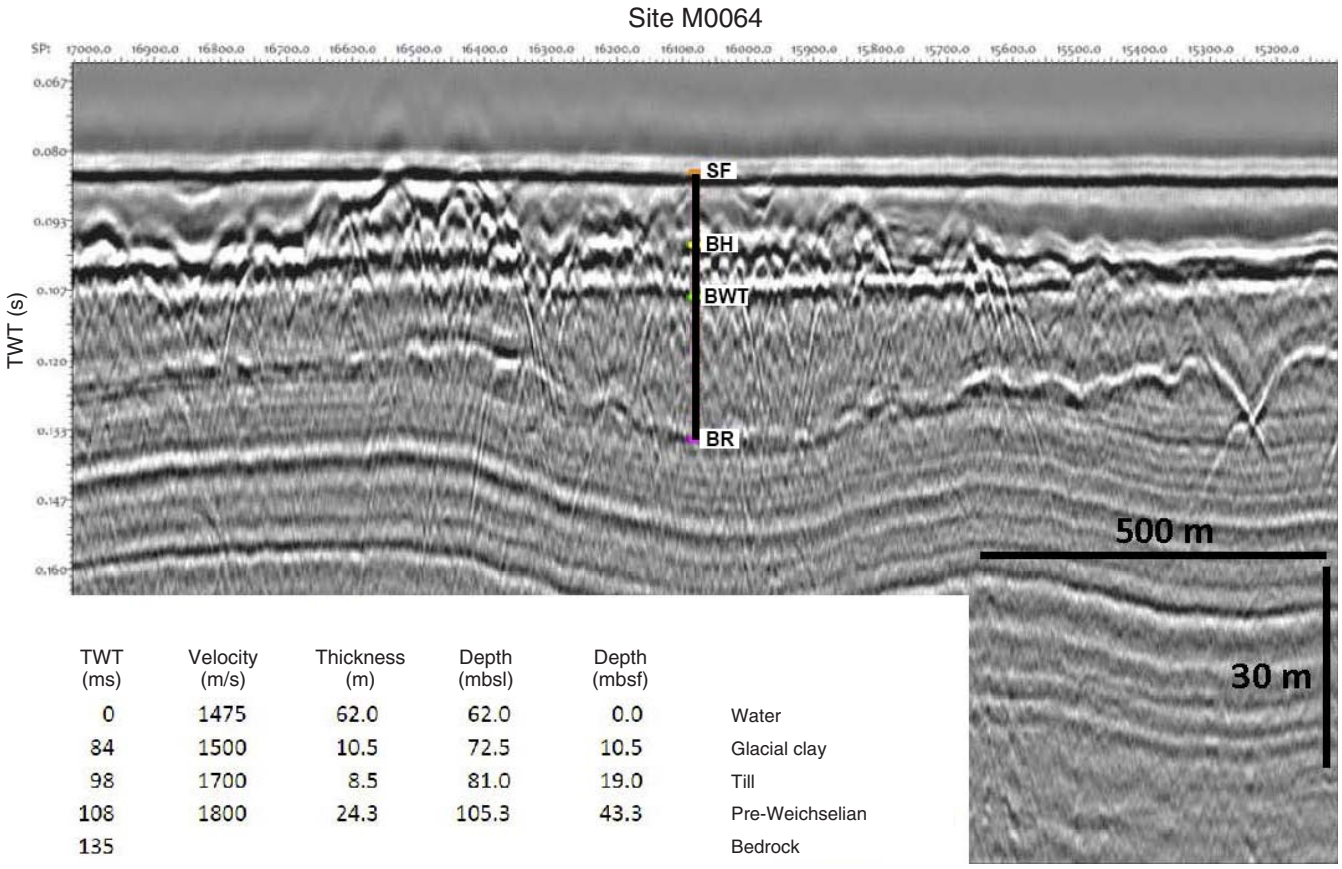

TWT (ms)	Velocity (m/s)	Thickness (m)	Depth (mbsl)	Depth (mbsf)	
0	1475	62.0	62.0	0.0	Water
84	1500	10.5	72.5	10.5	Glacial clay
98	1700	8.5	81.0	19.0	Till
108	1800	24.3	105.3	43.3	Pre-Weichselian
135					Bedrock

Figure F29. Detailed seismic track chart in the Bornholm Basin around Sites M0065 and M0066 (yellow squares). Green line = boundary of the ammunition dump area located to the southeast. Shallow gas may occur in the area delimited by the two dotted lines. In order to avoid any disturbances from gas, Sites M0065 and M0066 were located outside this area.

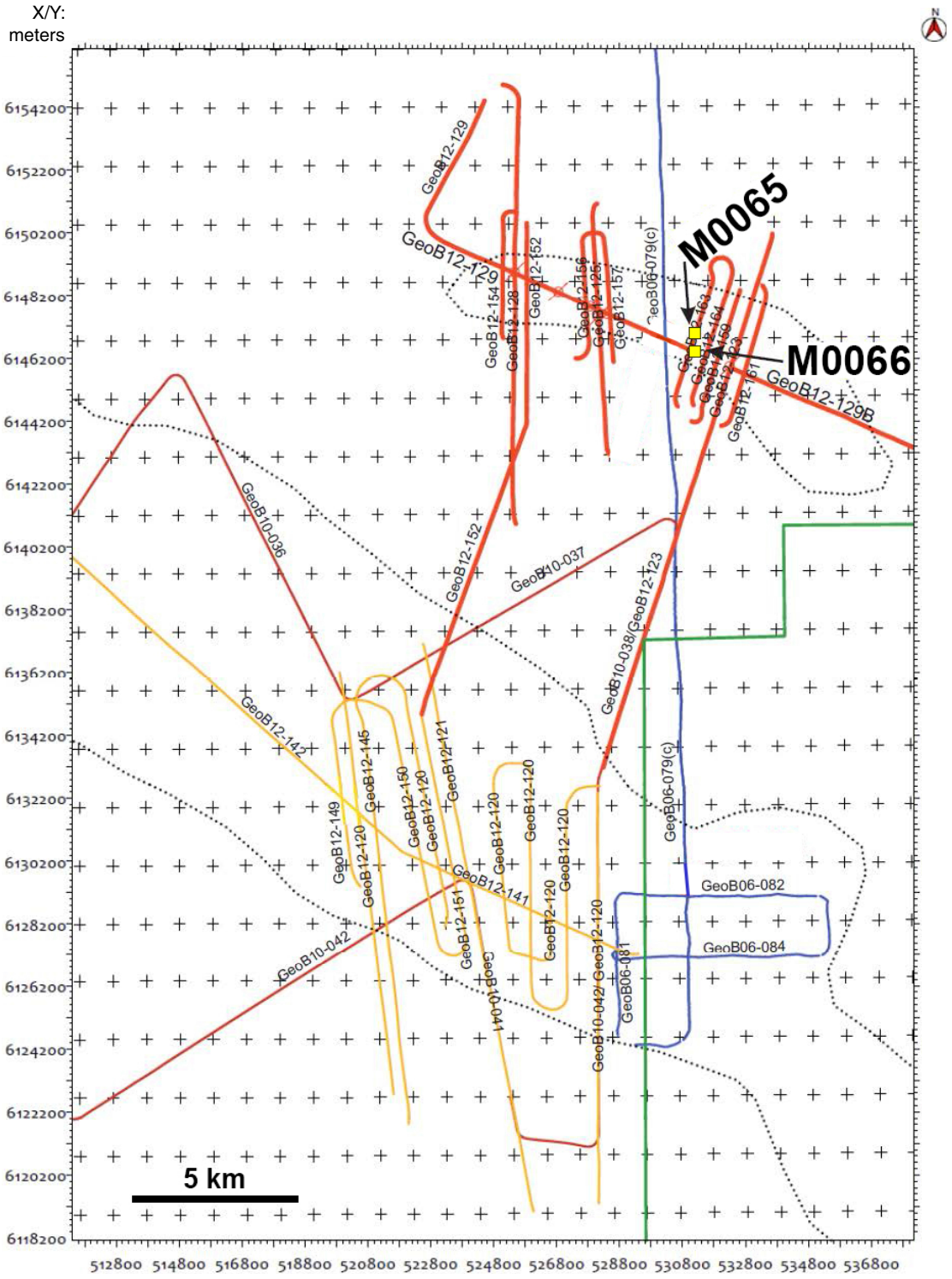

Figure F30. Seismic Line AL402-GeoB12-163 across Site M0065. Original interpretation of the seismic transect: SF = seafloor, BH = bottom of Holocene, LG1 = bottom of latest glacial Unit I, LG2 = bottom of latest glacial Unit II (Baltic Ice Lake), BR = bedrock. SP = shot point. TWT = two-way traveltime.

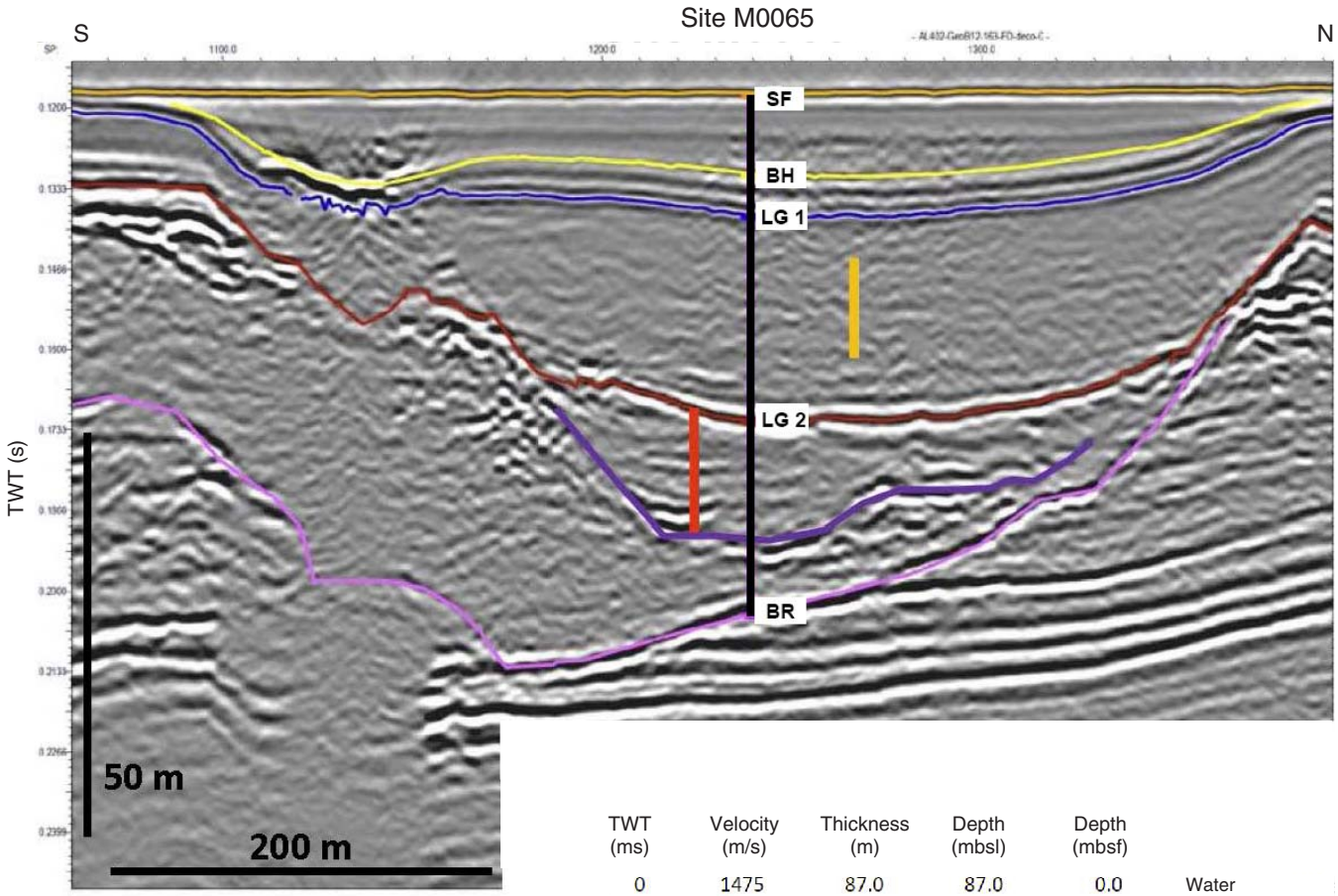

TWT (ms)	Velocity (m/s)	Thickness (m)	Depth (mbsl)	Depth (mbsf)	
0	1475	87.0	87.0	0.0	Water
118	1500	9.8	96.8	9.8	Holocene
131	1650	5.8	102.6	15.5	Late glacial
138	1700	28.9	131.5	44.4	Baltic Ice Lake
172	2000	32.0	163.5	76.4	Pre-Weichselian
204					Bedrock

Figure F31. Seismic Line AL402-GeoB12-129 across Site M0066. Original interpretation of the seismic transect: SF = seafloor, LG2 = bottom of latest glacial Unit II (Baltic Ice Lake), BR = bedrock. SP = shot point. TWT = two-way traveltime.

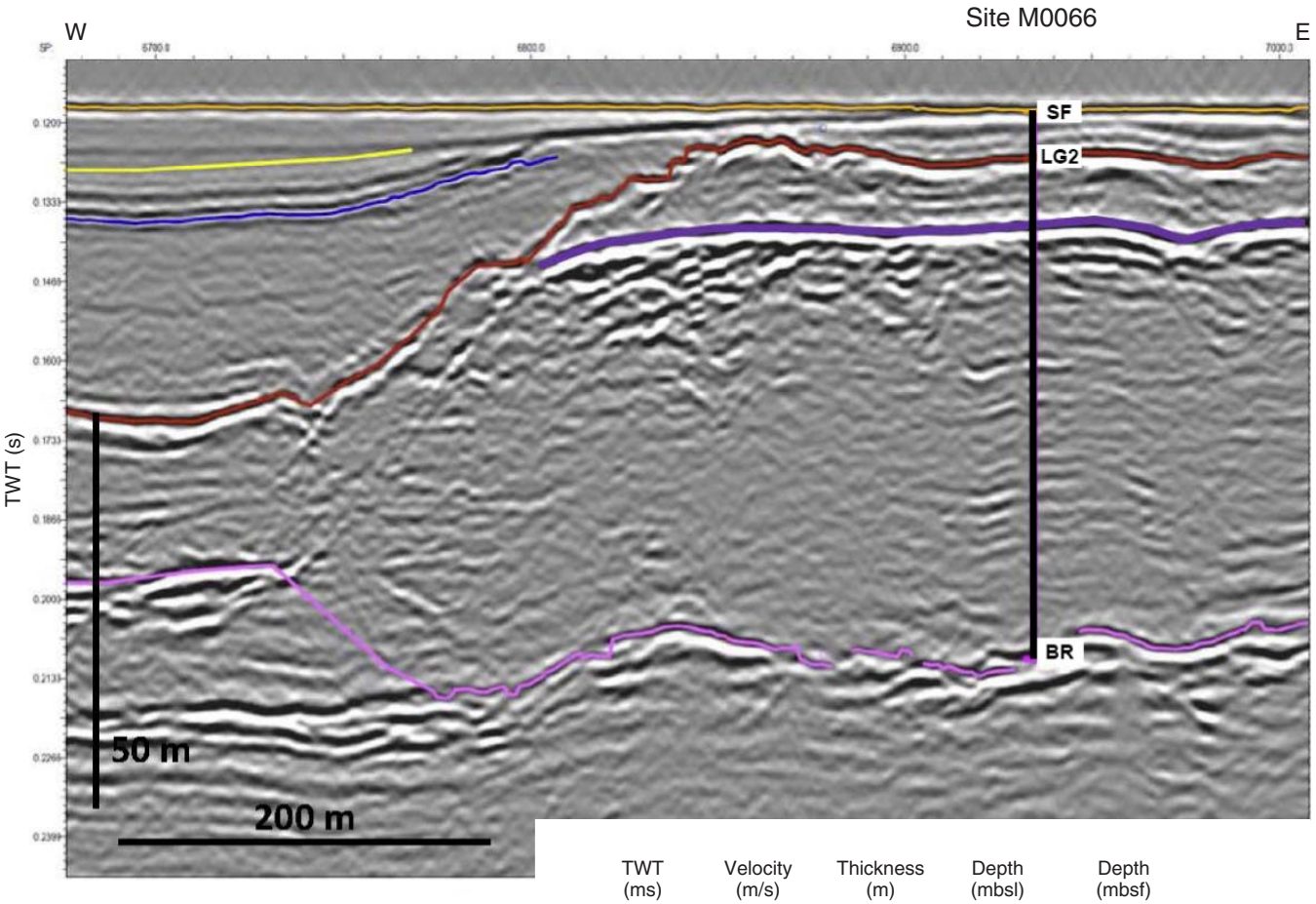

TWT (ms)	Velocity (m/s)	Thickness (m)	Depth (mbsl)	Depth (mbsf)	
0	1475	87.0	87.0	0.0	Water
118	1700	6.8	93.8	6.8	Baltic Ice Lake
126	2000	84.0	177.8	90.8	Pre-Weichselian
210					Bedrock

Figure F32. Polar diagrams of declination and inclination data obtained from discrete samples after alternating field demagnetization at 5 mT. Solid blue squares = normal polarity natural remanent magnetization (NRM) (positive inclinations), open red squares = reversed NRM (negative inclinations). Magenta circles = predictions of a geocentric axial dipole for the highest (inner) and lowest (outer) site latitudes drilled during Expedition 347.

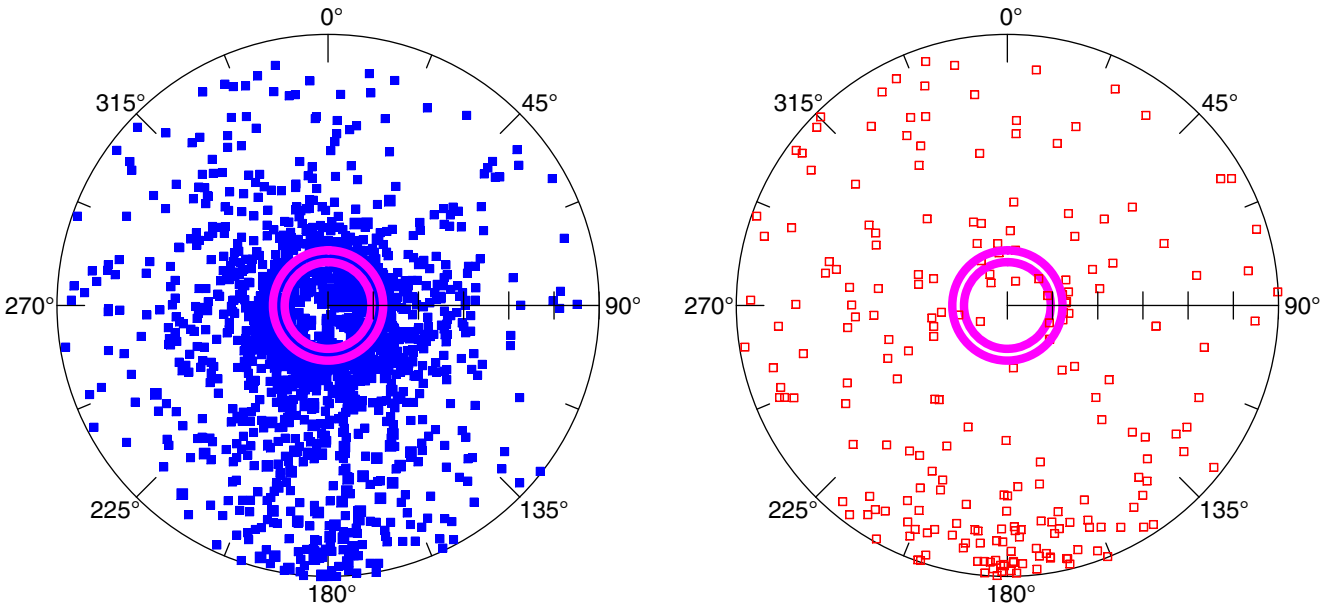

n = 1779

Figure F33. Biplot of mass-specific magnetic susceptibility (χ) vs. the intensity of natural remanent magnetization (NRM) after alternating field (AF) demagnetization at 5 mT.

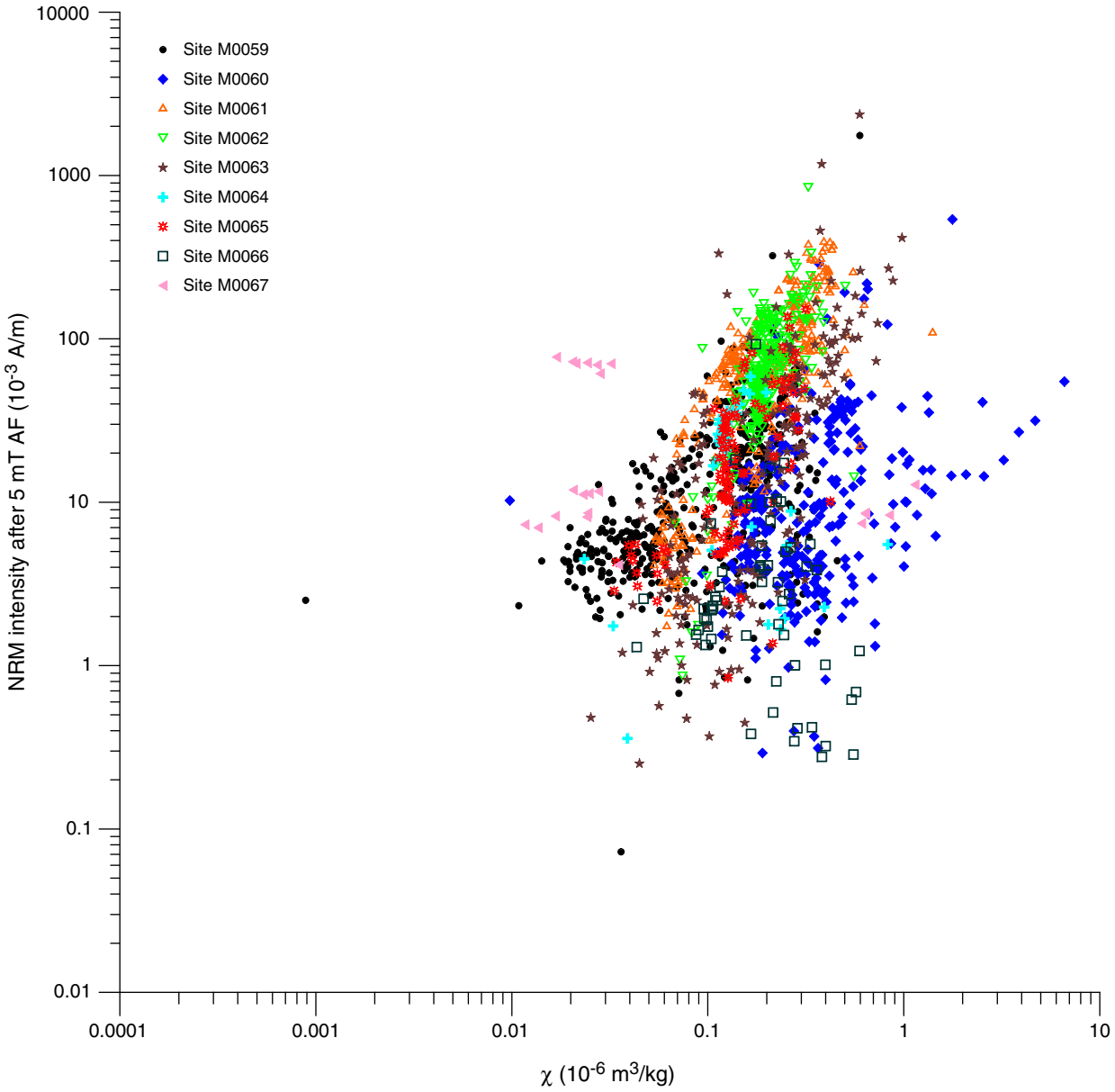

Table T1. Correlation between European and North American glacial terminology, approximate age, and marine isotope stage (MIS).

Northwest Europe	North America	Glacial/Interglacial	Age (ka)	MIS
Saalian	Illinoian	Glacial	200–130	6
Eemian	Sangamonian	Interglacial	130–115	5e
early Weichselian	Eo-Wisconsinan	Glacial	115–70	5a–5d
middle Weichselian	early/middle Wisconsinan	Glacial	70–30	3–4
late Weichselian	late Wisconsinan	Glacial	30–11.7	2–3
Holocene	Holocene	Interglacial	11.7–present	1

Table T2. Summary of the late glacial and Holocene Baltic Sea stages, approximate ages, inlets and outlets, salinity, and characteristic types of sediments.

Stage	Age (ka)	Inlet/Outlet	Salinity	Sediment type in Baltic proper
Baltic Ice Lake	~16–11.7	Öresund and south central Sweden	Freshwater	Clay, varved
Yoldia Sea	11.6–10.7	South central Sweden	Freshwater/weakly brackish water/ freshwater	Clay, weakly varved/homogeneous
Ancylus Lake	10.7–9.8	South central Sweden and later southern Baltic Sea area	Freshwater	Clay, homogeneous, sometimes sulfide banded or stained
Littorina Sea	9.8–3.0	Öresund/Great Belt	Brackish water	Gyttja clay/clay gyttja, alternating homogeneous and finely laminated
Post-Littorina	3.0–present	Öresund/Great Belt	Brackish water	Gyttja clay/clay gyttja, alternating homogeneous and finely laminated

Table T3. Summary of measurements, Expedition 347.

Greatship Manisha, offshore BSB	Onshore Science Party, BCR (Germany)
Core description	Core description
Core catcher description	Split-core visual core description
	Smear slide analysis
Micropaleontology	Micropaleontology
Foraminifers	Foraminifers
	Ostracods
	Palynology
	Diatoms
Geochemistry	Geochemistry
pH by ion-specific electrode	IW analysis by ICP-OES (major and trace elements)
Alkalinity by single-point titration to pH	IC (chloride, bromide, sulfate, and nitrate)
Salinity by refractometer	Sediment TOC, TC, and TS by LECO (carbon-sulfur analysis)
Ammonium by flow injection method	
Methane by GC	
Sampling for postcruise research for time-sensitive analyses	
Whole-core MSCL logging	Discrete sample moisture and density properties
Density	Compressional *P*-wave velocity
Velocity	Bulk, dry, and grain density
Magnetic susceptibility	Water content
Electrical resistivity	Porosity
Core imaging	Core imaging
Core catcher photography	High-resolution continuous digital line scanning of all split-core surfaces
Downhole logging	Other
Total gamma	Natural gamma radiation
Spectral gamma	Thermal conductivity
Resistivity	Color reflectance of split core surface at 4 cm intervals
Resistivity imaging (including caliper measurements)	Discrete paleomagnetic measurements
Sonic	Discrete magnetic susceptibility measurements
Microbiology	Microbiology
Sampling for postcruise research	Cell counts by fluorescent microscope
Sampling for PFC contamination tests	
Cell counts by flow cytometer and fluorescent microscope	

BSB = Baltic Sea Basin, BCR = Bremen Core Repository, GC = gas chromatograph, IW = interstitial water, ICP-OES = inductively coupled plasma-optical emission spectrometry, IC = ion chromatography, TOC = total organic carbon, TC = total carbon, TS = total sulfur, LECO = carbon/sulfur analyzer, TBC = to be conducted later, MSCL = multisensor core logger, PFC = perfluorocarbon.

Table T4. Operations, Expedition 347.

Hole	Latitude	Longitude	Water depth (mbsl)	Number of core runs	Interval cored (m)	Core recovered (m)	Core recovery (%)	Interval open holed (m)	Penetration depth CSF-A (m)	Time on site (days)
M0059A	55°0.295′N	10°6.491′E	37.1	29	90.2	85.41	94.68	0	90.2	2.56
M0059B	55°0.299′N	10°6.508′E	37.1	30	48.43	28.63	56.51	155.6	204.03	3.51
M0059C	55°0.289′N	10°6.469′E	37.1	84	105.77	104.42	97.82	52.91	158.08	3.09
M0060A	56°37.211′N	11°40.243′E	31.2	101	190.01	157.83	83.06	42.49	232.50	6.58
M0060B	56°37.204′N	11°40.229′E	31.2	28	85.7	87.62	98.32	0	85.7	1.77
M0061A	62°46.7′N	18°2.95′E	87.9	11	25.20	26.36	94.87	0	25.20	0.55
M0061B	62°46.706′N	18°2.93′E	87.9	9	28.7	28.46	97.98	0	28.7	0.30
M0061C	62°46.722′N	18°2.982′E	87.9	7	23.1	23.12	98.4	0	23.1	0.38
M0061K	62°46.722′N	18°2.982′E	87.9	1	1.0	0.97	97	0	1.0	*
M0061L	62°46.722′N	18°2.982′E	87.9	1	1.0	0.96	96	0	1.0	*
M0061M	62°46.722′N	18°2.982′E	87.9	1	1.0	0.92	92	0	1.0	*
M0062A	62°57.35′N	17°47.7′E	69.31	13	35.4	34.97	97.82	0.5	35.9	0.40
M0062B	62°57.357′N	17°47.682′E	69.31	8	23.1	23.3	98.57	1	24.1	0.21
M0062C	62°57.342′N	17°47.723′E	69.31	1	3.3	3.43	100	0	3.3	0.01
M0062D	62°57.343′N	17°47.718′E	69.31	7	19.5	19.99	100	1.5	21	0.41
M0062K	62°57.343′N	17°47.718′E	69.31	1	1	0.95	95	0	1.0	*
M0062L	62°57.343′N	17°47.718′E	69.31	1	1	0.92	92	0	1.0	*
M0063A	58°37.340′N	18°15.250′E	437.1	41	101.26	101.53	92.89	15	115.8	3.23
M0063B	58°37.345′N	18°15.232′E	437.1	14	29	41.12	99.28	0	29	0.80
M0063C	58°37.335′N	18°15.268′E	437.1	41	93.4	120.05	99.29	3	96.4	1.9
M0063D	58°37.350′N	18°15.260′E	437.1	41	87.1	114.13	98.59	0.2	86.8	2.07
M0063E	58°37.330′N	18°15.240′E	437.1	44	91.5	127.68	99.69	1.3	92.8	2.76
M0064A	55°43.273′N	15°13.585′E	60.5	32	41.5	29.59	66.82	0	41.5	1.08
M0064B	55°43.284′N	15°13.586′E	59.8	5	7.2	7.14	96.94	3	10.2	0.13
M0064C	55°43.262′N	15°13.584′E	59.8	36	43	37.81	74.98	2	45	0.85
M0064D	55°43.267′N	15°13.585′E	59.8	25	30.1	26.96	77.94	11.1	41.2	0.83
M0065A	55°28.094′N	15°28.631′E	84.32	43	45.82	48.48	99.19	28.08	73.9	1.34
M0065B	55°28.104′N	15°28.638′E	84.32	18	44.3	46.34	99.28	5	49.3	0.5
M0065C	55°28.084′N	15°28.624′E	84.32	15	45.9	48.59	99.61	2	47.9	0.75
M0066A	55°27.769′N	15°29.556′E	82.02	21	26.66	21.27	76.82	3.12	28	0.55
M0066B	55°27.773′N	15°29.539′E	82.02	14	25.25	22.51	78.61	2	27.25	0.41
M0067A	55°8.141′N	9°48.030′E	23.1	7	9.3	5.24	56.34	0	9.3	0.18
M0067B	55°8.151′N	9°48.029′E	23.1	6	6.4	8.17	97.03	4.5	10.9	0.18
M0059D	55°0.305′N	10°6.483′E	37.1	28	86.57	92.54	99.9	0	86.57	0.85
M0059E	55°0.285′N	10°6.499′E	37.1	37	100.8	95.35	90.02	0	100.8	2.04
			Totals:	801	1600.47	1622.76	91.24	334.3		

* = acquired while coring main holes. Percent core recovery adjusted for core expansion (recovery limited to 100% for expanded cores).